

Development of Form-Fitted Body-Worn Force Sensors for Space and Terrestrial
Applications

A Thesis
SUBMITTED TO THE FACULTY OF
UNIVERSITY OF MINNESOTA
BY

Mary Ellen Berglund

IN PARTIAL FULFILLMENT OF THE REQUIREMENTS
FOR THE DEGREE OF
MASTER OF SCIENCE

Adviser: Dr. Lucy E. Dunne

December 2016

Acknowledgements

I would like to genuinely express my gratitude to my advisor Dr. Lucy Dunne for the undeserved patience, invaluable comments, and general advice through the complicated learning process of this master thesis. Furthermore, I would like to thank Dr. Brad Holschuh for helping me translate technical jargon and interpret material that is seems beyond my breadth of knowledge and comprehension. I would also like to thank those closest to me who may have pondered my absence from society as I worked on this thesis.

Dedication

I dedicate this work to my mom, dad, and my best friend David Verwoest for being there for me throughout this entire process. I couldn't have done it without your words of encouragement, hugs, and grilled cheese sandwiches.

Abstract

Sensing force on the body is useful in the design of many on-body systems, including gas-pressurized space suits, for design diagnostics (e.g., determining where an on-body system is exerting potentially dangerous amounts of force) and for in-use monitoring. Mechanical Counter-Pressure (MCP) space suits have advantages over gas suits, and are an example of where measuring on-body force would be necessary. The development of an unobtrusive and practical means of measuring force in an MCP suit has yet to be established. Reasons for the absence of an established method for force-sensing within an MCP suit lie in the difficulties associated with integrating a force sensor, unobtrusively, into the under-layers of the user's garment. If the sensor introduces pressure points (e.g., is rigid or bulky), it will potentially cause harm to the user. This thesis describes the process of developing a soft and unobtrusive force sensor that avoids the use of a stiff apparatus. Specifically, the criteria for sensor selection and initial characterization of a variety of candidate sensor configurations when exposed to an applied load will be discussed. This thesis focuses on three experiments that were performed. The first experiment featured a commercial piezoresistive flex sensor as well as a custom coverstitched stretch sensor that were adapted to respond to normal forces and evaluated in a laboratory compression test. The flex sensor response displayed considerable noise, particularly evident in recovery artifacts when the load was fully removed from the sensor. The coverstitch sensor, on the other hand, had a more consistent, linear response in relation to the load being applied. Based on the findings and analysis of the first test, a second experiment was performed to examine the accuracy and

performance of different lengths and widths of the coverstitched stretch sensor. The findings concluded that the thin 2'' coverstitched sensor displayed the most promising results in terms of overall correlation with applied load and standard deviation between trials in relation to the other coverstitched samples that were tested. The final experiment extended the findings from the second experiment to test two different support structure substrates, rubber and silicone, each implemented in a topography of small hemispheres in varying size (small-diameter hemispheres, medium-diameter hemispheres, large-diameter hemispheres, and a flat topography). The results of the third experiment showed promise for the flat topography, which exhibited the strongest correlation between sensor response and applied load for both elastomer rubber and silicone substrate materials. Results were less favorable for the more extreme large-diameter hemisphere topography, which exhibited a weaker correlation indicating the larger the diameter the hemisphere was in the substrate material, the weaker the correlation between the load being applied to the sensor that was overlaid on the substrate material and the sensor's response (resistance readings). The development of an unobtrusive, form-fitted stretch sensor that measures force is a significant step forward for MCP suit design and controllability, as well as for many other domains in which sensing forces on the body is important. The results of this thesis study illustrate the difficulties associated with implementing a flex sensor onto a pliable surface. Additionally, this thesis study illustrates the potential that the coverstitched stretch sensor has for force-sensing applications.

Table of Contents

Abstract	iii
List of Tables	i
List of Figures	ii
I. Introduction.....	1
II. Background.....	6
A. Piezoresistance	8
a. Piezoresistive Pressure Sensing	9
b. Piezoresistive Strain Sensing	10
B. Piezoelectric sensing	23
a. Piezoelectric pressure sensing.....	24
a. Piezoelectric strain sensing	25
C. Capacitance	26
a. Capacitive pressure sensing	26
a. Capacitive strain sensing.....	27
D. Conclusion	29
III. Experiment 1: Sensor Type, Substrate, Topography, & Thickness	33
A. Method	33
B. Sample Characteristics	38
C. Data Collection	40
1. Analysis	43
2. Results.....	43
E. Discussion	47
1. Sensor Type	47
2. Supporting structure - Density	48
3. Supporting structure - Topography	50
4. Supporting structure - Thickness	51
5. Conclusion	52
IV. Experiment 2: Coverstitch Length & Width Testing.....	56
a. Method	56
b. Sample Characteristics	57
c. Data Collection	59
d. Procedure.....	59
i. Analysis	60
ii. Results.....	61
e. Discussion	64
1. Sensor Width.....	64
2. Sensor Length	65
3. Conclusion.	66
V. Experiment 3: Substrate Material & Topography	70

A. Method.....	70
B. Sample Characteristics	72
C. Data Collection	74
D. Procedure.....	74
1. Analysis	75
2. Results.....	75
E. Discussion	79
1. Substrate Material	79
2. Sphere Size	80
3. Conclusion	81
VI. Conclusion	84
Reference.....	90
Appendix A: Additional Figures for Experiment 1.....	95
Appendix B: Additional Figures for Experiment 2.....	119
Appendix C: Additional Figures for Experiment 3	129

List of Tables

Table 1. Requirements for the Design of a Force-Sensing Device to be Implemented into a Garment.....	6
Table 2. Characterization of Known Sensors	30
Table 3. Resistance Readings of Sensors (in OHMS) for Each Loading Cycle with Standard Deviation.....	34
Table 4. Coverstitched & Flex Sensor Test Parameters	41
Table 5. Mean R-square Values for the Coverstitch & Flex Sensor Tests	47
Table 6. Coverstitch & Flex Sensor Test Parameters	59
Table 7. Mean R-Square Values for Coverstitched Sensor Length & Width.....	64
Table 8. Substrate Material Test Parameters	74
Table 9. R-Square Values for Substrate & Topography Materials	77

List of Figures

Figure 1. Detecting stretch (left) vs. Detecting Force (right)	15
Figure 2. Attaching the Sensors to the Foam with Baste Stitches	38
Figure 3. Test Setup with VELCRO® Adhesion.....	41
Figure 4. Instron Unloaded (left) and Loaded (right) Sample	42
Figure 5. Squared Foam Topography. Relaxed vs. Depressed Sensor	42
Figure 6. Curved Foam Topography. Relaxed vs. Depressed Sensor	42
Figure 7. Mean R-square Coefficients of Sensor, Topography, Structure Thickness, & Material	44
Figure 8. Raw Data Traces of Load (red line) and Resistance (blue line) for Each Test Condition	45
Figure 9. Scatter Plot - Applied Load vs. Resistance	46
Figure 10. Coverstitched Stretch Sensor Thick (1/4") and Thin (3/16") Samples	57
Figure 11. Coverstitched Stretch Sensor Length and Width Samples	58
Figure 12. Coverstitched Stretch Sensor Basted on 1/2" 100% Polyester Densified Foam	59
Figure 13. Coverstitched Sensor Width and Length Mean R-Sq Values	61
Figure 14. Raw data traces of load (red line) and Resistance (blue line)	62
Figure 15. Scatter Plot - Applied Load vs. Resistance	63
Figure 16. Silicone & Rubber Samples with Various Size Diameter Hemispheres	73
Figure 17. Rubber Substrate Sample - Medium 1/2"-Diameter Hemisphere	73
Figure 18. Raw data Data Ttraces of Lload (red line) and R resistance (blue line).....	76
Figure 19. Diameter-Hemisphere Size and Substrate Material Mean R-Sq Value.....	77
Figure 20. Scatter Plot - Applied Load vs. Resistance	78
Figure 21. Coverstitch - 1" Green Polyester Curved	95
Figure 22. Coverstitch - 1" Green Polyester Curved	95
Figure 23. Coverstitch - 1" Green Polyester Squared	96
Figure 24. Coverstitch - 1" Green Polyester Squared	96
Figure 25. Coverstitch - 1" White Polyurethane Curved	97
Figure 26. Coverstitch - 1" White Polyurethane Curved	97
Figure 27. Coverstitch - 1" White Polyurethane Squared	98
Figure 28. Coverstitch - 1" White Polyurethane Squared	98
Figure 29. Coverstitch - 1/2" Green Polyester Curved	99
Figure 30. Coverstitch - 1/2" Green Polyester Curved	99
Figure 31. Coverstitch - 1/2" Green Polyester Squared	100
Figure 32. Coverstitch - 1/2" Green Polyester Squared	100
Figure 33. Coverstitch - 1/2" White Polyurethane Curved	101
Figure 34. Coverstitch - 1/2" White Polyurethane Curved	101
Figure 35. Coverstitch - 1/2" White Polyurethane Squared.....	102
Figure 36. Coverstitch - 1/2" White Polyurethane Squared.....	102
Figure 37 Coverstitch - 3/4" Green Polyester Curved	103
Figure 38. Coverstitch - 3/4" Green Polyester Curved	103
Figure 39. Coverstitch - 3/4" Green Polyester Squared	104
Figure 40. Coverstitch - 3/4" Green Polyester Squared	104

Figure 41. Coverstitch - 3/4" White Polyurethane Curved	105
Figure 42. Coverstitch - 3/4" White Polyurethane Curved	105
Figure 43. Coverstitch - 3/4" White Polyurethane Squared	106
Figure 44. Coverstitch - 3/4" White Polyurethane Squared	106
Figure 45. Flex Sensor - 1" Green Polyester Curved	107
Figure 46. Flex Sensor - 1" Green Polyester Curved	107
Figure 47. Flex Sensor - 1" Green Polyester Squared	108
Figure 48. Flex Sensor - 1" Green Polyester Squared	108
Figure 49. Flex Sensor - 1" White Polyurethane Curved	109
Figure 50. Flex Sensor - 1" White Polyurethane Curved	109
Figure 51. Flex Sensor - 1" White Polyurethane Squared	110
Figure 52. Flex Sensor - 1" White Polyurethane Squared	110
Figure 53. Flex Sensor - 1/2" Green Polyester Curved	111
Figure 54. Flex Sensor - 1/2" Green Polyester Curved	111
Figure 55. Flex Sensor - 1/2" Green Polyester Squared	112
Figure 56. Flex Sensor - 1/2" Green Polyester Squared	112
Figure 57. Flex Sensor - 1/2" White Polyurethane Curved	113
Figure 58. Flex Sensor - 1/2" White Polyurethane Curved	113
Figure 59. Flex Sensor - 1/2" White Polyurethane Squared	114
Figure 60. Flex Sensor - 1/2" White Polyurethane Squared	114
Figure 61. Flex Sensor - 3/4" Green Polyester Curved	115
Figure 62. Flex Sensor - 3/4" Green Polyester Curved	115
Figure 63. Flex Sensor - 3/4" Green Polyester Squared	116
Figure 64. Flex Sensor - 3/4" Green Polyester Squared	116
Figure 65. Flex Sensor - 3/4" White Polyurethane Curved	117
Figure 66. Flex Sensor - 3/4" White Polyurethane Curved	117
Figure 67. Flex Sensor - 3/4" White Polyurethane Squared	118
Figure 68. Flex Sensor - 3/4" White Polyurethane Squared	118
Figure 69. 4" Long 1/4" Thick	119
Figure 70. 4" Long 1/4" Thick	119
Figure 71. 4" Long 3/16" Thin	120
Figure 72. 4" Long 3/16" Thin	120
Figure 73. 3" Long 1/4" Thick	121
Figure 74. 3" Long 1/4" Thick	121
Figure 75. 3" Long 3/16" Thin	122
Figure 76. 3" Long 3/16" Thin	122
Figure 77. 2" Long 1/4" Thick	123
Figure 78. 2" Long 1/4" Thick	123
Figure 79. 2" Long 3/16" Thin	124
Figure 80. 2" Long 3/16" Thin	124
Figure 81. 1" Long 1/4" Thick	125
Figure 82. 1" Long 1/4" Thick	125
Figure 83. 1" Long 3/16" Thin	126
Figure 84. 1" Long 3/16" Thin	126

Figure 85. 1/2" Long 1/4" Thick	127
Figure 86. 1/2" Long 1/4" Thick	127
Figure 87. 1/2" Long 3/16" Thin	128
Figure 88. 1/2" Long 3/16" Thin	128
Figure 89. Flat Rubber	129
Figure 90. Flat Rubber	129
Figure 91. Rubber - 3/4" Diameter Sphere	130
Figure 92. Rubber - 3/4" Diameter Sphere	130
Figure 93. Rubber - 1/2" Diameter Sphere	131
Figure 94. Rubber - 1/2" Diameter Sphere	131
Figure 95. Rubber - 1/8" Diameter Sphere	132
Figure 96. Rubber - 1/8" Diameter Sphere	132
Figure 97. Flat Silicone	133
Figure 98. Flat Silicone	133
Figure 99. Silicone - 3/4" Diameter Sphere	134
Figure 100. Silicone - 3/4" Diameter Sphere	134
Figure 101. Silicone - 1/2" Diameter Sphere	135
Figure 102. Silicone - 1/2" Diameter Sphere	135
Figure 103. Silicone - 1/8" Diameter Sphere	136
Figure 104. Silicone - 1/8" Diameter Sphere	136

I. Introduction

The need for force sensing on the body is a key obstacle for many space, industrial, and terrestrial applications. Developing an unobtrusive and practical means of measuring force in these applications, such as in a mechanical counter-pressure (MCP) space suit, has yet to be accomplished. Force sensing not only provides post-hoc information about garment-wearer interaction – it can potentially provide real-time feedback for systems capable of providing dynamic counter-pressure control. Reasons for the absence of the established method for force sensing within an MCP suit lie in the difficulties associated with integrating a sensor that measures force, unobtrusively, into the under-layers of the user's garment. If the sensor introduces pressure points (e.g. is rigid, bulky), it will potentially cause more harm to the user.

Sensing force, particularly to measure the force of contact against the human body, has become an increasingly useful and beneficial function in everyday life. The majority of the research and applications pertaining to measuring the force of a contact surface against a body (or even the body against a contact surface) are in the domain of medical research, particularly health, safety, & prevention. Some injuries and illnesses require compression garments or casts to immobilize part of the body, and having the ability to determine the contact force of the cast and/or compression garment could improve the ability to design a more uniform contact force. Additionally, monitoring pressures exerted by pressure garments and analyzing the clinical outcome enables clinicians to adopt an understanding of the implications of particular pressures on scar outcome and

maturation rates (Robertson, Hodgson, Druett, & Druett, 1980). These measurements are usually done with commercially available interface pressure sensors, which will be discussed in the next section. Compression garments aid in the treatment of hypertrophic scarring following serious burns to the skin, and use of these garments is believed to “hasten the maturation process, reduce pruritus associated with immature hypertrophic scars, and prevent the formation of contractures over flexor joints” (Robertson et al., 1980). Despite the obvious benefits of obtaining measurements to determine exact pressure under a garment or medical appliance, no system has been established or identified as the only or best way to measure pressure for these applications (Partsch et al., 2006).

The human body is incredibly dynamic and complex, which makes it particularly difficult to accurately measure force exerted upon it. This is mostly due to the composition of the body, some of which includes the water content, tissue/skin types, muscle, contours, and fat percentage of the individual. Additionally, the human body is not stationary; it’s extremely mobile, and can perform wide ranges of motion. It is also soft, it bends, and moves, which can make it difficult to isolate forces being exerted in a particular direction, as many sensing mechanisms respond to force in any direction. The current methods for detecting and analyzing forces exerted on the body suffer from these outlined characterizations, mostly in relation to detecting “noise” and unwanted responses from movement of the user. Despite these difficulties, the need to accurately and unobtrusively detect force is present due to the numerous current and potential applications for which detecting force on the body is crucial. Detecting pressure points

within MCP spacesuits, for example, would help provide post-hoc information about garment-wearer interaction as well as potentially providing real-time feedback for systems capable of providing dynamic counter-pressure control.

Measuring force can be accomplished through force sensors either by measuring force more generally or by measuring pressure. The difference between force and pressure is that pressure is the amount of force per unit area exerted on a surface. Despite the existence of numerous types of sensors, there are only a small number of sensors with the capability of detecting force on the human body, due to the dynamic nature of the body. The human body requires a sensor that can both adapt to body movements, as well provide a consistent response regardless of the stability of the tissue over which the sensor is placed (for example, the soft fatty tissue on the thigh vs. the bony part of the ankle). Few sensors have the capabilities of bending (and even fewer stretching) to follow body movements, while reliably sensing force.

In this work soft, conformal force sensors were developed and characterized to be used with body-worn garments for space and terrestrial applications. In particular, the development of an unobtrusive, form-fitted force sensor that measures force is a significant step forward for active MCP suit design and controllability (as well as for many other domains in which sensing force on the body is important). Challenges associated with this type of integration relate to the dynamic nature of the human body. Integrating a manufacturable sensor that can sense force at various points on the body in real-time, while allowing the user to perform various tasks, is challenging. This thesis analyzed a set of sensors with the potential for 3D conformability to evaluate their

capability of sensing normal force accurately. The thesis included three separate experiments. The first experiment investigated two flexible sensors with potential for detecting force on the body (piezoresistive flex sensors & coverstitched strain sensors) over two varying substrate materials (100% high-density polyester foam & 100% polyurethane batting) of varying topography (“curved” & “flat”) and thickness ($\frac{1}{2}$ ”, $\frac{3}{4}$ ”, & 1”). The second experiment in the thesis was performed based on the results of the first experiment, which illustrated a better correlation between the force and sensor response for the coverstitched stretch sensor vs. the flex sensor. The second experiment was focused on determining the minimum viable size of the coverstitched sensor, through analysis of varying lengths ($\frac{1}{2}$ ”, 1”, 2”, 3”, & 4”) and widths ($\frac{1}{4}$ ” & $\frac{3}{16}$ ”) of the coverstitched stretch sensor. The results indicated that the 2”-long coverstitched stretch sensor had a stronger correlation with load and resistance compared to the other lengths, with the thinner $\frac{3}{16}$ ”-width coverstitched sensor performing slightly better than the wider $\frac{1}{4}$ ” width coverstitched sensor in terms of both correlation with load and standard deviation between trials. Paired with the results of the first and second experiment, a third experiment was performed which evaluated the response of the 2”-long, $\frac{3}{16}$ ”-wide coverstitched stretch sensor over two substrate materials (elastomeric rubber & silicone) with varying topography (flat, small $\frac{1}{4}$ ”-diameter hemisphere, $\frac{1}{2}$ ”-diameter hemisphere, & $\frac{3}{4}$ ”-diameter hemisphere) based on the results from the first experiment in this thesis study, which indicated a possible chance for a higher correlation between load and resistance when paired with a substrate material made of silicone. Overall results from this thesis show that there are difficulties associated with implementing a flex sensor onto

a pliable surface. Additionally, this thesis illustrates the potential that the coverstitched stretch sensor has for force-sensing applications.

II. Background

Sensing force being exerted on the body is required in many space, industrial, and terrestrial applications, but has proven to be challenging. An established method of integrating an unobtrusive force sensor that doesn't add bulk to the garment does not currently exist. The benefits of establishing a method, however, would be paramount due to the numerous applications for which force sensors used to detect force being exerted could provide safety, health, & prevention for the user. In order to integrate a mechanism into one of these applications, the material and type of sensor would require the ability not just to flex, but to allow for the potential of 3D drapability (i.e. conforming to bends along more than one axis). Additionally, these mechanisms would require a compact shape and the ability to fit on a contoured surface if they were to be integrated into a garment comfortably. The following table summarizes specific requirements for the design of a mechanism of the variety emphasized in this thesis, to be implemented into a garment to be worn on the body.

Table 1. Requirements for the Design of a Force-Sensing Device to be Implemented into a Garment

Parameter	Requirements
Force sensing direction	Normal to the body surface
Sensor output	Stable, repeatable, low hysteresis
Mechanical Properties	Flexible in more than one dimension, comfortable, thin
Fabrication	Simple mechanical integration with soft goods, low cost

Despite the existence of the variety of sensors that measure compressive forces, few are designed with the ability to bend or fit contours, which are conditions of the human body. These conditions would also affect the wearability of the sensor on the human body and its ability to be integrated into a garment that measures force. The ability to integrate the sensor into a garment also affects its manufacturability, in the sense that it can be worn comfortably and easily reproduced and manufactured without considerable expense in large-scale. Additionally, the sensor should be low-cost and have a form factor that is unobtrusive, which would help prevent injury to the individual due to potential snags, pressure points, and general discomfort. Its ability to be manufactured in-line with the current mass manufacturing methods of e-textiles would also contribute to the sensor's cost factor.

The sensors that fit this criterion generally use either capacitance, piezoelectric, or piezoresistive mechanisms to detect force. These mechanisms have been applied in different configurations to sense force, pressure, as well as strain. Pressure can be described as a force per unit area of a mechanical force in a controlled application, or a measurement of force applied to a contained gas or liquid. Strain occurs when a deformation of the material occurs, either by stretching or bending, which distorts the components due to the applied load. Using piezoresistive, piezoelectric, and capacitive sensing mechanisms with different kinds of materials and architectures, sensors that have the potential to flex can be implemented.

Capacitance sensors, piezoresistive sensors, and piezoelectric sensors respond to forces differently. Capacitive sensors rely on compression or stretch causing conductive

layers to get closer or further apart to issue a capacitive response, piezoresistive sensors are conductive materials that respond to being bent or flexed with a resistance change, and piezoelectric sensors respond to pressure or stress with a change in voltage. How these various mechanisms work, how they have been used to sense force (with particular emphasis on on-body sensing instances), as well as the pros and cons of each application will be discussed in the following sections. These include commonly-used commercially available techniques as well as sensors explored in research settings that have the potential for measuring compressive forces. Importantly, these mechanisms were chosen for their ability to detect forces applied perpendicular to a surface. This thesis will exclude types of force that act in other directions relative to the body surface and will only include the application of these sensing mechanisms in measuring normal forces through pressure (whether through a contained gas or fluid, or a force measurement with defined units of area) and through strain (through a material that responds to being deformed).

A. Piezoresistance

Force can be measured via resistance using piezoresistive materials. The piezoresistive effect is when the resistance of a material changes as pressure, force, or strain alters and deforms the material (Webster & Eren, 2014). Metals, such as platinum alloys or silver, are commonly-used piezoresistive materials (Liu, 2006). Examples of applications using piezoresistance to detect external forces through either pressure or strain of the sensor are described in the following sub-sections.

a. Piezoresistive Pressure Sensing

As stated earlier, pressure is the amount of force applied per unit area. Pressure requires an external force applied over either a contained gas, liquid, or controlled contact area. This sub-section will provide an example of an application that uses piezoresistance-based pressure sensors in a garment to measure pressure forces.

One study focused on contact pressure between body and contact surface analyzed where an individual was experiencing body-space suit contact in a Mark III space suit (A. P. Anderson & Newman, 2015). Donning the space suit and performing mission-related activities often causes health problems like skin and surface injuries due to the contact the body makes against the suit. This study focused on analyzing human-space suit interaction by assessing the body placement within the suit. Resistance-based pressure sensors were integrated into an athletic garment, over the arm (Anderson & Newman, 2015). Sensors were placed on the garment at anticipated “hot spots” where body- suit contact was likely to be made. The pressure sensing system (named the Polipo system) was comprised of 12 sensors, each 2.5 cm in diameter. The sensors had been measured to be highly repeatable in previous studies (A. Anderson, Hilbert, Bertrand, McFarland, & Newman, 2014), and were molded using a hyperelastic polymer cured to have a microfluidic channel into which liquid conductive metal is deposited (A. Anderson et al., 2014). When the conductive channels were deformed under an applied load, the sensors were able to measure normal pressure by the change in resistance of the conductive metal within the channels. Despite the sensors successfully being able to measure normal forces of pressure for this particular study as well as being repeatable

and stable, the sensor itself had limitations due to the complexity of manufacturing. Additional limitations included the expense of the system, as well as the mechanical properties of the sensor itself, which was relatively thick (4.8 x 3.6 x 1.3cm) and not entirely flexible with the silicone sensor being housed in a rigid structure. The sensors are also accurate when used under intended dynamic conditions, but are limited in their utility under static loading due to a creep as energy dissipates from the system, which results in a hysteresis of greater than 10% from loading and unloading as well as drift (11%) when exposed to higher pressures. The sensors were relatively stable, however, with a root mean square of error at 3 kPa. The manufacturing process of the sensors was also complex compared to other standard methods for both manufacturing electronics and textiles (manufacturing the sensors consisted of three steps of casting, bonding, and injection) as well as the sensor needing to be attached to a network of wires under the garment. Durability concerns were also raised from the internal copper wires, which were known to separate from the sensing element in previous studies using this Polipo system, possibly due to its rigidity (A. Anderson et al., 2014).

b. Piezoresistive Strain Sensing

When an element is strained, it undergoes a change in dimension. The resistance of a piezoresistive device is affected by these changes in cross-sectional area and length (Wilson, 2005). Examples of the resistance of the device changing through the use of strain exerted mechanically on the sensing element will be discussed in this sub-section. Additionally, these examples will illustrate the potential to sense strain-type forces in a

garment or on the body using piezoresistive materials and devices that contain all (or most) of the requirements specified in Table 1.

Strain can occur through either compressive (two points squeezing together) or through tensile (two points pulling apart) forces. The following examples used piezoresistance to sense compressive strain.

The first study evaluated helmet force impact performance using commercially available piezoresistive Flexiforce® sensors (Ouckama & Pearsall, 2011). Their goal was to better understand the dynamics at the small region of contact between the colliding object and the helmeted head due to the directly induced stresses caused by impact on those regions. They anticipated the inclusion of a loading force distribution to the cranium could help determine local tissue distress related to injury (Hardy et al., 2007). They used 13 Flexiforce® (A201-100 Tekscan, Boston) sensors, which were arranged on a 5 x 5 cm array over three various densities of foam to simulate helmet padding material, secured on a load cell. The Flexiforce® sensors used in this study were chosen due to their low cost (which average \$16 per sensor), discreet form (0.204mm x 191mm x 14mm, with an optional trim of the length) and flexibility (with the substrate material being made of polyester mylar and having the ability to bend and sense bi-directionally). These characteristics are necessary in order to conform to irregular curved surfaces within a worn helmet. The Flexiforce® sensors also have a typical repeatability performance of $\leq \pm 2.5\%$ of full scale based on their datasheets, are stable with a drift of $< 5\%$ per logarithmic time scale with a constant load of 111 N (25lb) and have a hysteresis performance of $< 4.5\%$ of full scale with a conditioned sensor at 80% of full force

applied. Other factors also included their ability to detect high speed impulses, as well as simple mechanical integration of the sensor over the foam used in the study, having a 3-pin Male Square Pin, which could be adhered to a conductive element with solder as well as using double-sided tape to adhere the film portion of the sensor to the foam during testing. Three densities of foam were placed over the sensor array and underwent repeated impact by a hemispherical impactor, in the same direction that normal force would be applied to the body. They found that the sensor array, which only covered 36% of the total area of the helmet padding material, possessed sufficient spatial and temporal resolution to capture dynamic load distribution patterns (Ouckama & Pearsall, 2011). They indicate that implementation of the force mapping system is not limited to just helmet testing, but possibly to other areas of the body vulnerable to contact injuries (Ouckama & Pearsall, 2011). They do suggest, however, that future designs incorporate a higher sensor count to increase the spatial resolution as well as the total coverage area to minimize the possibility of the impact distribution exceeding the sensor array boundaries (Ouckama & Pearsall, 2011). However, the system used for testing did not integrate the sensors over a varying curved surface (which would have been the next step in their research), which would more accurately reflect the nature of the inside of a helmet. This study is similar to many other studies pertaining to integrating sensors onto the body, in that the sensor's performance is not tested under "ideal" conditions (i.e. on the the human body). Instead testing is limited to a constrained laboratory set-up which may not translate directly to conditions that reflect the irregular shape and curvature of the human body.

An example of a study using piezoresistance to measure compressive strain forces on the body directly used foam sensors (soft open-cell foam with an electro-active polymer coating) integrated into garments on a closely-fitted, non-extensible chest strap to monitor respiration rate (Brady et al., 2005). The actual measurements of the sensor were not included in the study, but it was small enough to be integrated into a garment. The actual cost of the materials used to construct the sensor were also omitted from the study. They measured the change in resistance values when the foam-based sensor experienced force normal to the body surface due to the expansion of the ribcage when the subject inhaled. The sensor required a small measure of compression in order to register a response, which enabled the strap to be secured on the subject comfortably rather than in a tight manner. They found that the accuracy of the garment-integrated sensing system was comparable to a standard airflow breathing test, making such a garment a viable option compared to traditional sensors, which impede wearability by their physical structure or functional requirements (Brady et al., 2005). Vigorous activity appeared to have no impact on the accuracy of the recorded respiration rate compared to a standard airflow measurement. The sensor itself was low cost, easily manufacturable, and only required a small amount of compression to detect force. The sensor was shown to be accurate, with the data never differing more than 1 BMP from a wireless Mote system vs. the airflow data that was used to gather data, with a correlation coefficient of 0.99 and a standard error of 0.62. Data pertaining to the hysteresis and stability were also not found in the study. When comparing this sensor to Table 1, it does have the requirement of having the ability to detect normal force to the body. Unfortunately, the

soft open-cell foam had limitations, such as limited elasticity and possible limitations of where it can be placed on a garment. In addition, this study did not measure forces in an analog way (which would not be possible without a reference measure for force), measurement was limited to frequency of breaths and compared to an airflow-based breathing monitor.

Forces that are applied in a direction normal to the body surface are compressive forces. compressive stress usually shortens or compresses the material (Ripka & Tipek, 2007). However, tensile strain sensors could also be used to sense normal force. The forces acting upon tensile strain sensors usually deform the sensor through stretch or elongation, making the material longer. However, if a compressive force or force normal to the body surface could be translated into a tensile strain within the sensing material, a stretch sensor could be used to detect compressive forces normal to the surface of the sensor (or body).

Wang et. al investigated the fabrication of fabric tensile strain sensors capable of acting as normal force sensors by using a top and bottom “conversion layer” on either side of the tensile strain sensing element. The conversion layers were shaped in an interlocking tooth-like grid, which caused the sensing fabric between the conversion layers to extend over the “grooves” when a force was applied to the conversion layer. In this way, compression of the conversion layers is transformed into an in-plane strain of the sensing fabric, which ultimately changes the resistance of the fabric (Wang et al., 2011). The normal force sensor was fabricated by adhering a fabric tensile strain sensor to the top and bottom conversion layers. The conversion layers were made by molding

silicone elastomers within a frame used to attach the conversion layers. The whole setup was placed in an oven for vulcanization of the silicone. The fabricated sensors used had a very low profile and measured 10 mm x 16 x 4.8 mm. After 100,000 pressing cycles, the sensors were shown to obtain “repeatable and stable resistance and pressure data”, with a “small hysteresis”, but these qualities were not quantified. This study illustrates the potential for using normal force to induce strain in a tensile strain sensor. With this method, it is possible to sense normal force using tensile strain sensors. The success of the method relies on both the strain-sensing capabilities of the sensor itself as well as the amount of stretch induced in the sensor, which in this paradigm requires some type of underlying material or substrate (similar to Wang et al.’s “conversion layers”) to induce the stretch when a normal force is applied (Figure 1).

There are many sensing approaches that could be adaptable to this approach to

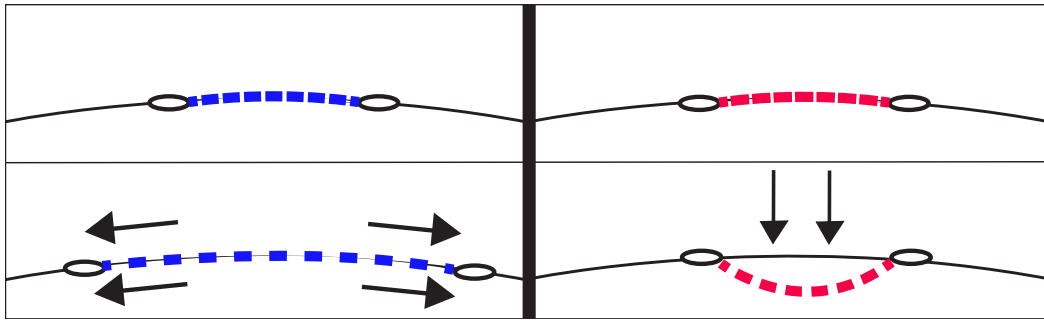


Figure 1. Detecting stretch (left) vs. Detecting Force (right)

using elongation sensors to detect normal forces. Stretch sensing technology and methods for measuring stretch or elongation on the body fall into three categories (Gioberto & Dunne, 2012): 1) piezoelectric or electro-active polymer materials or coatings that respond to stretch compression with a corresponding change in resistance, 2) implementation of suspended particles or electrodes in an extensible substrate, and 3)

implementation of a looped conductor. Measuring stretch or elongation on the body is particularly common in studies that focus on breathing patterns. One such study used deformation by extension to affect a change in resistance in a piezoresistive sensor integrated into a test garment. They developed a textile based sensor for remote monitoring of breathing of a user in a prototype garment using ELASTOSIL® conductive silicone (Guo et al., 2011). The sensor's primary purpose was to detect the various levels of spontaneous breathing patterns which are present in individuals that have medical conditions such as asthma, which could play an important role in detecting early signs of illness. They created a washable, flexible, and comfortable means of sensing measurements on the body that provided traditional comforts of everyday garments, which greatly increases the likelihood of being adopted by a user (Guo et al., 2011). The sensor was made from a conductive silicone that was coated over a textile substrate, which was a PA (polyamide fiber)/Lycra woven fabric used because it had good elasticity and recoverability. To detect breathing, the sensor was placed on the torso of the test garment, and recorded the resistance change caused by extension and deformation of the sensor, which was repeated mechanically to simulate breathing in an initial test followed by testing the breathing patterns of ten subjects. They found that the sensor could register both the frequency change and amplitude change of activities that were performed during the testing procedures, which included various breathing patterns while sitting still, walking, and jogging. The manufacturability of the garment was more in-line with a traditional method for manufacturing garments. The sensing element was also low-profile(100 mm x 10mm) and had elastic properties of silicone, so it was soft

and flexible in multiple directions as well as comfortable by not hindering or restricting the body movement of individuals during testing. Unfortunately, the sensing element itself was only placed and coated on two locations of the body (the abdomen and the chest), and the sensing element was not tested on different curvatures of the body to determine accuracy and performance. Additionally, the stability, repeatability, and hysteresis of the sensor were not clearly reported.

Further research that used tensile strain forces in piezoresistance implemented stretch sensors into the form of lycra fabric coated with carbon-loaded rubber and knitted electro-conductive yarn sensors into a skin-tight body suit to measure respiration (Paradiso, Loriga, & Taccini, 2005). The Wearable Health Care System used knitted fabrics with conductive and piezoelectric yarns, which they integrated into an elastic skin-tight body suit (Paradiso et al., 2005). This system of sensing elements is something that could be more easily manufacturable, particularly in the current standard textile industrial processes (Loriga, Taccini, De Rossi, & Paradiso, 2005). Their study emphasized and reinforced the notion that signals by fabric sensors are comparable with standard sensors (Scilingo et al., 2005). Additionally, the piezoresistive fabric sensors used in this study were low-cost, fit the contours of the body, flexible in multiple directions, and were low profile due to the commercially-available conductive yarns they used. The actual dimensions of the sensor were not reported and appeared to vary depending on the placement of the sensor on the body, but did not appear to be thicker than the knitted substrate material. The comfort of the sensors was not noted, but it can be assumed that the low-profile nature of the sensor paired with the knit textile substrate

added to the comfort of the sensor. It was also noted during testing that the more physical activity that the individual underwent while wearing the sensors, the stronger the influence of artefacts which interfered with the quality and stability of the signal. The repeatability of the sensor as well as the hysteresis were not given.

Another study developed a wearable gesture-sensing device designed for monitoring the flexion angle of elbow and knee movement (Shyr, Shie, Jiang, & Li, 2014). They made a textile strain sensor using an elastic conductive webbing in a plain weave structure made of conductive and elastic yarns which respond to stretch by compressing the filaments of the yarn together, with a corresponding change in resistance. A change in resistance of the elastic conductive webbing between two electrodes was measured during flexion-recovery movement. The flexion angle of the gesture sensing apparatus was recorded using a protractor. They then established a relationship between the flexion angle and the resistance of the elastic conductive webbing in the flexion-recovery cycles using an assembled gesture sensing apparatus that they constructed. They fixed the strain sensor onto a woven fabric (which they refer to as the “steady fabric”) to ensure the stability of the resistance when measuring the flexion angle-resistance. The sensor was placed between two woven fabric strips that were anchored to the body with a closure mechanism. They found the elastic conductive webbing, which consisted of 32 conductive yarns and 5 elastic yarns in the warp and one conductive yarn in the weft in a plain weave structure measuring 8mm wide by 2mm thick, had a good linear relationship during the stretch-recovery cycles in the resistance. The main advantages that were discovered for this device were the precision of

measurement, comfort (being textile-based), wearability, and the ability to monitor flexion angles during knee and elbow movements with no discomfort (Shyr et al., 2014). In addition, the sensor itself wasn't strictly woven into a full-sleeve garment, but rather had the two ends connected to the "anchor" fabric. The results indicated that the resistance of the elastic conductive webbing was proportional to the elongation performed during testing cycles, with a coefficient of determination of the linear regression curve being 0.98, indicating stable and repeatable measurements. No hysteresis from the results was evaluated. The conductive yarns used in this study, like the previous studies that have thus far used conductive yarns as the sensing element, were low-cost, low-profile, flexible in more than one dimension (being textile based), and easily manufacturable based on current textile industry standards.

Another study using piezoresistive fabric as sensors for measuring breathing (Rovira et al., 2011) found that the three piezoresistive fabric sensors that they tested exhibited different responses, but after applying a Butterworth filter to reduce noise, all were accurate and clear enough to imply that the sensors could detect accurate movements with precision. The piezoresistive fabric sensors were acquired from Eonyx (Eonyx Corporation, Pinole, CA 94564, USA). They concluded that the three various piezoelectric fabric sensors provided adequate means for monitoring respiratory rate based on the results they obtained from the fatigue machine they used for data collection to simulate breathing when worn on the body, but would need further testing to evaluate the behavior of the sensors in relation to temperature. Additionally, the sensors were tested on a linear flat surface, and were not integrated into a garment or on a body. The

sensors themselves were flexible in more than one dimension (having the same characteristics as drapable fabric), low-cost, and low-profile and thin (each sensor that was attached to the garment was 55mm x 20mm). While not explicitly evaluated, based on the graphs and data reported, it seems likely that the stability and repeatability of the sensor is similar to other textile-based sensors explored here. The hysteresis for the tests of the sensors, however, was not reported. The sensors can be cut to any size and shape, since they derive from piezoresistive fabric, but would require some measure of binding of the edges in order to prevent further fraying, as well as an additional step of attaching the sensor to the garment and testing it on the body. Given that, they would qualify as manufacturable in-line with current textile industry manufacturing methods

A similar study implemented conductive yarn-based instead of fabric-based piezoresistive sensors to explore the capability of measuring respiration signals. The sensors consisted of high-density piezoresistive fibers, elastic, and polyester fibers. The yarns were fabricated by wrapping polyester fibers, elastic, and piezoresistive fibers into a skein. The sensors were knitted into a single jersey fabric, which they referred to as yarn-based sensing fabric. A carbon-coated fiber (CCF) was used as the basic conductive material, which wrapped a core polyester and lycra yarn (50d/144f) to form a stable yarn structure (a single and a double yarn). They also sewed the fabric into a belt, which they refer to as yarn-based sensing, which they used in a simulation system to measure respiration rate. The simulation system consisted of a solenoid control valve connected to an air bag, which was used to create periodic pressure variation. The test sample was 6cm long, and they used an INSTRON tensile test apparatus and Fluke multi-meter to

measure the applied force and resistivity of the sample. The standard deviation of the resistance of the single wrap yarn (0.139) was larger than the double wrap yarn (0.0056), which may have been due to the symmetrical and constrained structure of the double yarns vs. the single wrap yarn. This indicates that the double-wrap yarns are more stable and repeatable. Hysteresis for the sensors was not indicated. Their study found that, aside from the successful capability of measuring the respiration rate of the user, yarn-based sensors were more comfortable to wear than textile-based sensors, could measure distributed strain, and can be easily fabricated by conventional textile processes (Huang, Tang, & Shen, 2006). Unlike fabric-based sensors, the yarn-based sensors were separated on the fabric, and were not continuously distributed over the whole fabric; even if there was only one yarn-based sensor on the fabric, similar results could be accomplished, though multi-yarn-based sensors could help ensure proper measurement if the application was not properly positioned (Huang et al., 2006). This type of sensor requires the use of a knitting machine for manufacturing, but the result is low-profile, flexible in multiple dimensions, and low-cost.

Gioberto et al. (2012) analyzed a sensor made using a similar principle: in this case, a top-thread coverstitched stretch sensor, (a sensor made using a common stitch used in apparel production) which was made from a conductive thread that increases in electrical resistance as the fabric is stretched, due to the geometry of the stitches (Gioberto & Dunne, 2012). In the implementation of a looped conductor, the resistance changes when the electrical length of the conductive pathway is increased or decreased as the sensor is stretched. There are several different loop structures feasible with an

industrial coverstitch, which affect the properties of the sensor response (e.g. either making the electrical length longer or shorter when stretched depending on the configuration of shorting behavior in the loop structure) (Gioberto & Dunne, 2012). The easily-manufactured coverstitched stretch sensor could be integrated into any garment, though elastic knits would provide more responsiveness in terms of resistance due to the ability for the sensor to stretch to the limitations of the fabric. This method of integrating a sensor is also low profile since the sensor itself is customizable and made from conductive yarns stitched directly onto a textile (the sensor used in the Gioberto study was 4.75'' in length), low-cost, comfortable (no hardware or stiff components used), flexible in multiple directions (being made from soft goods), and manufacturable using only a coverstitch machine (a common sewing machine in garment production). The use of conductive yarn as the sensing element instead of other sensing mechanisms discussed thus far has not shown a significant effect on sensor performance (Scilingo et al., 2005). The correlation coefficient of the resistance vs. load of the sensor was 0.83, indicating a stable, repeatable, and linear response (Gioberto & Dunne, 2012). The hysteresis area of the results was 12.63Ω (note that this study expressed the hysteresis differently than the other examples highlighted in this chapter). The coverstitched stretch sensor illustrates some of the best potential in terms of aligning with the requirements for a force-sensing device to be implemented into a garment (as highlighted in Table 1), which are its cost-effectiveness, flexibility, thickness of sensor, comfortability, simple mechanical integration, responsiveness and ability to detect normal force. These attributes are contributing factors to using this particular sensor in this thesis' experiments.

The concept of detecting normal force with a stretch sensor on the body by allowing the sensor to stretch inward (or “toward”) the body is possible without a conversion layer if the sensor can be allowed to deform with the body surface when a point of pressure is applied. Unfortunately, depending on the placement of the sensor on the body, the sensor could possibly be limited by the deformability of the tissues it is placed over a firm (i.e. a “bony” part of the body wouldn’t allow the sensor to stretch as much as a fleshy part, as illustrated in Figure 1.) Techniques (similar to the Wang. et. al., study) could be used, implementing a “conversion layer” to further induce (or “amplify”) the stretch response.

B. Piezoelectric sensing

Piezoelectric sensors rely on the piezoelectric effect, which is the generation of an electrical potential (or charge) in certain materials (such as crystals or quartz) when subject to a mechanical stress (Fraden, 2004). Unlike piezoresistance, which causes a change in resistance when a material or device is stressed, piezoelectricity generates an electrical charge in the material or device in response to stress. Common piezoelectric sensing materials include crystals (like quartz or topaz), ceramic, polymers, or biological matter, that generate a charge or voltage. The most common piezoelectric material that is currently used is a ceramic lead zirconate titanate, which is man-made, known as PZT (Robinson, 2016). Piezoelectric sensors can not be made in a manner that allows them to stretch along a surface, which may make it difficult to integrate them into a garment. There are some piezoelectric sensors, however, that can be easily shaped for any desired

application (Sirohi & Chopra, 2000). A piezoelectric effect can occur when a mechanical strain is applied, specifically pressure or force. The applications of piezoelectric force sensing for wearable applications will be described below.

a. Piezoelectric pressure sensing

The voltage change in a piezoelectric material is proportional to the amount of force being applied (Dirjish, 2012). Piezoelectric sensors generate an electric signal that decays rapidly, which can make it difficult to measure static forces. However, this makes them ideal for detection of explosions or dynamic pressures (“Pressure Sensors from Kistler,” 2016). The following example application senses force using piezoelectric response.

An early attempt at measuring the pressure exerted onto the body between the body and the garment was through the use of the Oxford Pressure Monitor (Harries & Pegg, 1989). The purpose of the study was to measure garment-scar interface pressure to be able to prescribe specific garments for certain body areas. The Oxford Pressure Monitor was a portable and battery operated device, with a digital display of 12 pressure values in mmHg. They placed pneumatic piezoelectric electrodes directly under the garments in a matrix of 12 in 3x4 array, which were connected to the Oxford Pressure Monitor device. They encountered difficulties when taking readings over soft-tissue areas, and required the use of a stabilizer (a piece of cardboard) placed over the electrode to aid in taking the readings. The authors recommend for future studies that sensors should be thin as not to disturb the presence of the surface being measured and not so thin as to distort the measurements if the surfaces are non-planar (Robertson et al., 1980). The

sensors themselves were not characterized in the study, but limitations in this study include the requirement of some sort of stabilizer to aid in the sensor readings and limited flexibility.

a. Piezoelectric strain sensing

One study developed a piezoelectric method of measuring the vertical contact stress (specifically the strain of the sensor) beneath the human foot by using piezoelectric ceramic transducers to make a prototype pressure-sensitive shoe insole (Hennig, Cavanagh, Albert, & Macmillan, 1982). The purpose was to obtain data pertaining to the force acting on the plantar surface of the foot while standing for the treatment of various disorders of lower limb and in the design of footwear. It was noted in the study that piezoelectric ceramic transducers are sensitive to variations in humidity and temperature. The prototype device consisted of a flexible array of 499 4.78 mm square, 1.2 mm thick, lead zirconate titanate transducers embedded in a 3-4 mm thick layer of highly resilient silicone rubber that was impervious to moisture and was electrically insulating (Hennig et al., 1982). A sheet of thin copper gauze cut to the shape of a US size 10 right foot was used, which had transducers with silver electrodes diffusion bonded to their major surfaces. They were able to successfully develop a system for the measurement of vertical contact pressure distributions, but suggestions for improving the design for the future included using a lower density rubber, thinner transducers, and thinner wires. The results of the tests in the study indicated hysteresis that was less than 1% and had less than 2% linearity which indicated repeatability of the sensor and was stable. Integration into soft goods was only performed on a shoe; no further indication of implementing the

sensor into soft goods was realized or characterized. The manufacturing cost of the sensor is also unknown, as well as an indication of the comfort of the sensor to the user.

C. Capacitance

Capacitance is essentially the ability for a mechanism to store an electrical charge. A capacitor relies on two parallel conductive plates that are separated by a distance or a dielectric material. In order to generate a capacitance change, a compressive or tensile external force must be applied to move the capacitor plates (Fraden, 2016). The forces that are used to generate a capacitive response will be described below, which include pressure forces and strain forces.

a. Capacitive pressure sensing

One study that used a capacitive-type sensor to detect pressure was implemented by integrating a pixelated 6 x 6 array of sensors to obtain spatial pressure information (Lee et al., 2015). Cotton fibers were used with PDMS-coated conductive fibers (silver nanoparticle/elastic rubber composite fibers) to weave the sensor array fabrics. The total area of the sensor array fabricated was 2 x 1.5 cm. In a capacitive pressure sensor, the area of the pressure sensor and the distance of the electrode separation affect the change in the capacitance. When the sensor is compressed by external pressure, the PDMS films used in this study changed in thickness, which reduced the distance of the electrode separation. The contact area between the two PDMS-coated conductive fibers was increased due to the deformability of the stretchy PDMS-coated fibers. Results showed “negligible” hysteresis, and had “good” stability, although these were not quantified.

Repeatability was also not quantified but also seemed to be similar to other sensors evaluated here, with the hysteresis and stability results corresponding with the response of the sensor to a load of 1.7N over 10000 cycles. This method was found by the authors to be favorable in terms of manufacturability (due to its ability to be integrated into current textile manufacturing methods) and cost (based on the materials used to produce the PDMS-coated conductive fibers. It also demonstrated the successful integration of the sensor and flexibility over a curved surface on the body (in this case, the fingertips).

a. Capacitive strain sensing

Capacitive sensors can be used as strain gauges if the force that induces strain pulls the capacitor plates apart. One particular study implemented an inexpensive means of measuring strain by using a differential capacitive sensor to detect respiration monitoring using a textile-based belt (Merritt, Nagle, & Grant, 2009). The belt itself was composed of four materials: screen printable fabric, rubber elastic, Velcro, and conductive elastic. The sensing-portion of the belt was comprised of capacitive displacement sensors, which measured the change in area between the two capacitor plates. They were fabricated by screen-printing a silver ink electrode pattern on two separate parts of a nonstretchable nonwoven textile and attaching them laterally with one-dimensionally stretchable nonwovens on opposite ends to enable the plates to slide in opposite directions when the sensor is stretched. The capacitive sensors that were used to fabricate the belt were 45mm in length for the bottom of the belt and 60mm for the top. The belt was intended to fit around the chest – so the device itself was somewhat large in length (specific measurements for the belt were not disclosed). When the subject takes a

breath, the fixed ends of the sensor are pulled apart, causing the overlapping area between the capacitor's plates to change. Instrumentation circuitry is used to measure this change in area, which produces a proportional change in capacitance. The friction between the two layers caused hysteresis in the measurements which was not quantified in the study, however visual assessment of the data presented graphically showed a linear response over time despite the presence of noise artefacts from the friction caused by the two layers. This sensor could be easily fabricated using conventional textile manufacturing processes.

Another example of a textile-based capacitive sensor in a garment is one that measured the capacitance changes from abdominal displacement in breathing (Se Dong Min, Yonghyeon Yun, & Hangsik Shin, 2014). They did so by constructing a five layered belt-type capacitive textile force sensor, which has a conductive layer and insulation layer. They used non-conductive woven interlining with electro-conductive fabric. To achieve capacitance, the two electric conductive fabrics were wound twice by non-conductive polyester woven fusible interlining. When a force was exerted on the sensor, it caused a change in capacitance due to it being strained. Comparable to the previous examples in terms of thickness, this sensor was relatively thick due to the need to manufacture the sensor with 5 layers. The height, width, and thickness were 830 mm x 38.6 mm x 1.35 mm. The coefficient of determination was 0.9933 for the capacitance vs. the force being applied during testing, indicating stability and repeatability. The hysteresis was not indicated in the results. It was also low-cost relative to standard sensing mechanisms, flexible (being made from textile and pliable materials), and

relatively easy to manufacture based on current methods of manufacturing textile-based goods.

D. Conclusion

E-textile sensing methods are one area of focus that could help fulfill the requirements of a sensor being drapable, flexible, and compact and better suited for a human body as well as being able to detect force, but unfortunately few e-textile sensors meet all of these performance requirements, as illustrated in Table 2 which is a representation of all of the sensors characterized in the studies reviewed thus far in this thesis' literature review section.

Table 2. Characterization of Known Sensors

	Force Sensing Direction	Sensor Output	Mechanical Properties	Fabrication
A. P. Anderson & Newman, 2015	✓ Mentioned that it can detect normal force to the body)	✓ Mentioned it being repeatable from previous tests, hysteresis: greater than 10% from loading and unloading pressure effect, 11% drift	✗ Mentioned it being NOT flexilbe, and the sensor is (4.8 x 3.6 x 1.3cm) , which is considered relatively "thick"	✗ Mentioned that the mechanical integration with soft goods is complex, as well as expensive
Ouckama & Pearsall, 2011	✓ Can detect normal force	✓ Repeatable (of <+2.5% of full scale), drift of <5% per logarithmic time scale, and a hysteresis of <4.5%	✓ Thin sensor (0.204mmx191mmx14mm), flexible bi-directionally	✓ Low cost (average \$16 per sensor), simple mechanical integration (all it requires is solder, double-sided tape)
Brady et al., 2005	✓ Can detect normal force	✗ No hysteresis, no data about stability, does indicate repeatability	✗ No measurements (~2") - look up paper by Dr. Dunne	✓ Easy manufacturable, no price listed
Guo et al., 2011	✓ Can detect normal force	✗ No hysteresis, no data about stability, does indicate repeatability	✓ Low profile - 100 mm x 10 mm, elastic, flexible in more than one direction, comfortable (didn't hinder movement and was soft)	✓ In-line with current textile manufacturing methods
Paradiso, Loriga, & Taccini, 2005	✓ Uses stretch, which can be used to detect normal force	✗ No hysteresis or repeatability, but stability was affected by influence of artefacts	✓ Flexible in multiple directions, Low profile sensor (varied in length, no dimensions given), comfort not known but can be assumed	✓ Easily manufacturable, particularly in the current standard textile undistrial processes
Shyr, Shie, Jiang, & Li, 2014	✓ Uses stretch, which can be used to detect normal force	✗ Stable and repeatable measurements (r ² value of 0.98), no hysteresis was indicated	✓ Comfortable (textile based), 8mm x 2mm thin, flexible in more than one dimension	✓ Easily manufacturable, particularly in the current standard textile undistrial processes
Rovira et al., 2011	✓ Uses stretch, which can be used to detect normal force	✗ Repeatable and stable, no indication of hysteresis	✓ Drapable and flexible in more than one dimension (have same characteristics as a textile), thin (55 mm x 20 mm).	✓ Low cost, easily manufacturable (uses methods in-line with industry textile manufacturing methods)
Huang, Tang, & Shen, 2006	✓ Uses elongation, which can be used to detect normal force	✗ LAUDIC wrap yarn stable and repeatable vs. the Single wrap yarn with a standard deviatino of 0.0056 vs. 0.139 , no indication of hysteresis	✓ Yarn-based sensors found to be more comfortable than even textile-based sensors, flexible in multiple dimensions	✓ Can be easily fabricated by conventional textile processes, low-cost
Wang et al., 2011	✓ Uses stretch to detect normal force	✓ Repeatable and stable resistance and pressure data obtained after 100,000 pressure cycle, small hysteresis	✓ Fabric pressure sensors measured 10 mm x 16 mm x 4.8 mm(low profile),	✗ Not a traditional textile manufacturing procedure - requires molding, ovens, etc to manufacture the sensing element
Gioberto et al., 2012	✓ Can use stretch to detect normal force	✓ Correlation coefficient of 0.83 in regards to resistance vs. load, indicating stability and repeatability. Hystersis area indicated as 12.63ohms (*Note hysteresis was measured differently than other examples shown)	✓ Low-profile, customizable length (length in study was 4.75"), comfortable (no hardware, made from soft goods), flexible in multiple directions	✓ Can be easily fabricated by conventional textile processes, low-cost
Harries & Pegg, 1989	✓ Can detect normal force to the body	✗ Characteristics of results not indicated. Not stable - difficulties associated with taking readings over curvature of body	✗ Characteristics of sensor not specified, but not thin, needed a stabilizer	✗ Sensor manufacturing techniques not specified in study
Hennig, Cavanagh, Albert, & Macmillan, 1982	✓ Can detect vertical pressure distributions	✓ Low hysteresis (less than 1%), less than 2% linearity (is stable/repeatable)	✓ 4.78mm square, 1.2mm thick lead zirconate titanate transducers embedded in 3-4mm thick layer of silicone, comfort of sensor unknown	✗ Flexible in several dimensions (not drapable though), no indication of how to implement into soft goods, unknown cost to manufacture
Lee et al., 2015	✓ Can detect normal force to the body	✓ A negligible hysteresis was observed, good stability , good repeatability (10,000 load cycle)	✓ Total area of 2 x 1.4 cm of sensor, Flexible in multiple directions, thin (uses conductive fibers), flexible/drapable	✓ Can be easily fabricated by conventional textile processes, low-cost
Merritt, Nagle, & Grant, 2009	✓ Can detect normal force to the body	✗ Has a hysteresis from the two layers rubbing together, linear response despite noise artefact	✗ Used capacitive sensors that were 60mm and 45 mm, various parts were nonstretchable but flexible in several dimensions, actual measurements not disclosed	✓ Inexpensive, Can be easily fabricated by conventional textile processes, flexible and drapable
Kotani et al., 2004	✓ Can detect normal force to the body	✓ R ² value of 0.9933, indicating high repeatability and stability. No hysteresis indicated	✓ Height, width, and thickness were 830 mm x 38.6 mm x 1.35 mm. Comfortable (made from fabric-based materials), flexible and drapable	✓ Can be easily fabricated by conventional textile processes, low-cost

Red sections indicate that the specific parameter of the sensor characterized in the study didn't meet the parameters outlined in Table 1, which indicate the requirements for the design of force-sensing devices to be implemented into a garment. Green sections indicate that they met the parameters, while the yellow sections indicate that they met most of the parameters save one aspect (i.e. not indicating a known hysteresis). One study of compression garments declared several key specifications for any pressure sensor that is to be used for measuring exact pressures under compression garments for medical purposes (Partsch et al., 2006). These specifications included that the sensor should be thin and flexible, should be adjustable in the sense that it can be optimized for different applications (such as the hand, leg, or feet) as well as measuring different "regimes" like for small areas for mapping a circumferential pressure pattern, large sensor areas, and for measuring the integral pressure of a larger area. The sensor should also be void of possible skin irritation if left against the skin for long periods of time, and the pressure measurement systems should allow continuous pressure measurement during passive or active movements. Finally, easy sensor calibration is desired, as well as multiple sensors which would allow concurrent measurement of pressures under the device at several anatomical sites (Partsch et al., 2006). Additionally, durability, reliability, overload tolerance, electronic simplicity, low cost, lost hysteresis, little creep, insensitive to temperature and humidity changes, and a linear response to applied pressure were preferred as well as the possibility for a variable sensor size.

Of the types of sensors that have the capability of detecting force, the only form in which a piezoelectric sensor could practically be implemented onto the body is in a thin-film form, but unfortunately this thin-film form has been proven to be unreliable and unstable (Zhou, Huang, & Yin, 2015). For this reason, piezoelectric sensors were omitted for selection for testing in this thesis. Similarly, due to the complexities in the fabrication and calibration of capacitive sensors, they also have been omitted. Tensile strain sensors are the most commonly-used force sensors in terms of their accuracy, size, and cost constraints (“How to Measure Pressure with Pressure Sensors,” 2012). While the focus of this work is on detecting normal forces, there are several ways in which a tensile strain sensor can be used to detect and measure normal forces.

The successful integration of a sensor into a garment to detect force is the driving force for this thesis. Designing a sensor with the characteristics defined in Table 1 is the first step. In addition to this, evaluating the sensor’s performance under varying conditions such as topography, curvature, and density of the substrate the sensor will be placed on, as well as evaluating the varying customizable features of the sensor such as length and width is important to understanding the performance limits of the sensor. Following this process, it is the intent of this thesis to determine a recommendation for a sensor that could be integrated into a garment to measure normal force exerted upon the body.

III. Experiment 1: Sensor Type, Substrate, Topography, & Thickness

A. Method

The ability to detect force being exerted onto the body is required for many situations in both industrial and terrestrial applications as well as in space. There are challenges, however, associated with this capability. The human body isn't static (which is the perfect condition for most sensors, and the type of condition for which they are designed for). The sensor that would be integrated into a garment to be worn on the body would require the ability to flex, drape in line with the fabric, be compact so as not to be obstructive, as well as being cost effective. In addition to these, it would also need to be responsive and accurate.

An initial exploratory test was conducted following a literature review of potential sensors with the potential for detecting force exerted on the body. This exploratory test preceded "experiment 1", which used the results from the initial exploratory test for sensor selection. The primary criteria for the sensor was to be cost effective, flexible, and produce responsive, promising, and accurate results (as outlined in Table 1). The sensors that were tested during this initial exploratory test were a 2.5" Pressure sensor (manufactured by Flexiforce), a 1.75" pressure sensor (manufactured by Flexiforce), a 3" flex sensor (manufactured by Spectra Symbol, Salt Lake City, UT, and a 4.5" custom coverstitch sensor (manufactured in a similar manner as the one analyzed in the study by Gioberto, et al., but used a bottom layer instead of a top layer stitch). The sensors were placed on a flat surface, and their resistance was measured following the placement of a 0.35 lb weight

(which was loaded off and on 5 times in 30 second intervals). The results are as follows with standard deviation of each sensor:

Table 3. Resistance Readings of Sensors (in OHMS) for Each Loading Cycle with Standard Deviation

	Pressure Sensor (2.5'')	Pressure Sensor (1.75'')	Coverstitch Sensor (4.5'')	Flex Sensor (3'')
Test 1	13	10.4	104.7	24.32
Test 2	14.2	11.6	104.81	24.33
Test 3	13.7	11.01	104.5	24.39
Test 4	13.2	11.6	104.9	24.36
Test 5	13.7	10.1	104.5	24.34
Standard Deviation	0.47	0.68	0.18	0.03

These preliminary results indicated that the 2.5'' and 1.75'' pressure sensors were less consistent and repeatable than the 4.5'' coverstitched stretch sensor and the 3'' flex sensor based on their standard deviation (Table 3). The pressure sensors (the 2.4'' and the 1.75'') were eliminated from the next portion of experimentation, which was designated as “experiment 1”. Repeatability was one requirement outlined in Table 1.

Following the analysis of the results of this initial exploratory test, further testing of the flex sensor and the custom coverstitched stretch sensor (Experiment 1) was then conducted. This portion of the thesis’ purpose was to determine which of these two sensors would be used moving forward based on their effectiveness in sensing normal forces when a substrate material of varying topography was placed beneath the sensor to enable normal

force sensing. The substrate material was used to allow the sensor to experience more deformation from normal force than if it were placed on a rigid surface (see Figure 1). The intent for this portion of the thesis was to analyze sensor performance more precisely and evaluate the independent variables of sensor type, supporting structure properties, topography of supporting structure, and supporting structure thickness. A hypothesis was formed following the initial exploratory test and literature review, which consisted of:

H1a. The coverstitched stretch sensor will respond to force being exerted upon it in a more repeatable manner than the flex Sensor as measured by the correlation between applied load and resistance response

H1b. Using a denser substrate material under the sensors will allow force to be sensed in a more repeatable manner than a less-dense substrate material

H1c. Using a substrate material that is thicker under the sensor will improve the repeatability of the sensor

H1d. A curved substrate material will have greater repeatability vs. a squared flat substrate material.

The coverstitched stretch sensor as well as the flex sensor were investigated in more depth, due their sensitivity and ability to respond repeatedly to pressure, and to conform effectively to flat, curved, and compressible surfaces (Figure 2), which could be used to aid in the transformation of normal force into flex and elongation strain. The independent variables during phase 2 were sensor type, supporting structure properties, topography of supporting structure, and supporting structure thickness.

The flex sensor (manufactured by Spectra Symbol, Salt Lake City, UT) is a flexible resistor measuring 112.25mm x 6.25mm x 0.43mm that increases resistance with flexion increased angle (Figure 1 & 3). When the metal pads bend and separate from one another, the resistance increases in the flex sensor. It is manufactured on a single thin flexible plastic substrate coated with metal piezoresistive elements. It is flexible in one direction, but since it takes a very narrow strip shape, it allows flexion of the supporting substrate in the orthogonal direction. It is made of a flexible plastic (which requires adhesion or another method of integration with soft goods), and has easily accessible solderable leads. It is stiffer than most textile fabrics but flexible enough to conform to many body surface and joint curves. The flex sensor is relatively low cost (less than \$13.00 per unit), and has a proposed long life cycle (>1 million). It has the potential to detect force normal to the body surface (through a conversion layer as previously discussed), and is stable, repeatable, and has been known to have a negligible hysteresis (Saggio, Riillo, Sbernini, & Quitadamo, 2016).

The coverstitched stretch sensor is a custom sensor manufactured made using a Juki MF-7723 high-speed, flat-bed coverstitch machine with conductive silver-plated Nylon 4-235/34 dtex 4-ply sewing thread purchased from Shieldex (Figure 4) stitched onto a fabric (for this study a 98% polyester 2% lycra knit fabric was chosen, which allowed the sensor to stretch relatively unhindered due to the properties of the knit). The dimensions of the coverstitched sensor vary due to its ability to be fabricated in any length, but based on the limitations of the Juki MF-7723, it can be manufactured in 3/16'' and 1/4''-widths. The conductive thread can be easily integrated into soft goods, since the thread can be used in

most standard sewing machines. In addition, depending on the material to which the conductive thread is stitched to (such as elastomeric knits), it can be repeatable, stable, and have a low hysteresis (Gioberto & Dunne, 2012).

The substrate material to which the sensors were attached to included a 100% high-density white polyurethane batting and a 100% densified green polyester foam. The samples included “squared” and “curved” samples, measuring in 1”, 3/5”, and 1/2” thicknesses (with final measurements of the sensor + batting combination at 4”x2.5”x1”, 4”x2.5”.75” and 4”x2.5”x.5”). The curved pieces were less obtrusive than the squared samples, but manufacturing specific rounded shapes in various foams was somewhat challenging (but could be refined with a different manufacturing process--scissors were the primary tool used to shave the foam into the desired rounded shape, as seen in Figure 4 & 5). The densified green polyester foam was easier to form into a specific shape and adhered better to the attached sensor to it due to its dense composition. The high-density polyurethane foam had stray fibers that were somewhat abrasive and shed from the sample, leaving a bit of a white fibrous residue wherever it was placed. It was also less dense than the densified polyester foam, making it more difficult to adhere a sample onto since there were less uniform anchoring points for the stitches, and the fibers that composed the batting were considerably looser, potentially leading to a slightly less secure sensor than the polyester foam. The densified polyester foam had greater recovery in terms of shape; it sprang back to its original shape quicker than the high-density polyurethane batting. The densified polyester had somewhat more resistance to being compressed, bent, or twisted than the high-density polyurethane batting, though both were flexible in all directions.

B. Sample Characteristics

The desired performance characteristics of the sensors that were chosen included requirements as outlined in Table 1, which include repeatability of sensor response, flexibility, cost-effectiveness, comfortable, simple mechanical integration, thickness of sensor, as well as having the ability to detect normal force. The properties of strain gauges could potentially allow for the deformation of the material to be converted into the normal force that is being applied.

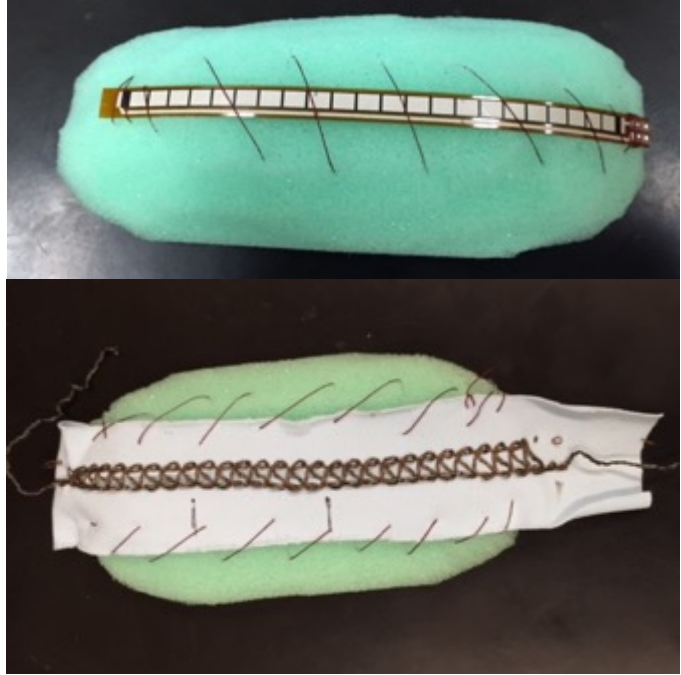


Figure 2. Attaching the Sensors to the Foam with Baste Stitches

Accentuating that deformation could potentially allow for a broader range of normal force ranges being applied. For this reason, supporting structures of various thicknesses and topography were chosen. The goal was not to characterize the sensor, but rather to characterize effect of the substrate material on the sensor response. Two supporting structures were chosen for their soft, semi-dense composition and accessibility. The variables that were tested in the experiment 1 investigation were sensor type (flex sensor vs. coverstitch sensor), supporting substrate material (high-density 100% polyurethane batting vs. densified compressed 100% polyester foam), supporting substrate thickness ($1/2''$, $3/4''$, and $1''$), and supporting substrate topography (squared vs. curved). These variables are outlined in Table 4. A dense

substrate with the ability to retain its shape while also being pliable was important in the material selection. It is necessary for the sensor to be flush against the garment, with little obstruction to prevent accidental triggering (or “noise”) of the sensor, as well as snagging and noticeability of the user, which is why substrate thickness was added as a variable; if a sensor can display similar response between a $\frac{1}{2}$ ” and a 1” thick material, a $\frac{1}{2}$ ” thick substrate would be ideal in the final selection for garment integration. The topography of the substrate was also explored due to the desire to have a shape that has few sharp corners and edges that could get caught or snag. A smooth, curved surface would minimize this risk. Densified 100% polyester foam and high-density 100% polyurethane batting were used for the tests. 1”, $\frac{3}{4}$ ” and $\frac{1}{2}$ ” thicknesses were tested for the high-density polyurethane batting and the densified 100% polyester foam. In addition to the square 4”x2.5”x1”, 4”x2.5”, .75” and 4”x2.5”x.5” samples, the high-density polyurethane batting and densified polyester foam also featured a set of samples that were rounded and curved pieces in 1”, $\frac{3}{4}$ ”, and $\frac{1}{2}$ ” thicknesses. The samples were adhered to the foam by baste stitching the sensor onto the foam (Figure 4). The flexibility of the coverstitched sensor adhered to a substrate material was limited to the properties of the foam and batting (which weren’t as elastic as the coverstitch sensor), but the flex sensor didn’t physically appear to be less flexible after being adhered to substrates. The flexibility of the coverstitch sensor and flex sensor were comparable after being adhered to the substrate, though the coverstitch sensor had less resistance to being adhered to the substrate material (i.e. return to it’s original form) than the flex sensor. The coverstitch sensor was also softer and less abrasive than the flex sensor after being adhered to the substrate.

C. Data Collection

The resistance response of the two sensors under variable loads normal to the sensor surface and in the testing conditions outlined in Table 4 was evaluated using an Instron tensile tester. For this particular test, compressive force (load), was applied by placing a sample (sensor plus “conversion layer” or supporting structure) on the Instron’s testing plate. The testing plate was covered with an acrylic structure base, and was compressed by the Instron machine, starting with a 1.25” gap between the Instron load mechanism and the rigid acrylic structure base (as illustrated in Figure 6). The Instron load mechanism loaded downwards onto the sample, moving 1” from its 1.25” initial start point, returning to its original starting point of 1.25”. This procedure was repeated 10 times in each trial. The 1.25” gap was used for the starting point for all samples, regardless of the thickness of the sample, such that the load mechanism did not contact any sample at the beginning of the test. The sensor’s resistance was measured using a Fluke 8845A 6.5 Digit Precision Multimeter. The test setup consisted of adhering the various foam samples with 1” x 3” long sticky back Velcro® strips to the Instron testing plate and the bottom of the samples (illustrated in Figure 5) to prevent the samples from shifting during pressure testing procedures. The sampling frequency of the Instron was recorded at 10.0Hz, while the DMM was recorded at 3.3Hz. The data were down-sampled using digital timestamps from both instruments, and manually aligned prior to analysis.

Each of 14 experimental setups (see Table 4) were evaluated. For each setup, 5 iterations of a 10-cycle loading pattern were performed. The setups were as follows: 1.) coverstitched sensor, no support structure, 2.) flex sensor, no support structure, 3.) coverstitched sensor,

Table 4. Coverstitched & Flex Sensor Test Parameters

Foam Thickness (Inches)	Coverstitched & Flex Sensor Tests			
	High-Density Green Foam		Densified White Foam	
	Curved	Squared	Curved	Squared
½"	5 Trials	5 Trials	5 Trials	5 Trials
¾"	5 Trials	5 Trials	5 Trials	5 Trials
1"	5 Trials	5 Trials	5 Trials	5 Trials

support structure, 14.) flex sensor, 1/2" densified compressed 100% polyester foam support structure.

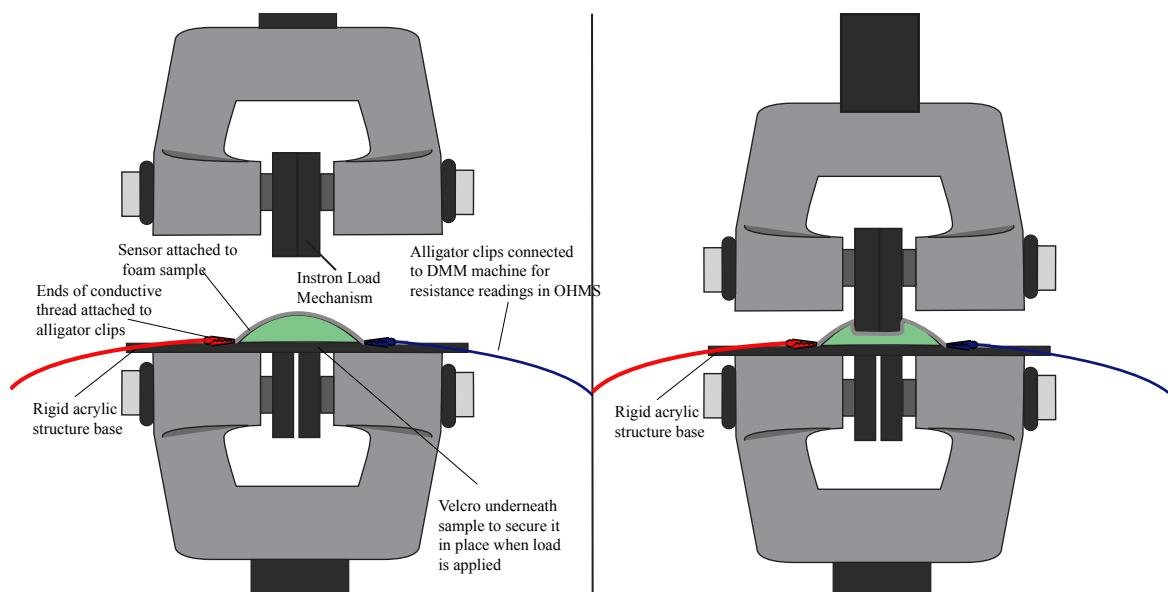


Figure 4. Instron Unloaded (left) and Loaded (right) Sample

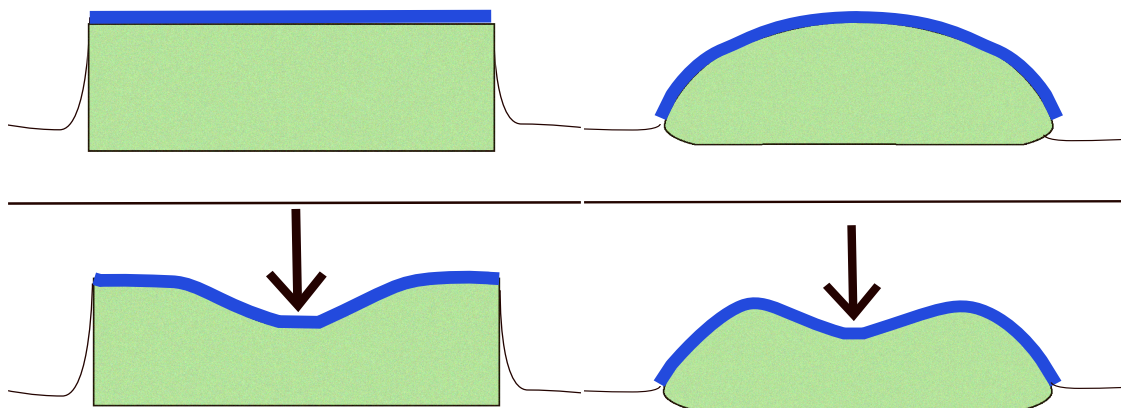


Figure 5. Squared Foam Topography. Relaxed vs. Depressed Sensor

Figure 6. Curved Foam Topography. Relaxed vs. Depressed Sensor

1. Analysis

The coverstitched stretch sensor and the flex sensor resistance responses were compared in each test to the load data captured by the Instron by visual analysis as well as by performing a linear regression between the datasets for each test. The linear regression was used as a metric to determine how repeatable and consistent the sensor's responses were because it provides an idea of the relationship between the variables (i.e. 0.1 signifies a weak relationship, and 0.9 indicates a strong relationship). The coefficient of determination (r-sq) was calculated for each test and mean and standard deviation of these coefficients was calculated for each test condition.

2. Results

The mean r-sq coefficients of the 14 test conditions are shown below (Figure 9). Example raw data traces of load (red line) and resistance (blue line) for each test condition are shown in Figure 10, as well as scatter-plot data of the applied load (lbf) vs. sensor output (resistance) shown in Figure 11.

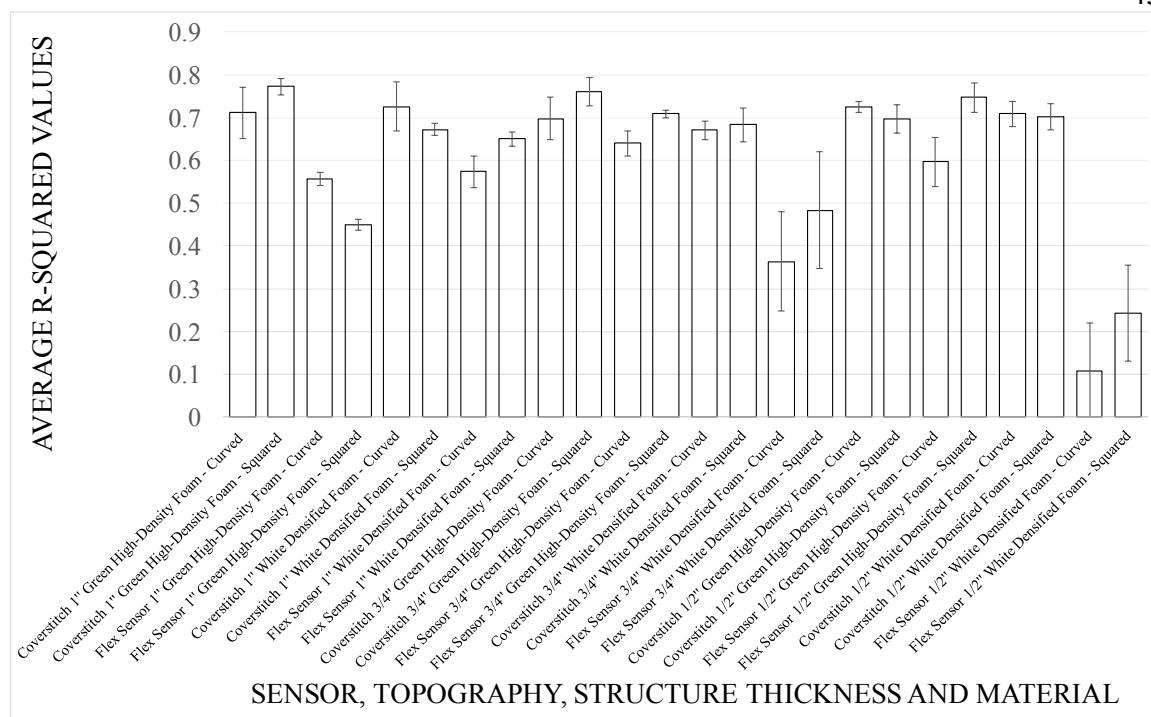


Figure 7. Mean R-square Coefficients of Sensor, Topography, Structure Thickness, & Material

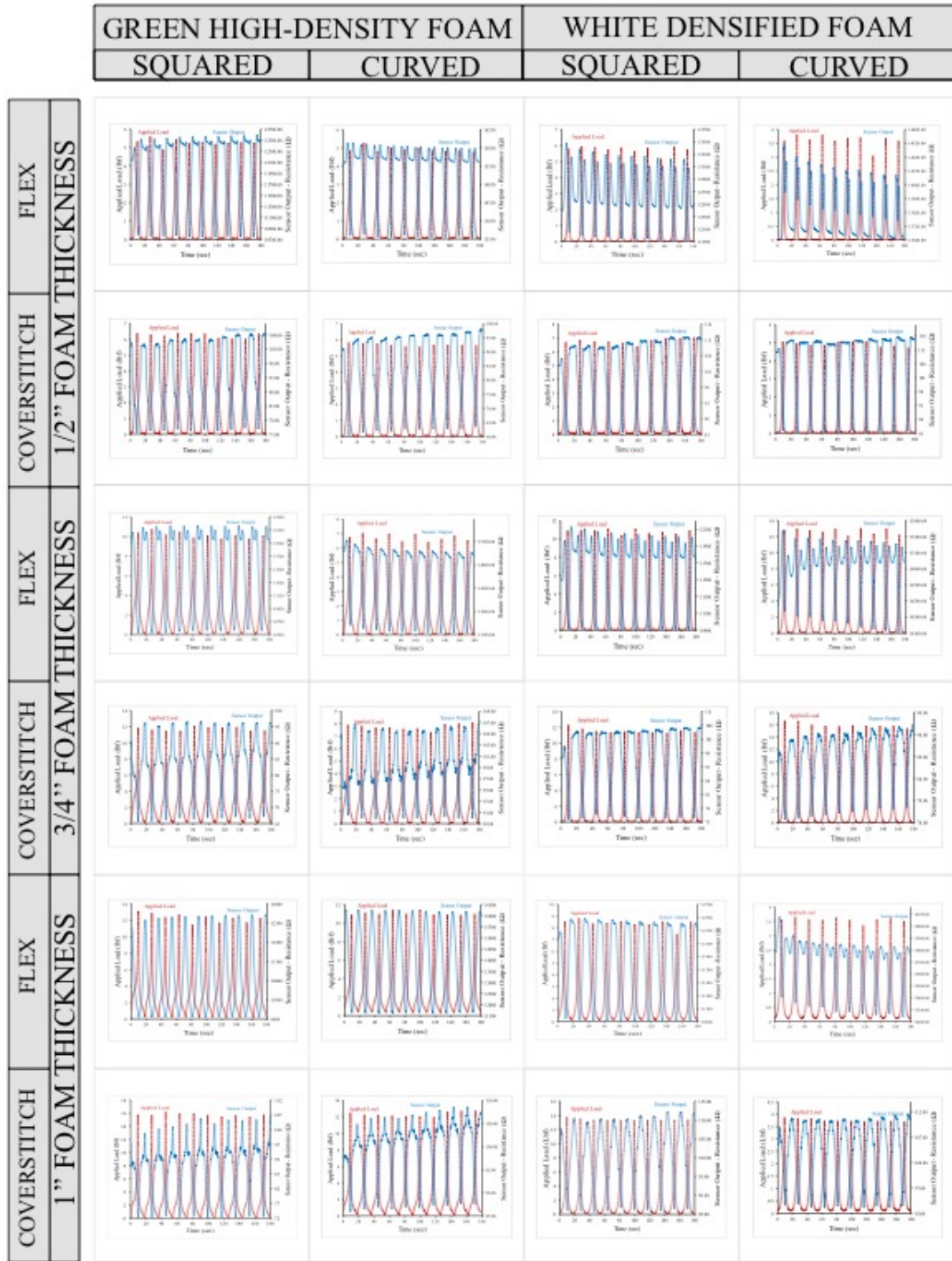


Figure 8. Raw Data Traces of Load (red line) and Resistance (blue line) for Each Test Condition

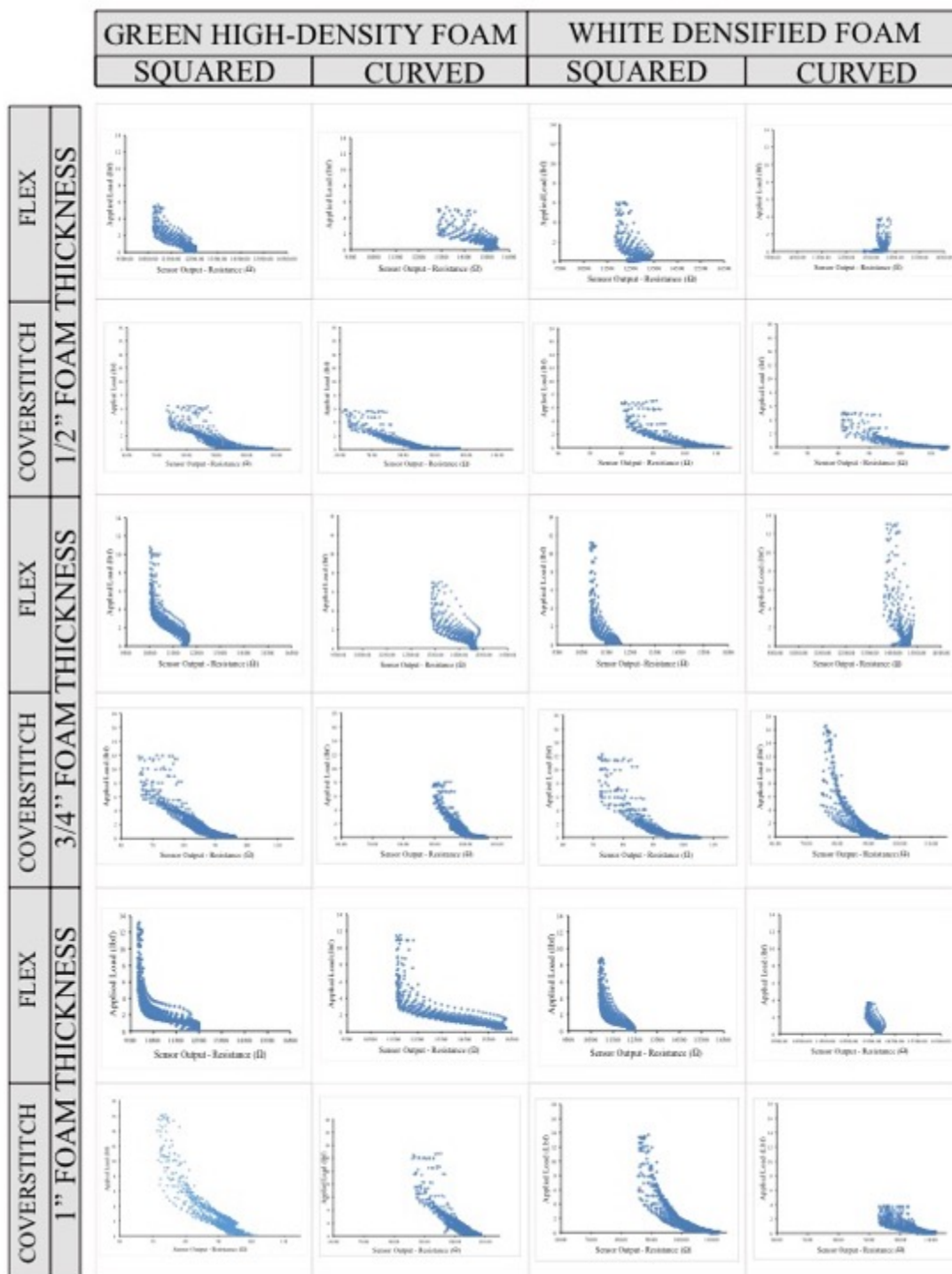


Figure 9. Scatter Plot - Applied Load vs. Resistance

Table 5. Mean R-square Values for the Coverstitch & Flex Sensor Tests

Foam Thickness (Inches)	Coverstitched & Flex Sensor Tests							
	High-Density Polyester Green Foam				Densified Polyurethane White Batting			
	Curved		Squared		Curved		Squared	
	Flex Sensor	Coverstitched Sensor	Flex Sensor	Coverstitched Sensor	Flex Sensor	Coverstitched Sensor	Flex Sensor	Coverstitched Sensor
½"	0.60	0.72	0.75	0.70	0.11	0.71	0.24	0.70
¾"	0.64	0.70	0.71	0.76	0.36	0.67	0.48	0.68
1"	0.56	0.71	0.45	0.77	0.57	0.72	0.65	0.67

E. Discussion

Varying results were observed for each independent variable, as discussed below.

1. Sensor Type

The coverstitched stretch sensor was visually more consistent and linear in the resistance readings as compared to the load applied. Its resistance response followed the load graph line visually and appeared to be more predictable, whereas the flex sensor appeared to deviate slightly and was more erratic. This supports the hypothesis H1a, which was that the coverstitch stretch sensor will respond to force being exerted upon it in a more repeatable manner than the flex sensor in correlation with applied load and resistance response. The flex sensor exhibited a considerable amount of “noise”, particularly evident in the recovery artifact that is observed when the load is removed from the flex sensor (Figure 10). The r-squared correlation coefficient values of both the coverstitched stretch sensor (with an average of 0.71 r-sq value across all coverstitched stretch sensor conditions) and the flex sensor (with an average of 0.51 r-sq value across all flex sensor conditions) support this visual analysis. A higher r-sq value indicates a closer relationship

between applied force and sensor response. The coverstitched stretch sensor's values were relatively consistent between testing conditions and had smaller standard deviation over all conditions (0.03), whereas the flex sensor, despite having one promising r-squared value, had an average standard deviation over all flex sensor conditions of 0.06. Additionally, the actual r-sq values vary drastically from one condition to another in the flex sensor (Table 5). The one promising r-squared value from the flex sensor, however, displays a considerable drift when the full load is exerted on the sensor, as well as a significant amount of recovery artifact when the load is fully removed from the sensor. However, the coverstitched sensor experienced a slight drift as well during the full load portion of the pressure testing based on a non-quantitative analysis of drift (Figure 10). The flex sensor visually appears to be less linear than the coverstitched stretch sensor in terms of the correlation between the force being applied and the sensor's resistance. The flex sensor readings appear to be erratic in terms of spontaneous jumps in the readings as compared to the coverstitched sensor, which is more consistent and has a more linear response.

2. Supporting structure - Density

Characterization of the coverstitched sensor indicates that the sensor response is influenced by the mechanical properties of the material to which it is attached to (Gioberto & Dunne, 2012). The sensor appeared to be reliable and repeatable, particularly paired with textiles with elastomeric fibers. The flex sensor performance without a supporting structure indicated repeatability based on previous research as well as this thesis' initial exploratory testing. The flex sensor appeared to respond with an increase in "noise"/recovery artifact when paired with the white densified 100% polyurethane batting, which is less dense in

structure than the high-density 100% polyester foam (Figure 10), as evident in the given r-sq value of 0.62 over the average of all flex sensors paired with 100% polyester foam vs. the r-sq value of 0.40 over the average of all flex sensors paired with the 100% polyurethane batting.

The average r-sq value for all of the 1'' white 100% polyurethane batting samples was 0.66, which is the only instance in which the average r-sq value for the white 100% polyurethane batting outperformed the average r-sq value for the green 100% polyester foam (Table 4). It also appeared based on visual analysis that the densified white 100% polyurethane batting experienced more hysteresis in recovery, failing to retain its form as well as the high-density 100% polyurethane batting. It should be noted, however, that it is difficult to dissociate the sensor response from the supporting structure response. Likewise, the white densified compressed 100% polyurethane batting appeared to lose its shape after extended cycles (in one set of graphs, particularly for the flex sensor, the drift moves “upward” for the green high-density foam in most trials, but the same tests done for the white densified foam, the drift goes downwards in most trials. This was most apparent on the ½'' samples.) The hypothesis H1b was that using a denser substrate material under the sensors would allow force to be sensed in a more repeatable manner vs. a less-dense substrate material. This hypothesis derived from the notion that a material that is less dense is more likely to reach “saturation”, or its limit, much quicker than a more-dense material. It was also based on the assumption that the less-dense material would be more porous and irregular in density/internal shape, which would translate to an irregular movement under mechanical loading, which would correspond to an irregular response in resistance of the

sensor. This idea is somewhat supported in the r-sq value results (except for the 1'' samples, in which the white polyurethane batting appeared to be more consistent in responsiveness).

3. Supporting structure - Topography

Topography of supporting structure (curved vs. squared/flat) affected the sensor response differently for each sensor type. There were no substantial differences observed between the coverstitched sensor based on topography of the supporting structure (the average r-sq value for the coverstitched sensor with the squared topography was 0.71, with the average r-sq value for the coverstitched sensor with the curved topography being 0.71, as well). See table below. Visually, the curved foam and batting samples as a whole displayed greater repeatability than the square foam and batting samples (Figures 10). This somewhat supports hypothesis H1d., which states that a curved substrate material will have greater repeatability vs. a squared sample, but not strongly due to some contrary r-sq values not displaying a substantial difference.

The flex sensor may have been more responsive to the curved topography vs. the squared topography due to the nature of the flex sensor themselves; they bend in one direction based on the thin film plastic materials they are manufactured, vs. the coverstitched sensor which can bend in both the x and y direction. For the curved topography, the sensor is in a slightly bent position when applied over the curve, and when the Instron testing machine puts a load upon the flex sensor, it bends inward at a greater flex than would be capable if it were attached to a flat (or in this instance, "squared") surface. Moving forward, despite the squared topography samples exhibiting only a slightly

higher average r-sq value than the curved topography samples (0.59 vs. 0.63), it would be advised to further explore variances in topography due to the visually even and linear responses from the curved topography samples. Additionally, it appeared that the thicker the supporting structure paired with a curved topography, the better the average r-sq value was. Based on these results, it would be advised to further explore a type of topography that has further variances in the thickness of the substrate material and/or topography. The thickness could be providing the sensors further ability to stretch and/or flex, which allows for a further range of resistance changes and responses.

4. Supporting structure - Thickness

Supporting structure thickness also affected the results slightly. The 1'' thick high-density 100% polyurethane batting samples appeared to have the highest r-sq value of 0.62 over all of the 1'' high-density 100% polyurethane batting samples, which can be translated to more favorable performance, particularly with the coverstitched stretch sensor samples (which had an average r-sq value of 0.74 over all of the 1'' high-density 100% polyurethane batting samples paired with a coverstitched stretch sensor vs. the r-sq value of 0.50 over all of the 1'' high-density 100% polyurethane batting samples paired with a flex sensor) (Table 5). The hypothesis H1c indicated that using a thicker material under the sensor would improve the repeatability of the sensor, which is supported by the r-sq values. The average r-sq value for all of the 1''-thick samples was 0.64. The average r-sq value for all of the $\frac{3}{4}$ ''-thick samples was 0.63. The average r-sq value for all of the $\frac{1}{2}$ ''-thick samples was 0.57. It appears that the thicker the substrate material, the higher the average r-sq value over all of the samples tested, however the difference between the 1'' and $\frac{1}{2}$ '' samples is

minimal. The ½” high-density 100% polyurethane batting samples had small irregularities appear in visual analysis of the graphs (Figure 10). Since the sensors’ responses to constant load were not evaluated in this test, differences in responses to constant load may affect the results. Both the flex sensor and the coverstitched sensor experienced a considerable amount of drift during the full-load portion of the ½” high-density foam tests (Figure 10).

5. Conclusion

Moving forward, the coverstitched stretch sensor appears to be a viable option for further exploration, particularly paired with the thicker supporting structures. The coverstitched stretch sensor could provide flexibility needed when paired with a bendable “squishy” support structure, which was a limitation on several studies that focused on measuring pressure in a garment, such as the soft open-cell foam study example conducted by Brady, et. al (2005). Additionally, the manufacturability of the coverstitched sensor is extremely promising. Manufacturability of the sensor would allow for the sensor to be implemented into a standard textile manufacturing process. One requirement from Table 1 was simple mechanical integration with soft goods. The sensors that were reviewed in the literature review (as well as being outlined in Table 2) had varied levels of difficulty in integration into soft goods. The coverstitched sensor had an advantage over the flex sensor as well as most of the other sensors reviewed in the literature review in regards to this parameter, as it can be made with easily-accessible equipment, whereas the flex sensor (as well as several of the other sensors highlighted in Table 2) would require some sort of adhesive, molding, or layering process to be attached to a textile (adding to complexity and cost). Adhesive methods also raise durability concerns, unlike the coverstitch sensor which

is directly sewn onto the textile. For both sensors investigated here, evaluating exposure to longer periods of fatigue and sweat would need to be further explored and characterized prior to field use.

An additional parameter outlined in Table 1 pertained to the mechanical properties of the sensor. These mechanical properties include the ability of the sensor to be flexible in more than one dimension, to be comfortable, and thin. The thinnest substrate material was $\frac{1}{2}$ ", for which a squared polyester green foam paired with a flex sensor appeared to have the greatest repeatability (r-sq value is 0.75), with the coverstitched sensor paired with a curved $\frac{1}{2}$ " polyester green foam piece close behind with an r-sq value at 0.72. The coverstitched sensor has an advantage over the flex sensor in regards to being comfortable to the user due to its greater flexibility, however, it is also easier to manufacture and to attach to the substrate material. The thin plastic substrate material that the flex sensor is manufactured in can be sharp and uncomfortable against the skin, and doesn't have the same radius of bending that the coverstitch sensor has. The bend of the flex sensor plus substrate material assembly was limited by the properties of the flex sensor. The coverstitched sensor has a minimal effect on the stiffness and other mechanical properties of the textile or foam that it is sewn onto, unlike the flex sensor which is considerably stiffer than most textiles. The flex sensor also has limits in its physical size and shape based on the availability of the manufacturer. The coverstitched sensor, however, is completely customizable and can be manufactured to many different specifications. The repeatability of the coverstitched sensor also seemed relatively unchanged across all thicknesses (lowest r-sq value = 0.67, highest r-sq value = 0.77), unlike the flex sensor which had a broader

and more extreme range of r-sq values across all thicknesses (lowest r-sq value = 0.11, highest r-sq value = 0.75), further reinforcing the idea of the coverstitched sensor's customizability and adaptability to various specifications (such as substrate thickness). The elastic properties of the stiffer flex sensor also result in resistance to bending forces, which might result in inaccurate sensor responses in loosely-fitted garments or under very small loads as compared to the less-elastic textile-based coverstitched sensor.

There were several limitations to this study. The first limitations for this particular test revolve around the use of only two types of structure, material, density types, as well as being unable to dissociate the sensor from the supporting structure itself. For further testing it would be suggested to use varying materials, particularly an elastomeric material. The softness or hardness ("Shore hardness") of an elastomeric material can be tailored to a range of values. By being provided a specific Shore hardness for a specific elastomer, analyzing the effects of the supporting structure's hardness (or softness) on the sensor's accuracy could be more precisely determined by testing the sensor with a variety of elastomers with different Shore harnesses'. Additionally, creating an experimental set-up that would allow for dissociating the sensor from the supporting structure (as needed) to better analyze the effects of the supporting structure on the sensor itself would be advised. The thicknesses of the supporting structure was primarily dependent on the commercial availability of the foam or batting; the high-density 100% polyurethane batting is available in ½'' and 1'' thicknesses, where as the densified 100% polyester foam is only available in ½'' and ¾'' thickness. The foam was either cut down/shaved to reflect the availability of the other material (i.e. a 1'' piece of polyurethane batting was shaved down to ¾'' to

reflect the availability of a $\frac{3}{4}$ ''-thick polyester foam). Thicker material options were unavailable for the polyurethane batting. Alternative means of adhesion of the sensor to the supporting structure would also ideally be explored. Additionally, performing Instron tensile tests that don't fully load onto the samples (which was experienced for the $\frac{1}{2}$ '' samples) would provide more consistent testing conditions for comparison between thinner and thicker samples.

Due to the promising results demonstrated by the single-size coverstitched sensor used in this study, the coverstitched sensor was chosen moving forward for further testing to investigate variables of length and width of the sensor (which would allow the physical form of the sensor to be reduced and/or optimized) and how those variables affect the responsiveness of the sensor itself, and to further investigate the performance of this sensor when paired with varying supporting substrate mechanical properties and topographies. The ultimate goal of the sensor is to be integrated onto the body, which would require a relatively thin and compact sensor in order to be successful.

IV. Experiment 2: Coverstitch Length & Width Testing

a. Method

Determining the response and repeatability of a sensor is paramount when deciphering the appropriateness of implementing it into a garment, particularly if the sensor is to be used to detect normal force exerted on the body. The first experiment in this study analyzed the results of a coverstitched stretch sensor and a flex sensor over substrate material of varying topography and thickness. Based on these results, the coverstitched sensor indicated the most promise in regards to its repeatability, particularly over various substrate materials. The coverstitched stretch sensor was investigated in more depth for this next experiment. This investigation sought to investigate the effect of the length and width of the sensor on the sensor response to loading. The independent variables evaluated here were coverstitched stretch sensor width and coverstitched stretch sensor length. The following hypotheses were formed and were to be tested for the next experiment (“Experiment 2”) with this in mind:

H2a. Longer coverstitched sensors will be more repeatable than shorter coverstitched sensor

H2b. Thicker coverstitched sensors will be more repeatable than thinner coverstitched sensors

b. Sample Characteristics

The coverstitched stretch sensor used here was the same stretch sensor used in experiment 1. Two variations of the custom coverstitched stretch sensor were chosen (a “wide” width sample measuring $\frac{1}{4}$ ” in width and a “thin” width sample measuring $\frac{3}{16}$ ” in width (Figure 12) due to the intent of implementing the sensors into a garment in the

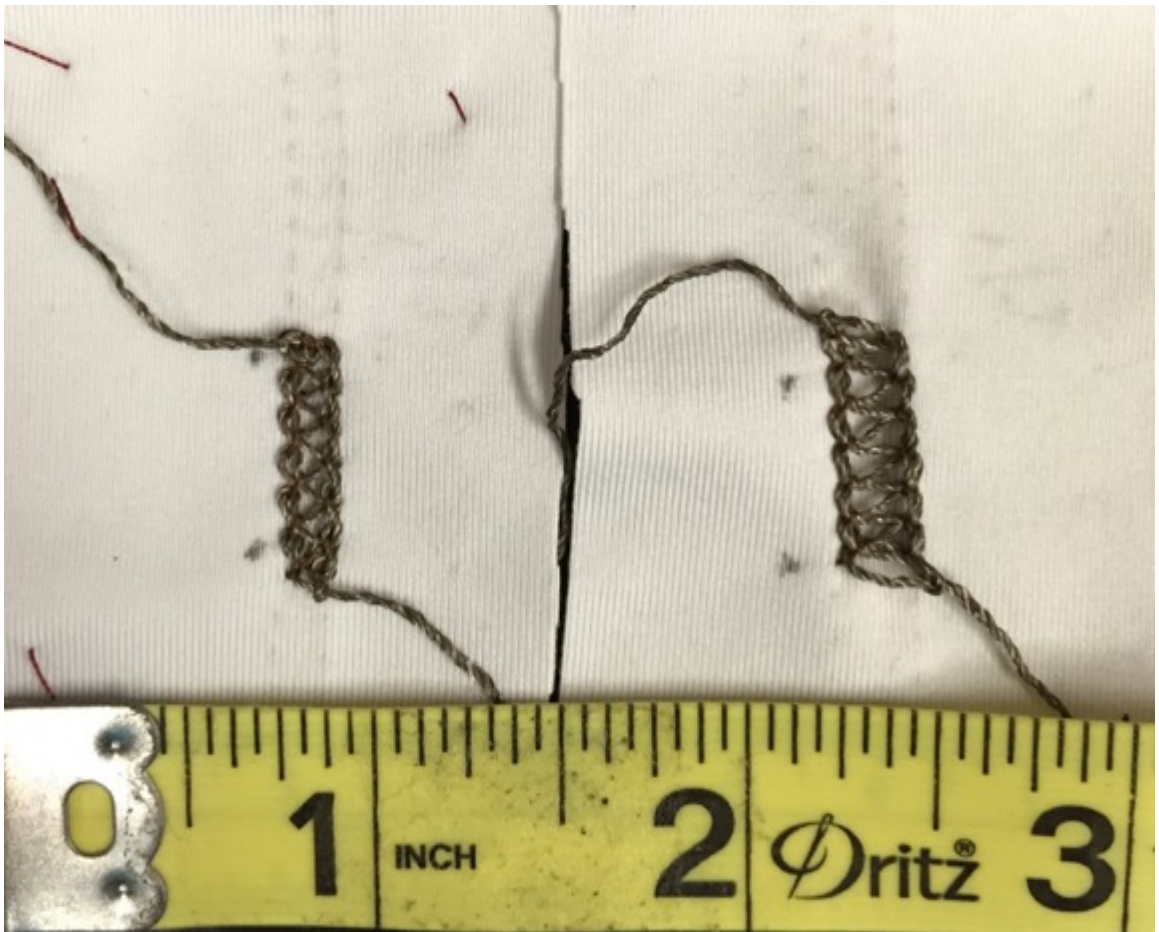


Figure 10. Coverstitched Stretch Sensor Thick ($\frac{1}{4}$ ") and Thin ($\frac{3}{16}$ ") Samples

future, and the need to verify the unexplored length and width variables and associated accuracy of the coverstitched stretch sensor width and lengths for manufacturing purposes. The Juki MF-7723 machine, a common type of coverstitch machine used in mass

manufacturing, has the ability to manufacture two stitch widths and unlimited stitch lengths. The conditions that were tested during experiment 2 were two sensor widths ($1/4''$ or 'thick' vs. $3/16''$ or 'thin') and 5 sensor lengths ($4''$, $3''$, $2''$, $1''$, $1/2''$) (Figure 13). The 100% polyester densified green foam was used as a support substrate for all tests. The samples were adhered to the foam by baste stitching as shown in Figure 14.

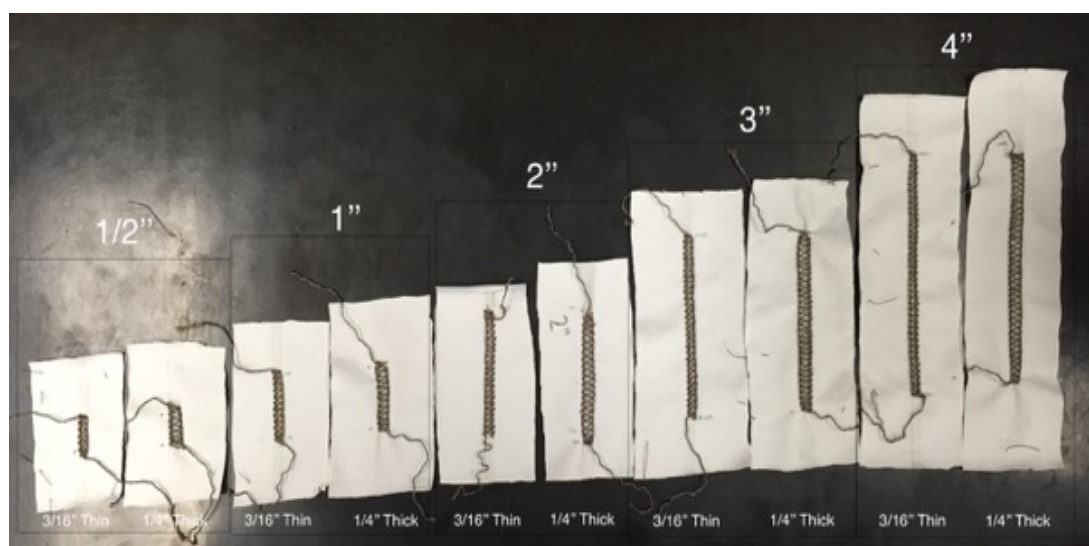


Figure 11. Coverstitched Stretch Sensor Length and Width Samples



Figure 12. Coverstitched Stretch Sensor Basted on 1/2" 100% Polyester Densified Foam**c. Data Collection**

Data were collected in the same manner as the previous test. The resistance response of the two sensors under variable loads and in the testing conditions outlined in Table 6 was evaluated using an Instron tensile tester. For this particular test, compression (load), was performed as illustrated in Figure 5, by placing a sample on the Instron's testing plate and having the other plate exert a load onto the sample 10 times in sequence and measuring the resistance. The data were down-sampled using digital timestamps from both instruments, and manually aligned prior to analysis.

Table 6. Coverstitch & Flex Sensor Test Parameters

Coverstitch Sensor Length (Inches)	Coverstitch Sensor Length & Width Tests	
	Thick Coverstitch Sensor (1/4")	Thin Coverstitch Sensor 3/16")
1/2"	5 Repetitions	5 Repetitions
1"	5 Repetitions	5 Repetitions
2"	5 Repetitions	5 Repetitions
3"	5 Repetitions	5 Repetitions
4"	5 Repetitions	5 Repetitions

d. Procedure

Each of 10 experimental setups (see Table 6) were evaluated. For each setup, 5 iterations of a 10-cycle loading pattern were performed. The setups were as follows: 1.) 1/4"-thick 1/2"-long coverstitched sensor, 2.) 3/16"-thin 1/2"-long coverstitched sensor, 3.) 1/4"-thick 1"-long coverstitched sensor, 4.) 3/16"-thin 1"-long coverstitched sensor, 5.) 1/4"-thick 2"-long coverstitched sensor, 6.) 3/16"-thin 2"-long coverstitched sensor, 7.)

$\frac{1}{4}$ ''-thick 3''-long coverstitched sensor, 8.) $\frac{3}{16}$ ''-thin 3''-long coverstitched sensor, 9.)

$\frac{1}{4}$ ''-thick 4''-long coverstitched sensor, 10.) $\frac{3}{16}$ ''-thin 4''-long coverstitched sensor.

i. Analysis

The coverstitched stretch sensor responses for length and width conditions were compared in each test to the load data captured by the Instron by visual analysis as well as by performing a linear regression between the datasets for each test, similar to the analysis from Experiment 1. The coefficient of determination (r-sq) was calculated for each test and mean and standard deviation of these coefficients was calculated for each test condition.

ii. Results

The mean r-sq coefficients of the 10 test conditions are shown below (Figure 15).

Example raw data traces of load (red line) and resistance (blue line) are shown in Figure 16, as well as scatter-plot data of the applied load (lbf) vs. sensor output (resistance) shown in Figure 17.

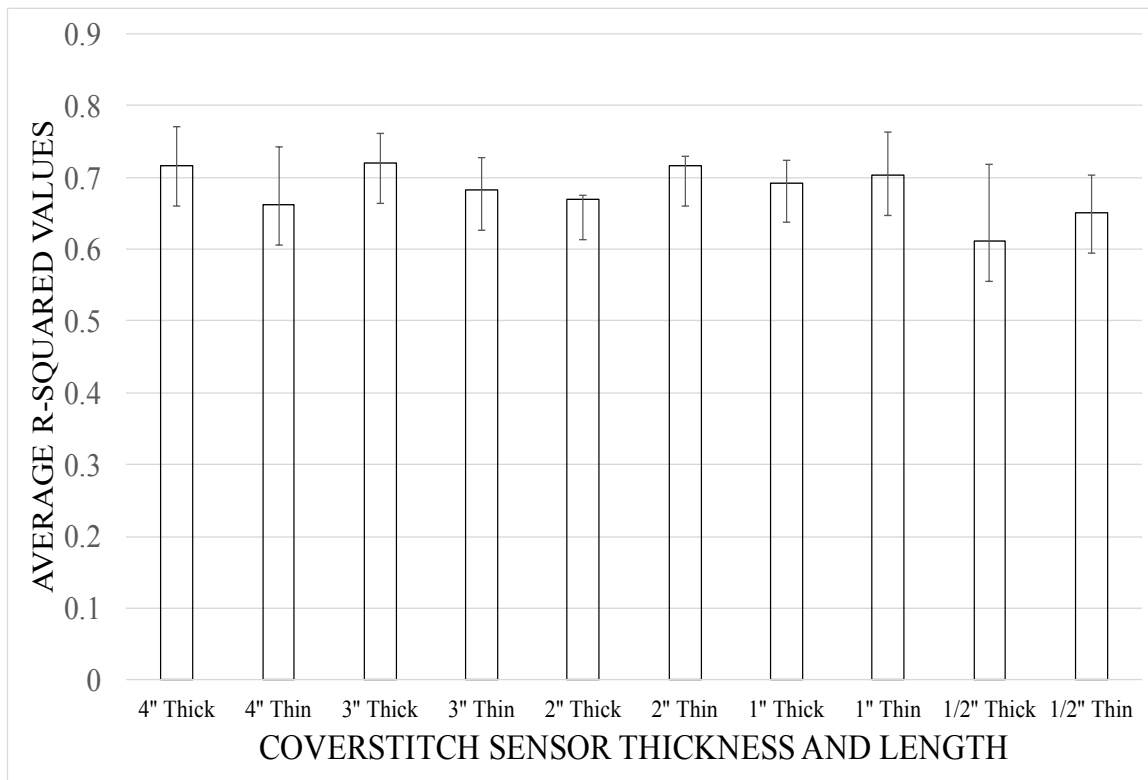


Figure 13. Coverstitched Sensor Width and Length Mean R-Sq Values

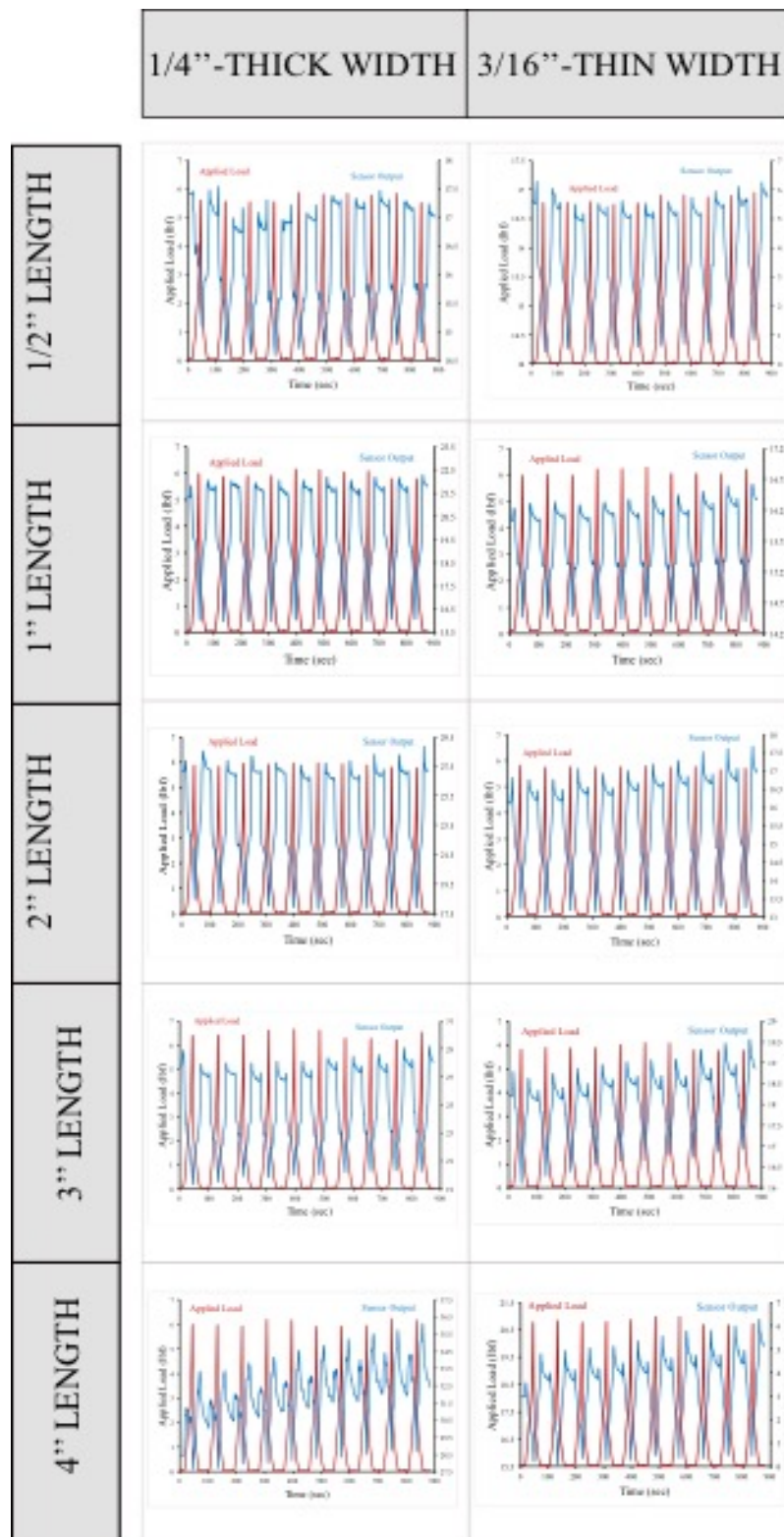


Figure 14. Raw data traces of load (red line) and Resistance (blue line)

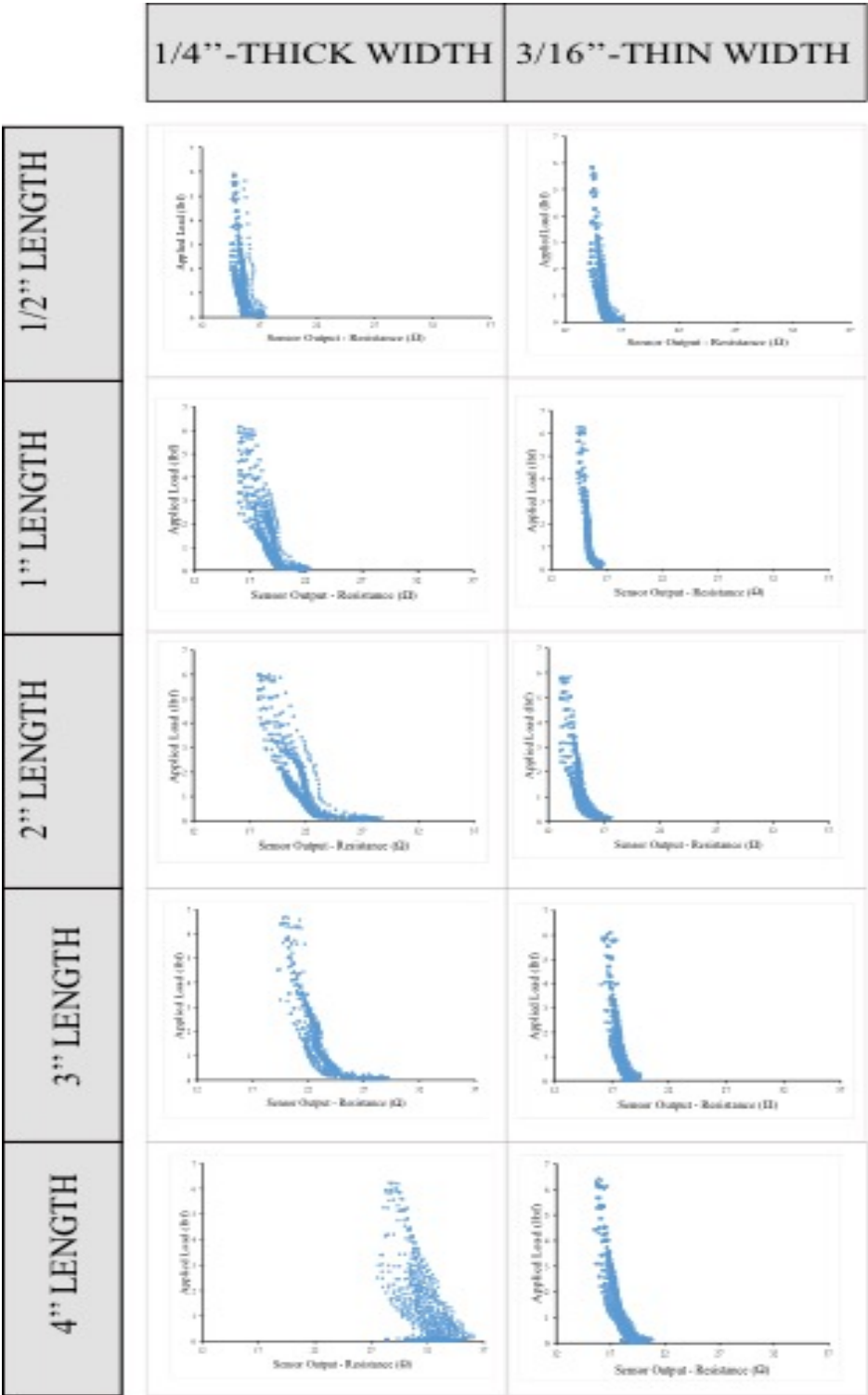


Figure 15. Scatter Plot - Applied Load vs. Resistance

Table 7. Mean R-Square Values for Coverstitched Sensor Length & Width

Coverstitched Sensor Length (Inches)	Coverstitched Sensor Length & Width Tests	
	Thick Coverstitched Sensor (¼'')	Thin Coverstitched Sensor 3/16'')
½''	0.61	0.65
1''	0.69	0.70
2''	0.69	0.72
3''	0.72	0.68
4''	0.62	0.66

e. Discussion

Varying results were observed for the sensor width and sensor length independent variable, as discussed below.

1. Sensor Width

The coverstitched stretch sensor responses across width conditions were comparable, with the thinner coverstitched stretch sensors having slightly more favorable r-sq values (0.68 average across all thin sensors) than the thicker coverstitched stretch sensors (0.68 average across all thick sensors) used. This does not support hypothesis H2b which states that thicker coverstitched sensors would be more repeatable than thinner coverstitched sensors. The 3'' thick coverstitched stretch sensor had the overall highest average r-sq value of 0.72, but had a standard deviation of 0.042. In terms of consistency, the 2'' thin coverstitched stretch sensor illustrated the most consistent responses, with an average r-sq value of 0.72 and a standard deviation of 0.01. Though comparable in terms of r-square values, the narrow coverstitched stretch sensor appeared

to have minimally more consistent responses as evidenced by r-sq values than the thicker counterpart.

2. Sensor Length

The hypothesis H2a which pertained to the sensor length predicted that the longer coverstitched sensors would be more repeatable than the shorter coverstitched sensors. There was no clear relationship, however, between sensor length and correlation between sensor response and applied load in the observed results. The 2'' coverstitched stretch sensor appeared to display the most consistent relationship, the lowest standard deviation of 0.01 and an average r-sq value of 0.69 across both the thick and thin 2'' coverstitched stretch sensors. The ½'' coverstitched stretch sensors had an average of 0.63 r-sq value, the 1'' had an r-sq average value of 0.70, the 3'' had an average r-sq value of 0.70, and the 4'' had an average r-sq value of 0.69. The ½'' stretch sensors had the weakest r-sq correlation with load, as well as the largest standard deviation, with the ½'' thick coverstitched stretch sensors having an average standard deviation of 0.11 and the thin ½'' coverstitch stretch sensor having an average standard deviation of 0.05. The 4'' coverstitched stretch sensor response had just slightly more reliable relationship to load than the ½'' stretch sensor, with an average r-sq value between the thick and thin 4'' coverstitched stretch sensors of 0.69 and the 4'' thin coverstitched stretch sensor having an average standard deviation of 0.08 and the 4'' thick coverstitched stretch sensor having an average standard deviation of 0.06. However, the lack of variance in repeatability amongst the sensor lengths allows more customization in the implementation of the coverstitch sensor. If the repeatability of the sensor response

varied based on the length of the sensor, then it could present limitations on placement and configuration of the sensor on the body.

3. Conclusion.

Based on the results, further exploration with the narrower coverstitched stretch sensor would be advised because that sensor showed better repeatability based on r -sq value. Additional suggestions would also be to vary the type of conductive thread used for the sensor, as well as varying the type of textile material the coverstitched stretch sensor was sewn onto (i.e. lycra, spandex, etc), and exploring different textile elasticity and stiffness to determine if there is a correlation between repeatability and load with concerns to sensor width and paired textile stiffness and elasticity. An appealing aspect of the coverstitched sensor is the cost, which is one parameter outlined in Table 1. The cost for the coverstitched sensor is still considerably less expensive than the other sensors outlined in Table 2. The primary cost for the coverstitched sensor is the conductive thread. Analyzing the various costs and effectiveness of the market-available conductive thread would further illuminate the cost range for the coverstitched sensor. A driving factor for most commercial textile businesses is the ability to manufacture inexpensively; if the cost for the main element used in this study could be varied without significant hindrance to the other important parameters from Table 1, then that should be explored. Additionally, some applications could afford certain variances in the repeatability, stability, and hysteresis of the sensor, which may correlate with cost. The coverstitched sensor showed promise in terms of sensing on-body by illustrating its ability to conform and perform well under variable conditions, particularly with variations in the sensor

length. Although the longer coverstitched sensor would be ideal in terms of physical form to sense on-body by covering a greater amount of area over the body, the shorter length coverstitch showed the most promise in terms of repeatability and accuracy, complimented with the narrow-width. The 2''-long coverstitch in the narrow 1/18''-width will be used moving forward with this investigation based on the repeatability of the results. It will be tested over urethane rubber and silicone substrate materials manufactured in various topographies. This length of the sensor (2''-long) attached to the polyester squared substrate material (4''x 2''x1'') is comparable (but still larger) to the majority of the sensors characterized in Table 2 and the literature review. Maintaining a low and discrete profile is an important aspect for the requirements of the mechanical properties of the sensor. Therefore, in order to be lower profile and discrete, the substrate material to which the sensor is adhered to should be minimized as much as possible in terms of the thickness, length, and width. The coverstitch sensor is customizable, so it can be manufactured to match the lower-profile and more discrete characteristics. The thinnest substrate used in this thesis was 1/2'' (with the thickest being 1''), and aside from the 3/4''-thick substrate, no other thicknesses were characterized. Further characterization of substrate thicknesses with the sensor would be recommended, particularly in regards to exploring thinner substrates less than 1/2''-thick to further generate a more discrete form with the sensor.

Limitations associated with this study include statistical limitations; in other words, only coarse statistical analysis of the correlation between the sensor response and the applied load was performed and there weren't many clear or obvious trends amongst the

sensor lengths. Further testing and quantitative evaluation of sensor performance parameters would be necessary to discover more clear or obvious trends in specific performance characteristics such as sensitivity, response range, drift, and hysteresis, or to validate the lack of correlation between repeatability and sensor length, as well as testing beyond the 4''-length sensor. Further evaluation of the shorter $\frac{1}{2}$ '' sensor under more optimal testing conditions procedure would also be advised, considering the experimental procedures used here relied on an Instron testing mechanism that may not have been suited well for testing the $\frac{1}{2}$ '' samples (i.e. the "clamps" for the Instron were larger than the $\frac{1}{2}$ '' sensors and extended past the sample size). Based on the current results, however, which demonstrate consistency in terms of average r-sq value and standard deviation, the 2'' narrow coverstitched stretch sensor would be suggested for use in future testing. The first and primary condition derived from Table 1 is the ability of the sensor to detect normal force. The coverstitched sensor's ability to detect normal force may be inhibited depending on the length to which it is manufactured, because of effects of length on the strain experienced by the sensor. This threshold needs to be established.

Additional limitations for this particular test pertained to the inability to explore beyond the two widths of coverstitched stretch sensor due to the manufacturing capabilities within the lab used to conduct the research for this thesis. It would be ideal to explore beyond just the two widths of coverstitched stretch sensor. Additionally, determining the maximum stretch of both the narrow and the wide coverstitched stretch sensor was not determined, which could play a factor when needed to implement the sensor into a garment that requires a variable amount of stretch. If the narrow coverstitched stretch

sensor is unable to accommodate the need to stretch a certain length within a garment, despite its potential to be more responsive and consistent than the wide coverstitched stretch sensor, it would not be a viable option due to this obvious handicap.

V. Experiment 3: Substrate Material & Topography

A. Method

Additional exploration with substrate material, rubber and silicone respectively, under a coverstitched stretch sensor w 3/16''-thin 2''-long coverstitched stretch sensor were investigated in more depth, due to the variable results indicated in the previous experiments by substrate materials, as well as results indicated by a study conducted by Wang et. al that utilized “tooth-like” substrate materials over a sensing element. The substrate structure in their study used “teeth” induce stretch in the sensing element when a normal force was applied, which in turn, caused a change in resistance. This experiment investigates the potential of using one layer of substrate material with a variable topography of hemispheres, which are placed under the sensor (which is sensitive to tensile strain). The underlying assumption is that the topography of the substrate material (hemispheres that protrude from the surface) may allow the sensing element (the coverstitched stretch sensor) to stretch further than it would if it were flat or supported by the simple support structures used in the previous experiments. A larger stretch would then result in an increased change in resistance when a normal force is applied. The 3/16''-thin 2''-long coverstitched stretch sensor was chosen based on the results of the previous experiment, because its resistance response showed the closest correlation with load and the lowest standard deviation between trials. The independent variables during this experiment were substrate material type, as well as a variation in diameter of the sphere size of the substrate material. The following hypotheses were formed and were to be tested for experiment 3:

H3a. Sensors over a larger-sphered substrate topography will have more repeatable responses than those a flatter substrate topography

H3b. Sensors over rubber substrates will have less repeatable responses than those over silicone substrates due to rubber's stronger elastomeric properties

B. Sample Characteristics

The custom coverstitched stretch sensor made using a Juki MF-7723 high-speed, flat-bed coverstitch machine with conductive thread was again used as the sensing element, (the same type of sensor used in Experiment 1 and 2). This experiment varied the type of substrate, either urethane rubber (Poly PT Flex 50, BITY, Richardson, TX) or silicone (Dragon Skin® 30, Smooth-on, East Texas, PA). The custom coverstitched sensor for all trials was 3/16''-wide and 2''-long.

In addition to varying substrate material type (rubber vs. silicone), the topography of the substrate was also varied. Each topography was composed of hemispheres protruding from a flat surface, varying in hemisphere diameter. 1/8'', 1/2'', 3/4'' - diameter hemispheres were implemented as well as a flat substrate, as illustrated in Figure 18. These variables are outlined in Table 8. The hemispherical bumps were chosen partly from literature review, as well as the potential ability for the hemispherical shapes to further increase the stretch of the sensor from a perpendicular force acting on the sensor overlaying the bumps. The symmetrical and repeated shape of the spheres would allow the sensor to be overlaid in any direction, and still experience a similar stretch when the perpendicular force acts upon it (as opposed to a tooth structure, which would enforce one sensing direction). The coverstitched stretch sensor was attached to the substrate material, which was then adhered to a piece of 100% polyester foam with sticky-back Velcro to the Instron testing set-up (Figure 5). Each sample was 2'' long and 1.5'' wide with various thicknesses depending on the diameter hemisphere density/size (Figure 19).

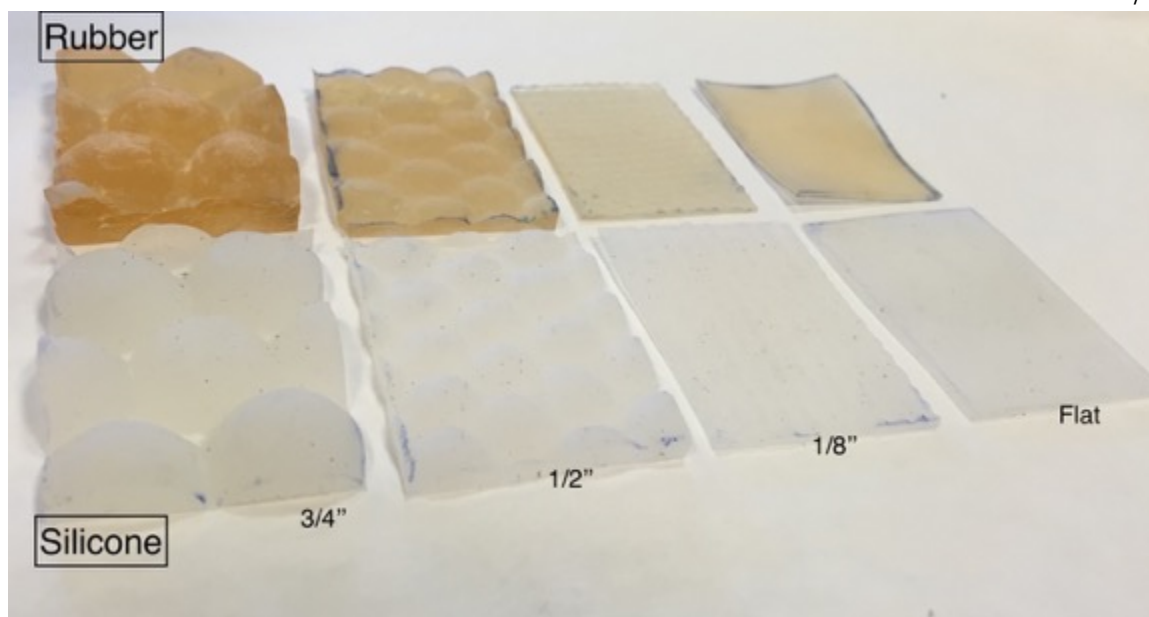


Figure 16. Silicone & Rubber Samples with Various Size Diameter Hemispheres

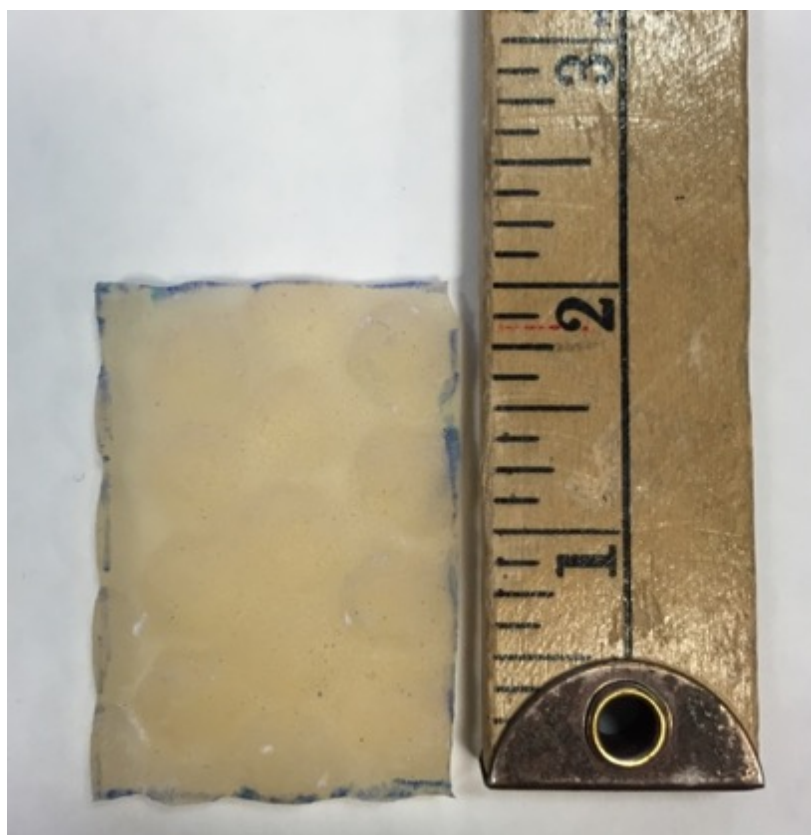


Figure 17. Rubber Substrate Sample - Medium 1/2'-Diameter Hemisphere

C. Data Collection

Data were collected in the same manner as experiment 1 and 2. The resistance response the coverstitched stretch sensor under variable loads and in the testing conditions outlined in Table 8 were evaluated using an Instron tensile tester. Compression (load) was applied using the Instron tensile testing machine 10 times in each trial. The sensor's resistance response was measured, recorded, and down-sampled as described in the previous experiments.

Table 8. Substrate Material Test Parameters

Topography	Substrate & Topography Material Testing with 2'' Coverstitched Sensor	
	Rubber Substrate	Silicone Substrate
Flat	5 trials	5 trials
Small-Diameter Sphere (1/8'')	5 trials	5 trials
Medium-Diameter Sphere (1/2'')	5 trials	5 trials
Large-Diameter Sphere (3/4'')	5 trials	5 trials

D. Procedure

Each of 8 experimental setups (see Table 8) were evaluated. For each setup, 5 iterations of a 10-cycle loading pattern were performed. Each sample had a 1/2'' layer of densified polyester foam beneath the substrate so that all samples (including the flat topography) could experience normal force being applied to it, which would cause some level of deformation. Additionally, a 3/16''-thin 2''-long coverstitched sensor was used on top of the substrate. The setups were as follows: 1.) 3/16''-thin 2''-long coverstitched

sensor over a flat rubber substrate, 2.) $3/16''$ -thin $2''$ -long coverstitched sensor over a flat silicone substrate, 3.) $3/16''$ -thin $2''$ -long coverstitched sensor over a $1/8''$ small-diameter sphere rubber substrate, 4.) $3/16''$ -thin $2''$ -long coverstitched sensor over a $1/8''$ small-diameter sphere silicone substrate 5.) $3/16''$ -thin $2''$ -long coverstitched sensor over a $1/2''$ medium-diameter sphere rubber substrate, 6.) $3/16''$ -thin $2''$ -long coverstitched sensor over a $1/2''$ medium-diameter sphere silicone substrate, 7.) $3/16''$ -thin $2''$ -long coverstitched sensor over a $3/4''$ large-diameter sphere rubber substrate, 8.) $3/16''$ -thin $2''$ -long coverstitched sensor over a $3/4''$ large-diameter sphere silicone substrate.

1. Analysis

The response of the coverstitched stretch sensor over the various substrates was compared in each test to the load data captured by the Instron. As in previous tests, visual analysis was performed as well as linear regression between the load and resistance datasets for each test. The coefficient of determination (r-sq) was calculated for each test and mean and standard deviation of these coefficients was calculated for each test condition.

2. Results

Example raw data traces of load (red line) and resistance (blue line) are shown in Figure 20. The mean r-sq coefficients of the 8 test conditions are shown below (Figure 21), as well as scatter-plot data of the applied load (lbf) vs. sensor output (resistance) shown in Figure 22.

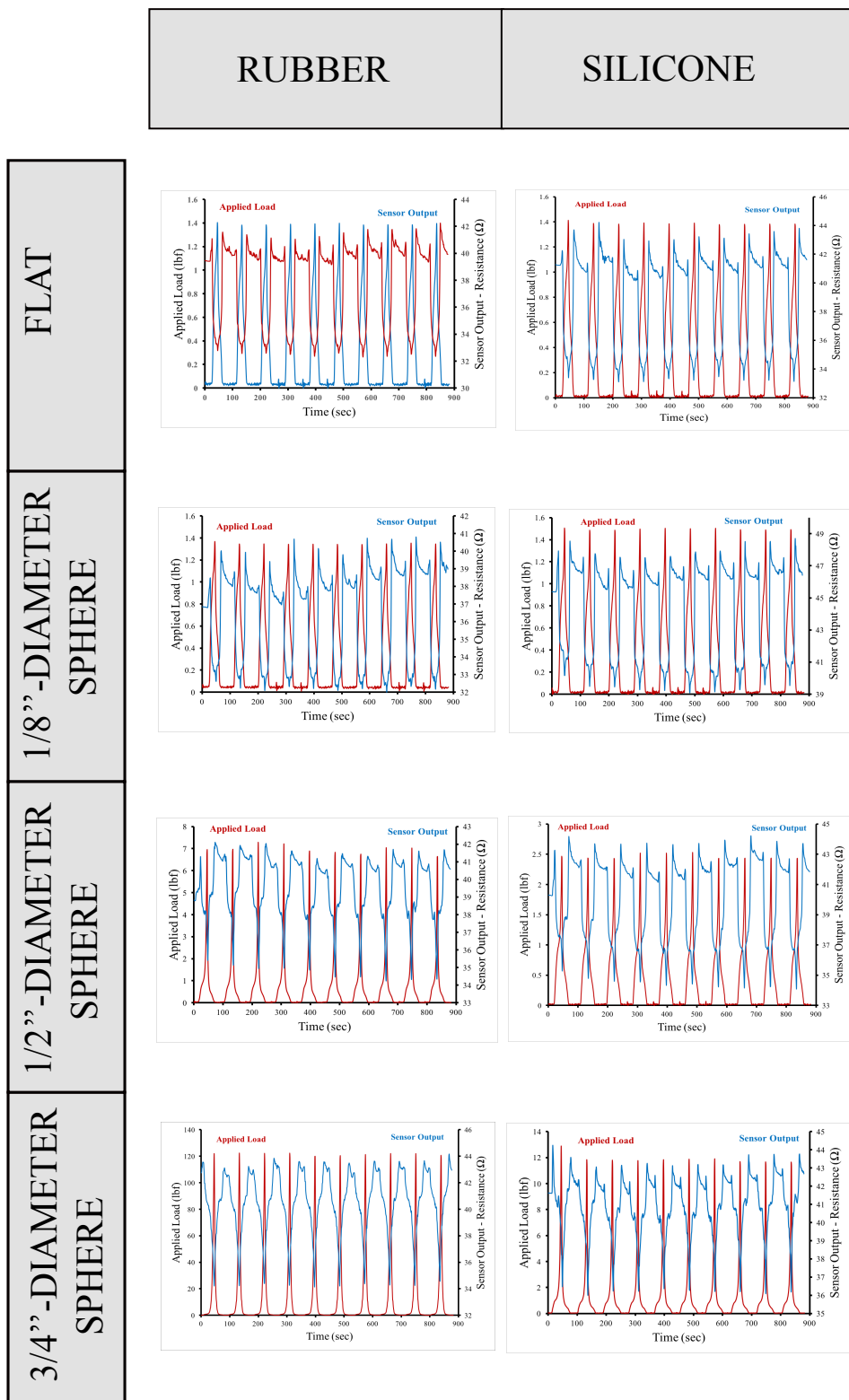
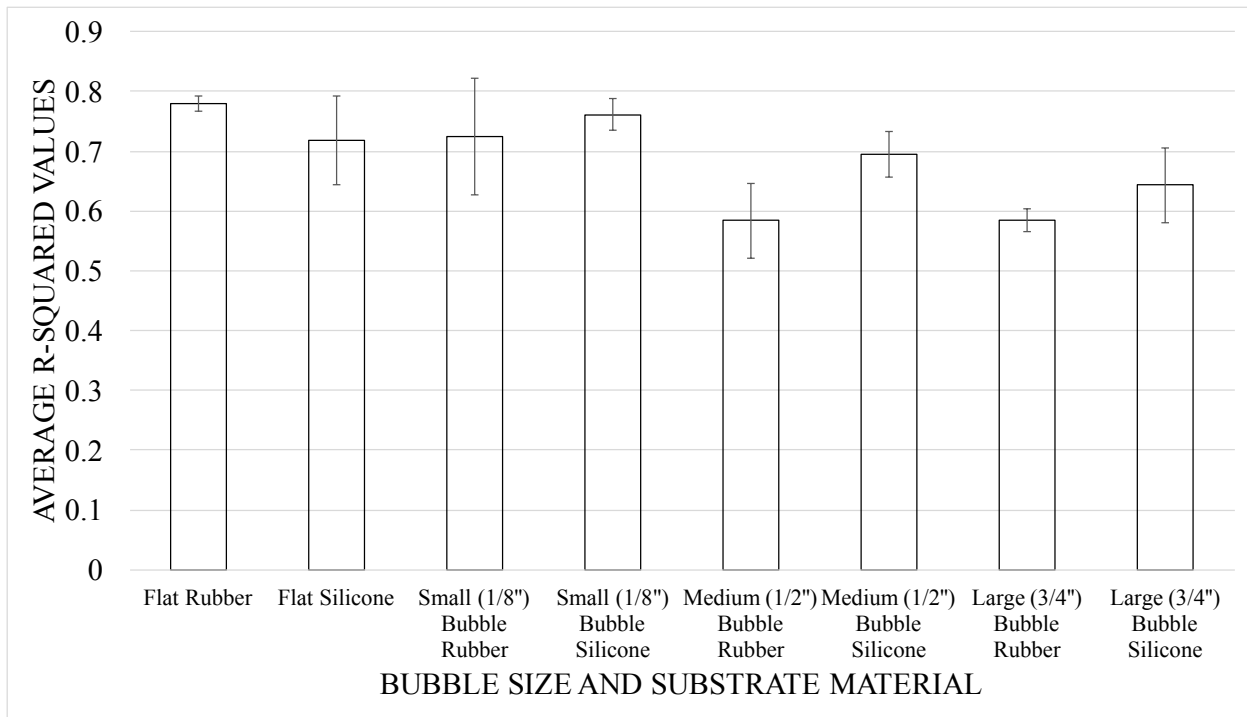


Figure 18. Raw data Data Ttraces of Load (red line) and R resistance (blue line).

Table 9. R-Square Values for Substrate & Topography Materials

Topography	R-Square Values for Substrate & Topography Material Testing with 2'' Coverstitched Sensor	
	Rubber Substrate	Silicone Substrate
Flat	0.78	0.72
Small-Diameter Sphere (1/8'')	0.72	0.76
Medium-Diameter Sphere (1/2'')	0.58	0.70
Large-Diameter Sphere (3/4'')	0.58	0.64

**Figure 19. Diameter-Hemisphere Size and Substrate Material Mean R-Sq Value**

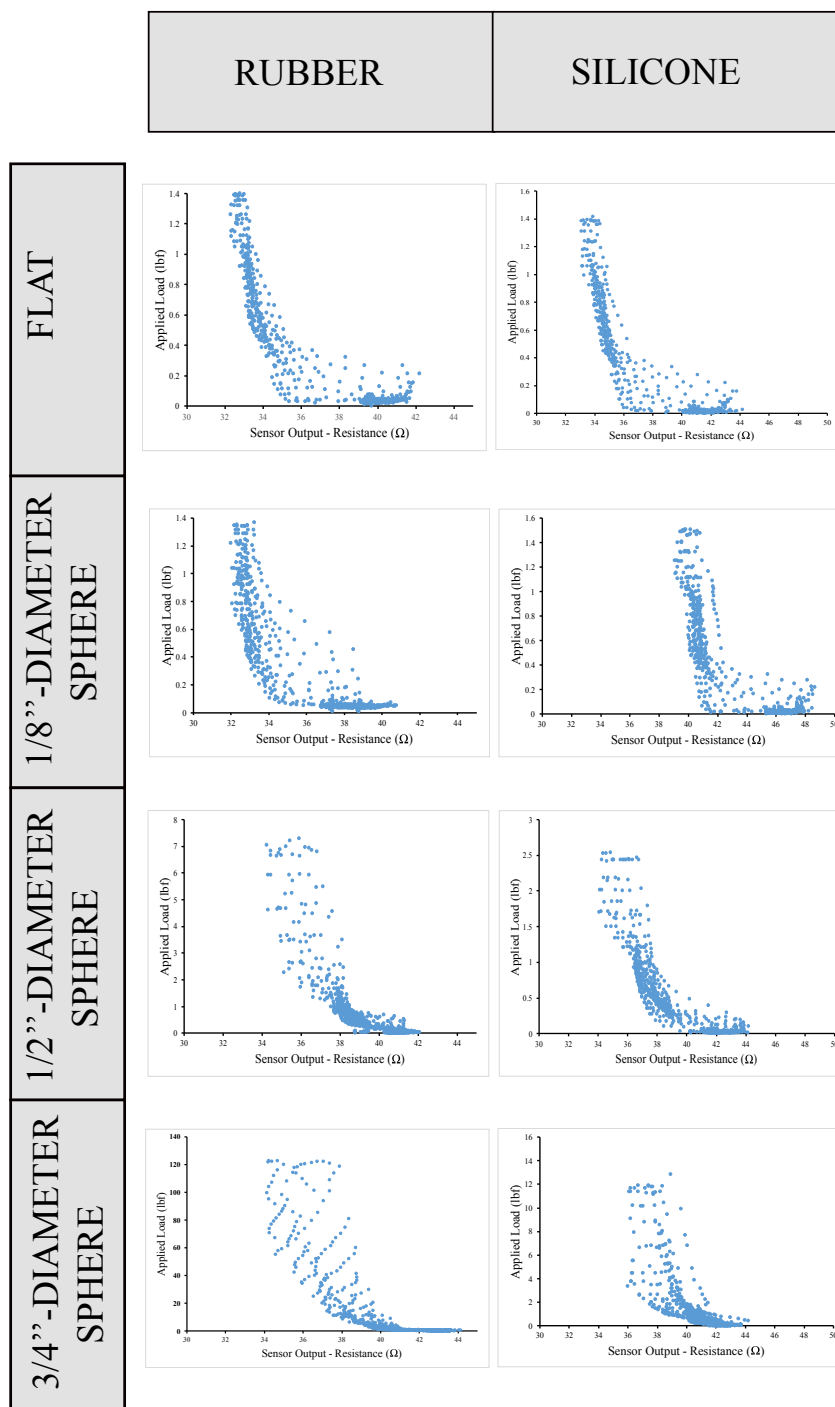


Figure 20. Scatter Plot - Applied Load vs. Resistance

E. Discussion

Varying results were observed for the substrate material and sphere size independent variable, as discussed below.

1. Substrate Material

The silicone substrate material appeared to have more consistent, linear, and predictable results visually, as evident with the average r-sq value of 0.70 vs. the average r-sq value of 0.67 of the average rubber substrate material samples. This provides some support for the hypothesis H2B which states that the samples made using a rubber substrate (which has stronger elasticity than silicone) would be less repeatable than the samples using a silicone substrate. This hypothesis was formulated based on the assumption that the weaker elasticity of silicone wouldn't inhibit the stretch of the coverstitch sensor like the stronger rubber samples. By allowing the samples to stretch, it allows them to detect a broader range of changes in resistance. The rubber substrate material had slightly less predictable results, which had the highest standard deviation of 0.10 for the 1/8''-diameter sphere substrates vs. silicone's highest standard deviation of 0.07 for the flat substrate material. Additionally, the rubber also had the lowest standard deviation reading of 0.01 for both the flat substrate material, with the lowest standard deviation reading for the silicone being 0.03.

Figure 20 further illustrates the weaker correlation of the coverstitched stretch sensor when paired with rubber and an applied load vs. the silicone with the coverstitched stretch sensor and an applied load. These results could be due to the substrate material thickness variance, with the rubber being slightly more stiff/thicker than the silicone substrate material, which allowed it more ease and allowance for the sensor to make contact as the Instron testing machine was enacting force upon the sensor over the silicone substrate material.

2. Sphere Size

The flat substrate samples had the most favorable results in terms of average r -sq value over all samples, as illustrated in Table 9. These results differ from the hypothesis H3a, which is based on previous work using substrate material and do not support the initial hypothesis for this experiment, which expected improved more repeatable sensor response when paired with a substrate that allows the sensor to further bend/stretch over a textured surface. However, this assumption assumes that the range of sensor response (which would in theory be enabled by the larger support structure topography used in this test) correlates with repeatability of the sensor. However, in this experiment the response range of each sensor was not evaluated. Since the repeatability as measured with r -sq correlation was only marginally different, investigating response range in more quantitative depth would be advised.

It appears that the flatter the surface of the substrate, the more favorable the results are in terms of r -sq value, as visually represented by Figure 20. However, the difference is marginal and could be due to a variety of reasons, such as the stiffness of the

silicone and rubber used in making the large-diameter sphere substrates, as well as the absence of a “top” layer conversion layer, which in previous work translated a force that caused the sensor to extend between two shaped layers substrate material.

3. Conclusion

Moving forward, despite the rubber substrate material having both a better overall average standard deviation, it also had both the lowest individual standard deviation and the highest individual standard deviation, implying a more irregularity and unpredictability than the mean standard deviation would imply. The silicone substrate was significantly more consistent in terms of the standard deviations across all tests. For this reason, it would be suggested that further testing with types of elastomers, specifically silicones, would be advised. A softer flatter surface may also be more optimal for further testing. Further (and more exhaustive) testing of the various sphere-shapes and sizes would also be recommended, specifically in terms of the overall shape and manufacturing method of the substrate topography

In terms of parameters outlined in Table 1, the silicone substrate material was slightly more flexible than the rubber substrate material samples. Despite not using an adhesive on the samples to attach the sensor, it would be assumed that the silicone samples would be slightly easier to penetrate (if need be) for manufacturing purposes (i.e. stitching on the silicone directly). The silicone, however, had a longer cure time of 16 hours (vs. the 60-minute cure time of the rubber). The prices of both silicone and rubber were comparable in price (roughly \$30 for 2 lb. of material). The rubber material was also slightly heavier than the silicone samples. The objective of the sensor is to be as less

cumbersome and unobtrusive as possible, so a more pliable and less dense substrate material would be ideal. The silicone and rubber Shore value can be manipulated to the needs of the user (i.e. less dense/denser/quicker mold time), which could help produce a substrate that is less noticeable. Making a thinner sample would also be recommended to further evaluate the sensor in terms of a discrete thin object. The examples illustrated in the literature review and in Table 1 that used an elastomer did so to house or cushion a more rigid sensor, or had the silicone housed by a rigid object (such as the A.P. Anderson & Newman (2015) study, which utilized the Polipo system which had a rigid body casing surrounding and protecting the less-rigid sensor). The sensor highlighted in this thesis wishes to eliminate hard components altogether to further aid in flexibility and comfort of the user, which are one of the main parameters in Table 1. The elastomers used in this study are existent to further aid in the sensor to detect normal force to the body, and should be as minimal as possible and should not obstruct the sensor from sensing or flexing. Therefore, further determining a minimal and discrete shape for the sensor that would be comparable to the smallest-size sensors highlighted in Table 1 (such as the study by Wang et al., (2011), which had a 10mm x 16 mm x 4.8mm sensor) and the substrate would be recommended.

One limitation of this thesis was the use of one substrate layer, (rather than two, which was how the experiment in the study by Wang et. al was performed). Using the two-layer approach would help further determine the responsiveness of the sensor by integrating it between two layers of substrate. Despite using two varying types of elastomers (the silicone and the substrate), the actual stiffness of the two elastomers was

not varied enough to fully make a determination that the stiffness of the elastomer played a role in the responsiveness to the sensors. An additional limitation associated with this thesis include the lack of a more extensive range of substrate materials, specifically elastomers. A broader range of elastomers, with specifically given Shore values would be recommended in order to associate substrate material stiffness/density with sensor responsiveness. Ideally, a sensor that is low-profile and thin is suggested in order to keep it as close to the body as possible, but at the same time, the sensor needs allowance to stretch perpendicular to the body, which would require some type of substrate that would thicken the sensor.

VI. Conclusion

Sensing normal force being exerted on the body could help prevent situations that could result in injury. However, the process of sensing on the body is more complicated than simply sensing on a flat surface. The body moves and bends, and isn't a flat hard surface. Discovering a sensor that could go over the body and still successfully detect normal force being exerted on it, despite these additional variables, is the ultimate challenge.

The coverstitched stretch sensor shows promise for sensing forces normal to the body surface based on the results presented in this thesis. Despite the accuracy that the flex sensor showed during the full-load portion of the tests, the recovery artifact that follows full loading discounts its accuracy. In implementation of the coverstitched sensor, placing the sensor over a curved, rather than flat, surface should improve the repeatability of the sensor, as well as utilizing a smaller-length, narrow-width coverstitch stretch sensor (here, 2"-length). When implementing one layer of substrate material, silicone showed marginally more favorable results in terms of r-squared value and standard deviation than rubber, and a flatter surface marginally increased consistency in the resistance readings of the coverstitched stretch sensor. When comparing the rubber and silicone substrate material to the initial foam and batting samples, the results are somewhat contradictory. For the foam and batting samples, the flatter the surface was, the less repeatable the sensor response. However, in the substrate samples, the flatter the silicone and rubber samples, the greater the repeatability of the sensor response. This could have been affected, however, by the difference in sensor lengths that were used in each experiment. The hardness factor of both the substrate materials could also have been a factor; the urethane rubber and

silicone samples had significant more rigidity/stiffness vs. the foam and batting samples. Overall, the rubber and silicone substrate materials were comparable to the samples adhered to foam in terms of repeatability.

Creating two layers of substrate material, rather than one, would be recommended (similar to the study conducted by Wang, et. al.) for further research. Creating two layers would help create consistency in the direction of the applied load. Additionally, a thinner layer of substrate material would also be suggested due to the need of maintaining a thin and unobtrusive measuring device. Testing these varying thicknesses, particularly with the silicone, would be highly recommended.

Future work will focus on refining the testing methods and better characterizing the coverstitched sensor, with particular emphasis on further testing the variance in accuracy associated with length in the coverstitched sensor. One of the advantages of using a coverstitched stretch sensor is its customizable physical properties, such as its length and width. Determining the absolute limits of the repeatability, stability, and hysteresis in terms of the length of the sensor would help further determine its characteristics if it were to be implemented into a garment. This could potentially limit the placement of the sensor, and would be a determining factor for the layout and construction of the garment. Additional elastomer topography structures and materials should also be explored, particularly with varying Shore values.

Finally, implementing the coverstitched stretch sensor into a realized garment that was tested for longer durations and exposed to stress and sweat would be necessary in order to conduct tests under the dynamic conditions associated with testing on the human body.

Many studies appear to successfully integrate various types of sensors into garments with promising results, but fail to realize the sensor in an actual garment that is worn on-body. Many of the studies outlined in Table 2 and in the literature review highlight sensors that are conditioned and tested in a laboratory environment with little to no regard for the material to which the sensor is attached to or to whom the sensor would be worn by. The physical properties of the sensor plus substrate combination, as well as the relationship of the sensor's physical properties to the physical properties of the body on which it is mounted, have as much influence on the accuracy of the sensing system as the sensor properties themselves. A seamless integration further reinforces a comfortable and invisible sensor, which has been an over-arching goal for many wearable technology applications. As with the studies presented here, several studies outlined in Table 2 didn't fully realize the sensor in a wearable garment. This step would prevent the researchers from identifying whether the sensor had true 3D-drapable capabilities, which is a contributing factor to the success of the sensor for on-body sensing. This final step is the true determining factor for the success of a sensor to be used to detect normal force being exerted onto the body. It's not only important to be able to integrate the sensor into soft goods, but to integrate it into soft goods that can be worn onto the body (with all that entails). Design recommendations for the final design of the sensor, with regards to the criteria outlined in Table 1, would be to minimize the size of the sensor. The sizes of the various sensors (as outlined in Table 2) in the literature review varied in size, with the smallest sensor being 10 mm x 16 mm x 4.8 mm from the Wang et al. (2011) study and the largest being 4.8 cm x 3.6 cm x 1.3 cm by the Anderson et al. (2015) study (although the

coverstitch sensor had the potential to be longer (with the longest being 4''x 2.5''x 1'', and the shortest being 2''x1.5''x1'' with the sensor paired with a substrate material); it just had yet to be characterized at a longer length). Minimizing the size of the sensor would allow the sensor to be integrated in numerous spots over the body, as well as avoiding noise and could better isolate the location of the force. This could also further aid in its ability to be stable and repeatable, which are just as important as the sensor's ability to be integrated and worn comfortably on the body which, unfortunately, appears to be the current conundrum of currently available sensors; they tend to lean heavily on one end of that spectrum or the other. The Hennig et al.(1982) study for example, with the 4.78mm-length sensor, had the smallest sensor but it was not truly bendable in multiple dimensions, minimizing its success to be worn for a prolonged period of time in a garment. Based on the guiding principle that the sensor would ultimately need to be implemented into a garment, a thinner more discrete sensor with a broad range of flexibility would be ideal. However, a minimal shape and size could allow for a variety of placements over the garment and would also minimize the requirement for flexibility, which is more important in larger sensors. A sensor that minimized the complexity of the manufacturing process would also likely be more cost effective, which is another important parameter outlined in Table 1 in regards to requirements needed for sensors to be integrated into a garment. The low-cost nature of the coverstitched sensor is also one of its leading attributes, but could be further analyzed and improved upon based on the ever-expanding conductive thread market, which (like electronics), is getting less expensive every day. The mechanical properties of the conductive thread used to make the coverstitched sensor are the most

significant influence on the mechanical properties of the sensor itself, but are less significant than the properties of the supporting substrate. Overall durability and repeatability of the sensor should be investigated in more depth, including the effect of oxidization of the silver used to coat the threads which could contribute to a lack of long-term repeatability. The sensor presented in this thesis has the potential to balance evenly between that spectrum with further testing and paired with the appropriate materials and characteristics.

In summary, the sensors evaluated in this thesis have shown promise due to their demonstrated ability to sense normal forces reliably, as well as their customizable physical structure. Although the experiments used in this study did not surpass the most discrete forms observed in the literature review, their customizable nature could allow for further testing to be conducted in this regard which could help establish the physical limits on the sensor's form factor. In addition to the potential of creating a lower-profile sensor, the manufacturing costs and complexities associated with making the coverstitched sensor are only comparable to the studies that used fiber-based sensors (such as the study conducted by Wang et al., 2011, which made fabric pressure sensors), and present an improvement over many fiber-based sensor manufacturing processes. Limiting the amount of resources and complexities associated with sensor fabrication are important, especially if it were to be used in traditional textile and garment manufacturing processes. A means of implementing the sensor onto a substrate material in a more streamlined process should also be further explored (as well as determining if parts of the human body have enough deformability to allow the sensor to respond accurately to normal force without a substrate

conversion layer). Complexities associated with manufacturing the sensor can make it difficult for textile manufacturers to adopt (such as the study conducted by A.P. Anderson & Newman, 2015, which developed and characterized the Polipo sensors). These complexities can also increase the cost associated with manufacturing the sensor. Cost associated with manufacturing textiles and electronics is also very competitive, so introducing a technique for sensing that is comparable to a sensor that is seemingly more complex but easier to manufacture would more likely be utilized and manufactured. The sensors highlighted in Table 2 all had relatively low profiles, but some had limited flexibility and stretch, such as the study conducted by Merritt, Nagle, & Grant (2009). The coverstitched sensor itself, independent of the substrate conversion layer, is comparable to the most flexible sensors introduced in Table 2 (the non-textile based samples tended to be less flexible, like the Merritt, Nagle, & Grant (2009) study) which used various parts that were nonstretchable and not as flexible as the other examples). However, the properties of the conversion layer must also be taken into account in this sensing scenario. The sensors that utilized fibers also displayed a higher level of comfort from the user, which is another important factor to consider. While a lack of quantitative data in the literature and in this thesis makes the repeatability of the coverstitched sensor relative to other examples difficult to assess, it appears comparable to many examples in Table 2. The manufacturability and potential for positive physical properties of the sensor/substrate ensemble combined with the promising sensing behavior observed here make this approach viable and interesting for future investigation.

Reference

- Anderson, A., Hilbert, A., Bertrand, P., McFarland, S., & Newman, D. J. (2014). In-Suit Sensor Systems for Characterizing Human-Space Suit Interaction. *International Conference on Environmental Systems*.
- Anderson, A. P., & Newman, D. J. (2015). Pressure sensing for in-suit measurement of space suited biomechanics. *Acta Astronautica*, 115, 218–225.
<https://doi.org/10.1016/j.actaastro.2015.05.024>
- Brady, S., Dunne, L. E., Tynan, R., Diamond, D., Smyth, B., & O'Hare, G. M. P. (2005). Garment-Based Monitoring of Respiration Rate Using a Foam Pressure Sensor (pp. 214–215). IEEE. <https://doi.org/10.1109/ISWC.2005.23>
- Dirjish, M. (2012, April 18). What's The Difference Between Piezoelectric And Piezoresistive Components? Retrieved September 28, 2016, from <http://electronicdesign.com/components/what-s-difference-between-piezoelectric-and-piezoresistive-components>
- Fraden, J. (2004). *Handbook of modern sensors: physics, designs, and applications* (3rd ed). New York: Springer.
- Fraden, J. (2016). Physical Principles of Sensing. In *Handbook of Modern Sensors* (pp. 69–154). Springer International Publishing. https://doi.org/10.1007/978-3-319-19303-8_4
- GioBERTO, G., & Dunne, L. (2012). Theory and characterization of a top-thread coverstitched stretch sensor (pp. 3275–3280). IEEE.
<https://doi.org/10.1109/ICSMC.2012.6378296>

Guo, L., Berglin, L., Li, Y. J., Mattila, H., Mehrjerdi, A. K., & Skrifvars, M. (2011).

“Disappearing Sensor”-Textile Based Sensor for Monitoring Breathing (pp. 1–4).

IEEE. <https://doi.org/10.1109/ICCASE.2011.5997723>

Hardy, W. N., Mason, M. J., Foster, C. D., Shah, C. S., Kopacz, J. M., Yang, K. H., &

King, A. I. (2007). A Study of the Response of the Human Cadaver Head to

Impact. *Stapp Car Crash Journal*, 51, 17–80.

Harries, C. A., & Pegg, S. P. (1989). Measuring pressure under burns pressure garments

using the Oxford Pressure Monitor. *Burns*, 15(3), 187–189.

[https://doi.org/10.1016/0305-4179\(89\)90180-0](https://doi.org/10.1016/0305-4179(89)90180-0)

Hennig, E. M., Cavanagh, P. R., Albert, H. T., & Macmillan, N. H. (1982). A

piezoelectric method of measuring the vertical contact stress beneath the human

foot. *Journal of Biomedical Engineering*, 4(3), 213–222.

[https://doi.org/10.1016/0141-5425\(82\)90005-X](https://doi.org/10.1016/0141-5425(82)90005-X)

How to Measure Pressure with Pressure Sensors. (2012, November 15). Retrieved from

<http://www.ni.com/white-paper/3639/en/>

Huang, C. t, Tang, C. f, & Shen, C. l. (2006). A Wearable Textile for Monitoring

Respiration, Using a Yarn-Based Sensor. In *2006 10th IEEE International*

Symposium on Wearable Computers (pp. 141–142).

<https://doi.org/10.1109/ISWC.2006.286366>

Lee, J., Kwon, H., Seo, J., Shin, S., Koo, J. H., Pang, C., ... Lee, T. (2015). Conductive

Fiber-Based Ultrasensitive Textile Pressure Sensor for Wearable Electronics.

Advanced Materials, 27(15), 2433–2439.

<https://doi.org/10.1002/adma.201500009>

Liu, C. (2006). *Foundations of MEMS*. Upper Saddle River, NJ: Pearson/Prentice Hall.

Loriga, G., Taccini, N., De Rossi, D., & Paradiso, R. (2005). Textile Sensing Interfaces for Cardiopulmonary Signs Monitoring (pp. 7349–7352). IEEE.

<https://doi.org/10.1109/IEMBS.2005.1616209>

Merritt, C. R., Nagle, H. T., & Grant, E. (2009). Textile-Based Capacitive Sensors for Respiration Monitoring. *IEEE Sensors Journal*, 9(1), 71–78.

<https://doi.org/10.1109/JSEN.2008.2010356>

Ouckama, R., & Pearsall, D. J. (2011). Evaluation of a flexible force sensor for measurement of helmet foam impact performance. *Journal of Biomechanics*, 44(5), 904–909. <https://doi.org/10.1016/j.jbiomech.2010.11.035>

Paradiso, R., Loriga, G., & Taccini, N. (2005). A Wearable Health Care System Based on Knitted Integrated Sensors. *IEEE Transactions on Information Technology in Biomedicine*, 9(3), 337–344. <https://doi.org/10.1109/TITB.2005.854512>

Partsch, H., Clark, M., Bassez, S., Benigni, J.-P., Becker, F., Blazek, V., ... Neumann, M. (2006). Measurement of Lower Leg Compression In Vivo: Recommendations for the Performance of Measurements of Interface Pressure and Stiffness. *Dermatologic Surgery*, 32(2), 224–233. <https://doi.org/10.1111/j.1524-4725.2006.32039.x>

Pressure Sensors from Kistler. (2016). Retrieved from

https://www.kistler.com/us/en/products/components/pressure-sensors/#piezoelectric__pressure__sensor__p_e_250_bar_3625_psi_601_c_a_a

Ripka, P., & Tipek, A. (Eds.). (2007). *Modern sensors handbook*. Newport Beach, CA: ISTE USA.

Robertson, J. C., Hodgson, B., Druett, J. E., & Druett, J. (1980). Pressure Therapy for Hypertrophic Scarring: Preliminary Communication. *Journal of the Royal Society of Medicine*, 73(5), 348–354. <https://doi.org/10.1177/014107688007300509>

Robinson, G. (2016, September 7). What is a Piezoelectric Transducer? Retrieved September 26, 2016, from <http://www.wisegeek.org/what-is-a-piezoelectric-transducer.htm>

Rovira, C., Coyle, S., Corcoran, B., Diamond, D., Stroiescu, F., & Daly, K. (2011). Integration of textile-based sensors and Shimmer for breathing rate and volume measurement. In *2011 5th International Conference on Pervasive Computing Technologies for Healthcare (PervasiveHealth)* (pp. 238–241).

Saggio, G., Riillo, F., Sbernini, L., & Quitadamo, L. R. (2016). Resistive flex sensors: a survey. *Smart Materials and Structures*, 25(1), 13001. <https://doi.org/10.1088/0964-1726/25/1/013001>

Scilingo, E. P., Gemignani, A., Paradiso, R., Taccini, N., Ghelarducci, B., & DeRossi, D. (2005). Performance Evaluation of Sensing Fabrics for Monitoring Physiological and Biomechanical Variables. *IEEE Transactions on Information Technology in Biomedicine*, 9(3), 345–352. <https://doi.org/10.1109/TITB.2005.854506>

- Se Dong Min, Yonghyeon Yun, & Hangsik Shin. (2014). Simplified Structural Textile Respiration Sensor Based on Capacitive Pressure Sensing Method. *IEEE Sensors Journal*, 14(9), 3245–3251. <https://doi.org/10.1109/JSEN.2014.2327991>
- Shyr, T.-W., Shie, J.-W., Jiang, C.-H., & Li, J.-J. (2014). A Textile-Based Wearable Sensing Device Designed for Monitoring the Flexion Angle of Elbow and Knee Movements. *Sensors*, 14(3), 4050–4059. <https://doi.org/10.3390/s140304050>
- Sirohi, J., & Chopra, I. (2000). Fundamental Understanding of Piezoelectric Strain Sensors. *Journal of Intelligent Material Systems and Structures*, 11(4), 246–257. <https://doi.org/10.1106/8BFB-GC8P-XQ47-YCQ0>
- Wang, Y., Hua, T., Zhu, B., Li, Q., Yi, W., & Tao, X. (2011). Novel fabric pressure sensors: design, fabrication, and characterization. *Smart Materials and Structures*, 20(6), 65015. <https://doi.org/10.1088/0964-1726/20/6/065015>
- Webster, J. G., & Eren, H. (2014). *Measurement, Instrumentation, and Sensors Handbook, Second Edition: Spatial, Mechanical, Thermal, and Radiation Measurement*. CRC Press.
- Wilson, J. S. (Ed.). (2005). *Sensor technology handbook*. Amsterdam ; Boston: Elsevier.
- Zhou, W., Huang, G., & Yin, S. (2015). A surface chemical potential and instability of piezoelectric thin films. *Journal of Applied Physics*, 117(14), 145303. <https://doi.org/10.1063/1.4917045>

Appendix A: Additional Figures for Experiment 1

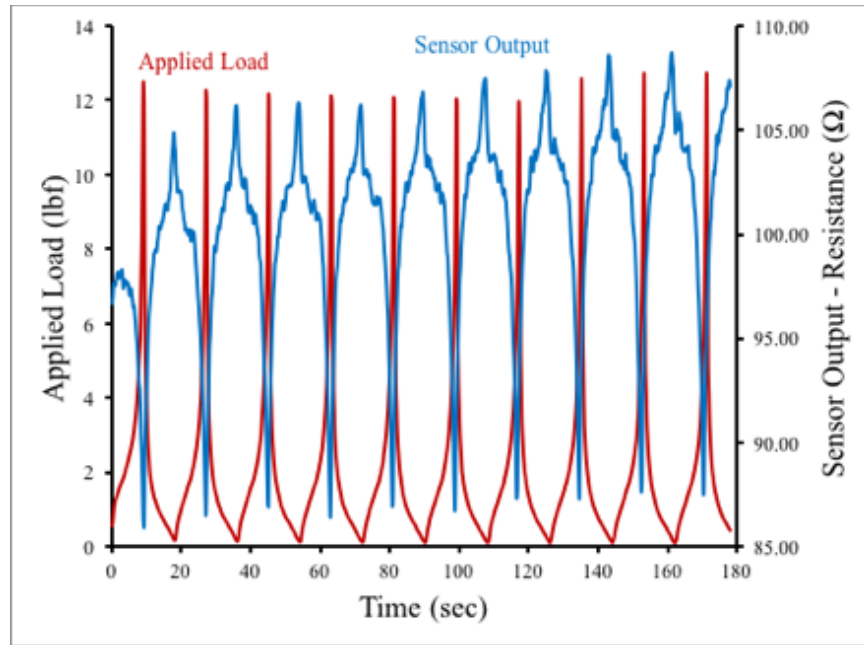


Figure 21. Coverstitch - 1" Green Polyester Curved

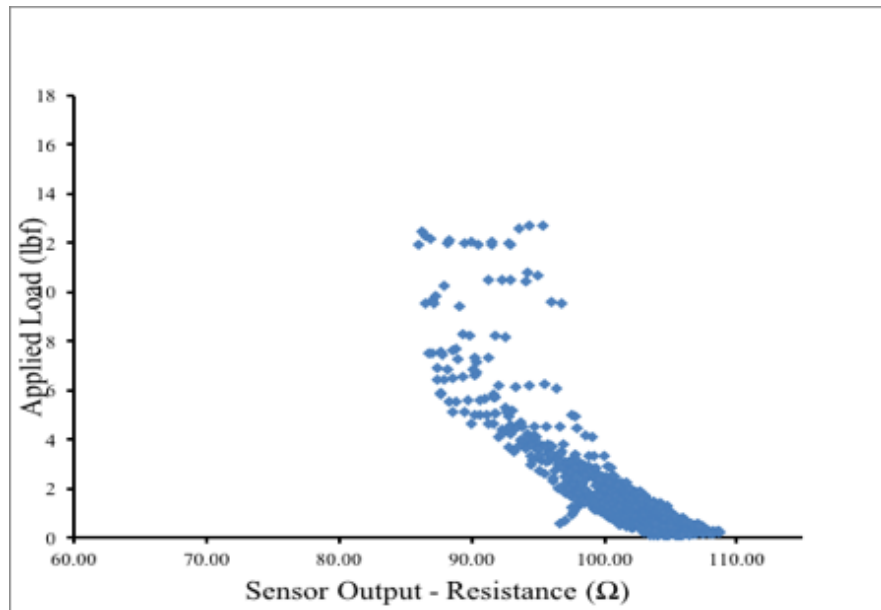


Figure 22. Coverstitch - 1" Green Polyester Curved

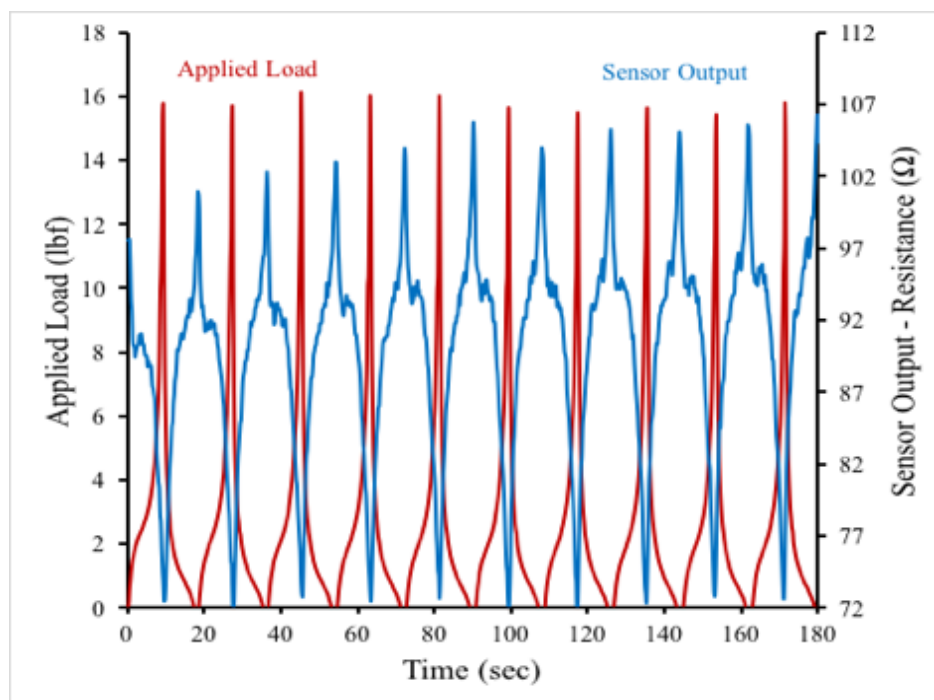


Figure 23. Coverstitch - 1" Green Polyester Squared

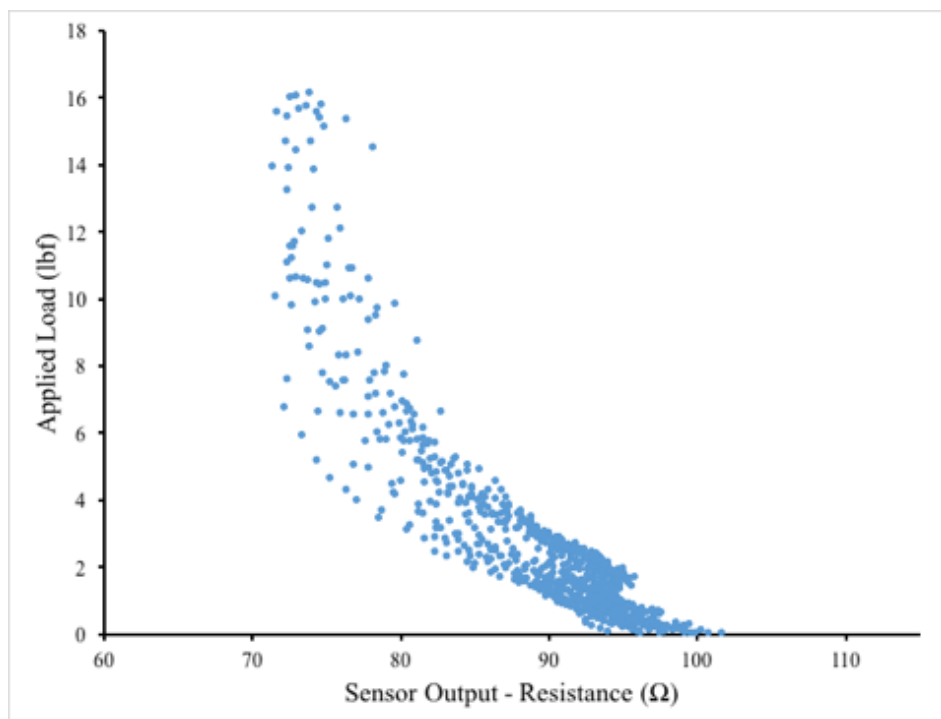


Figure 24. Coverstitch - 1" Green Polyester Squared

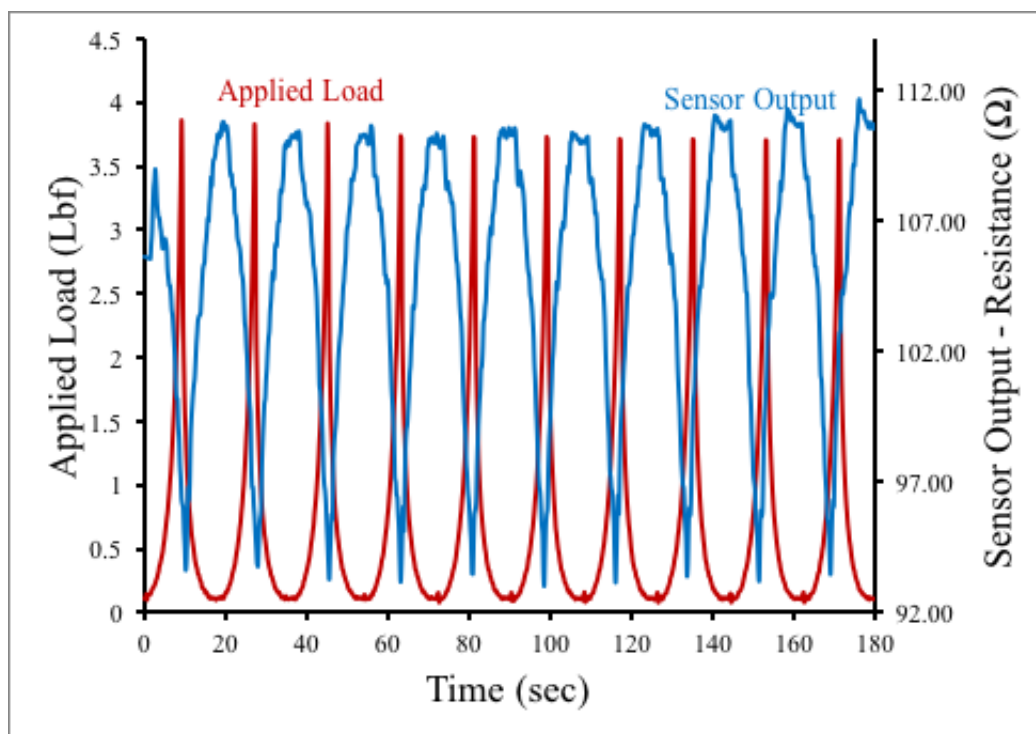


Figure 25. Coverstitch - 1" White Polyurethane Curved

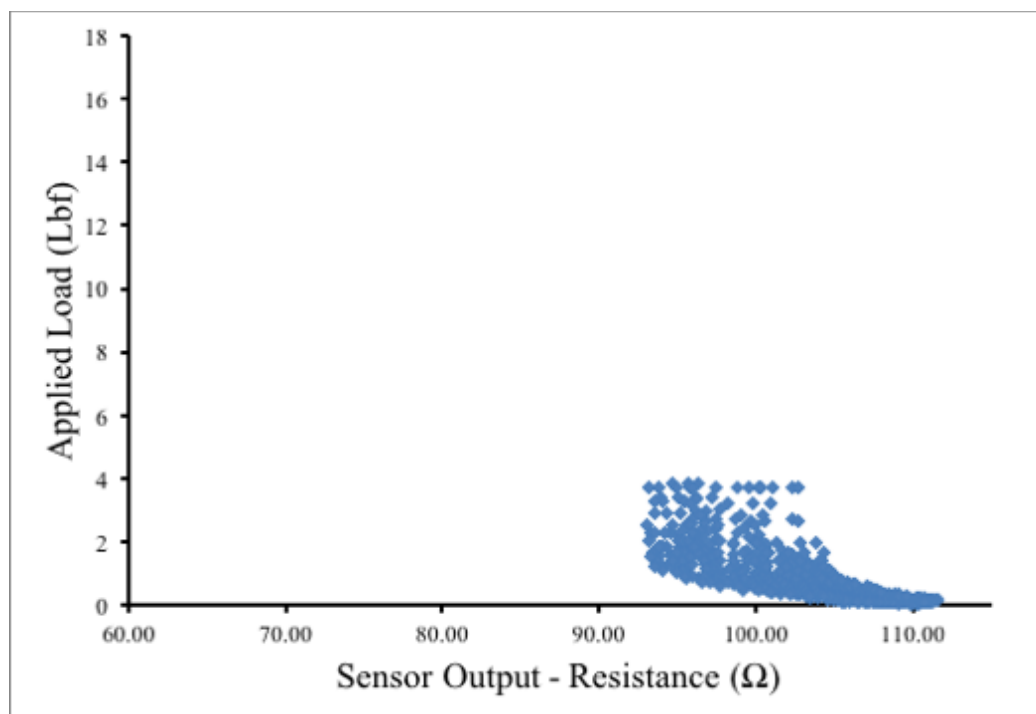


Figure 26. Coverstitch - 1" White Polyurethane Curved

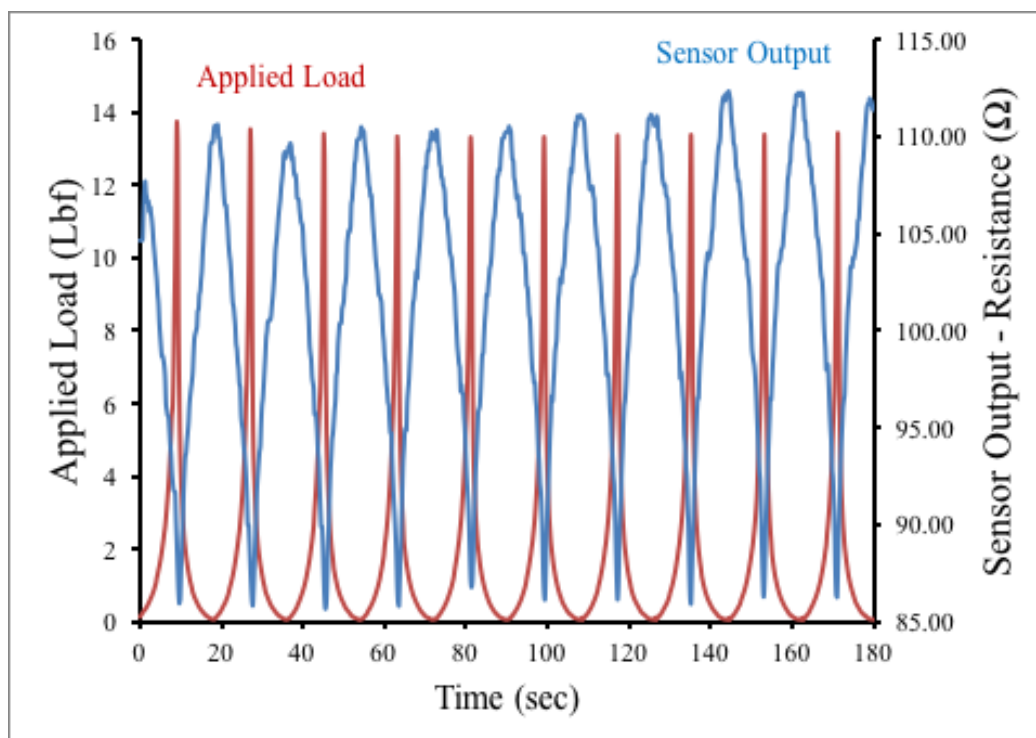


Figure 27. Coverstitch - 1" White Polyurethane Squared

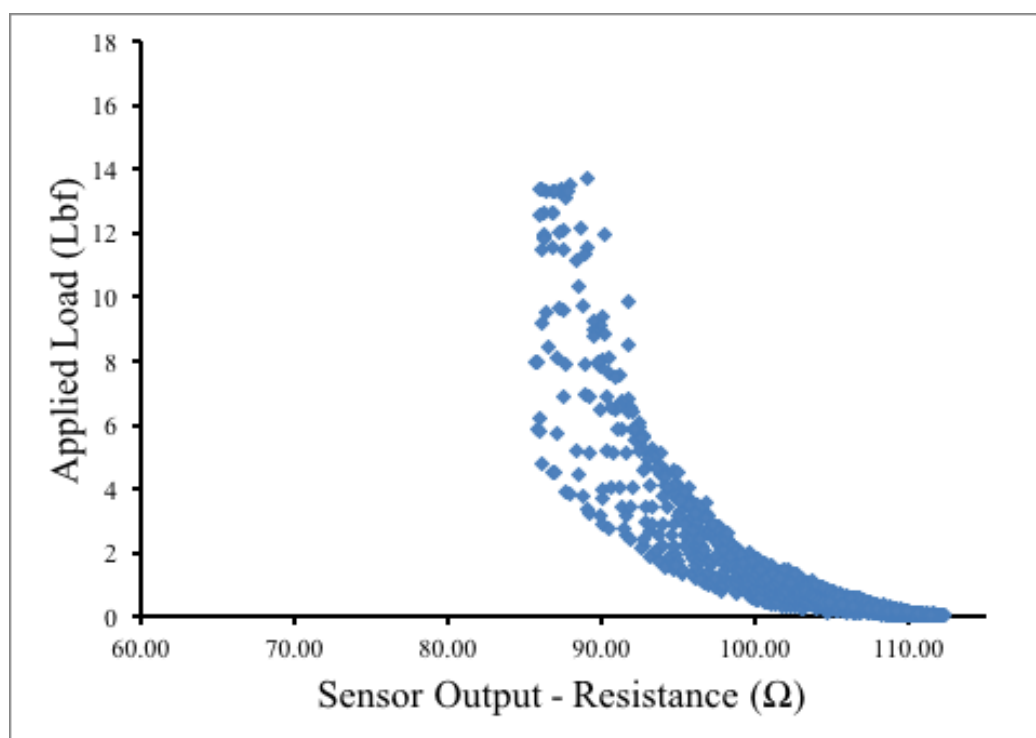


Figure 28. Coverstitch - 1" White Polyurethane Squared

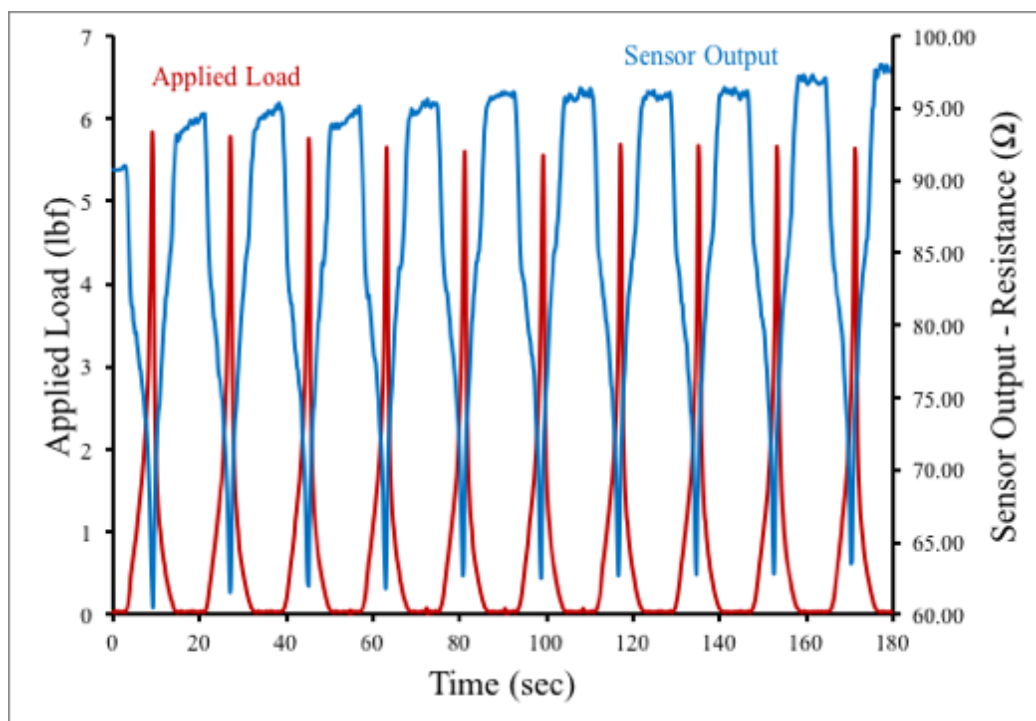


Figure 29. Coverstitch - 1/2" Green Polyester Curved

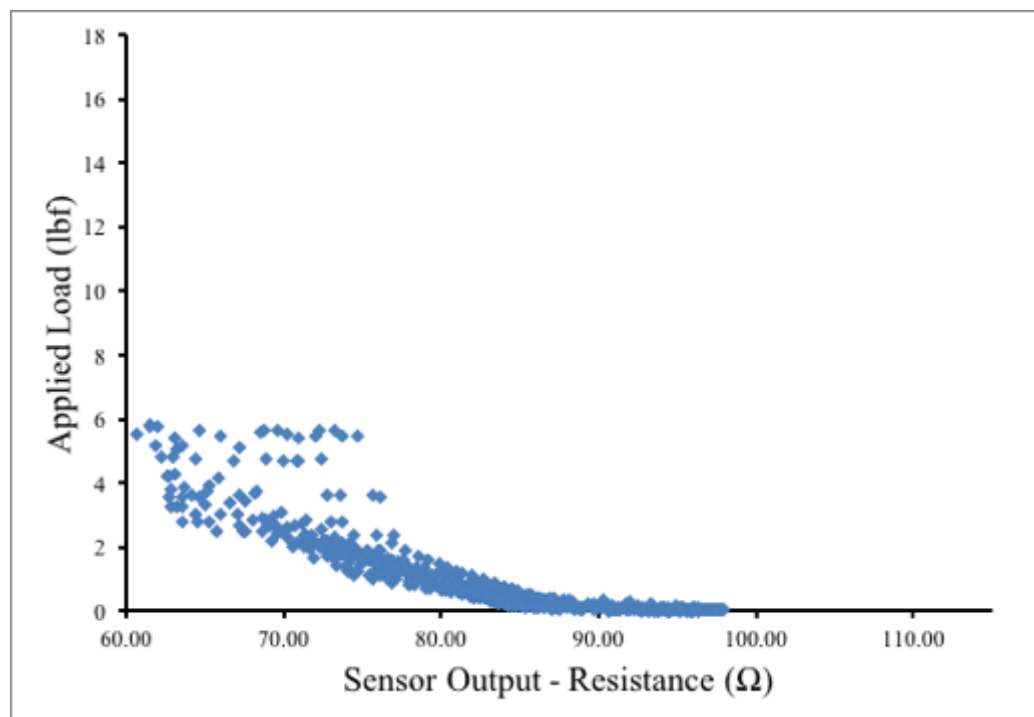


Figure 30. Coverstitch - 1/2" Green Polyester Curved

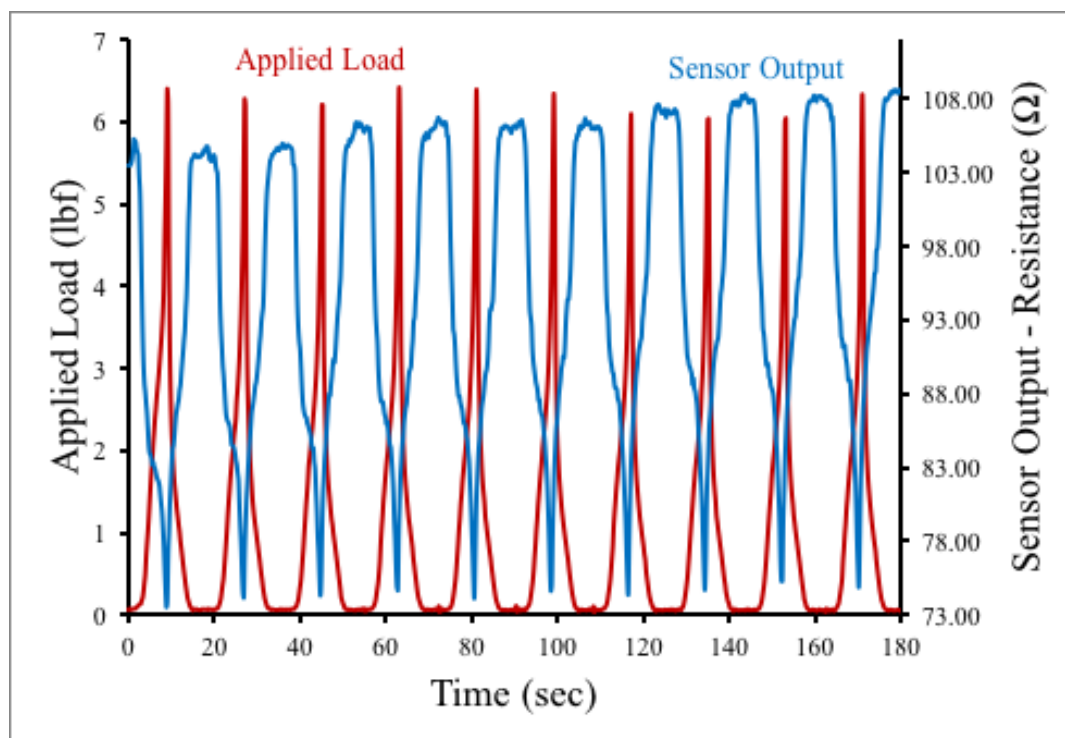


Figure 31. Coverstitch - 1/2" Green Polyester Squared

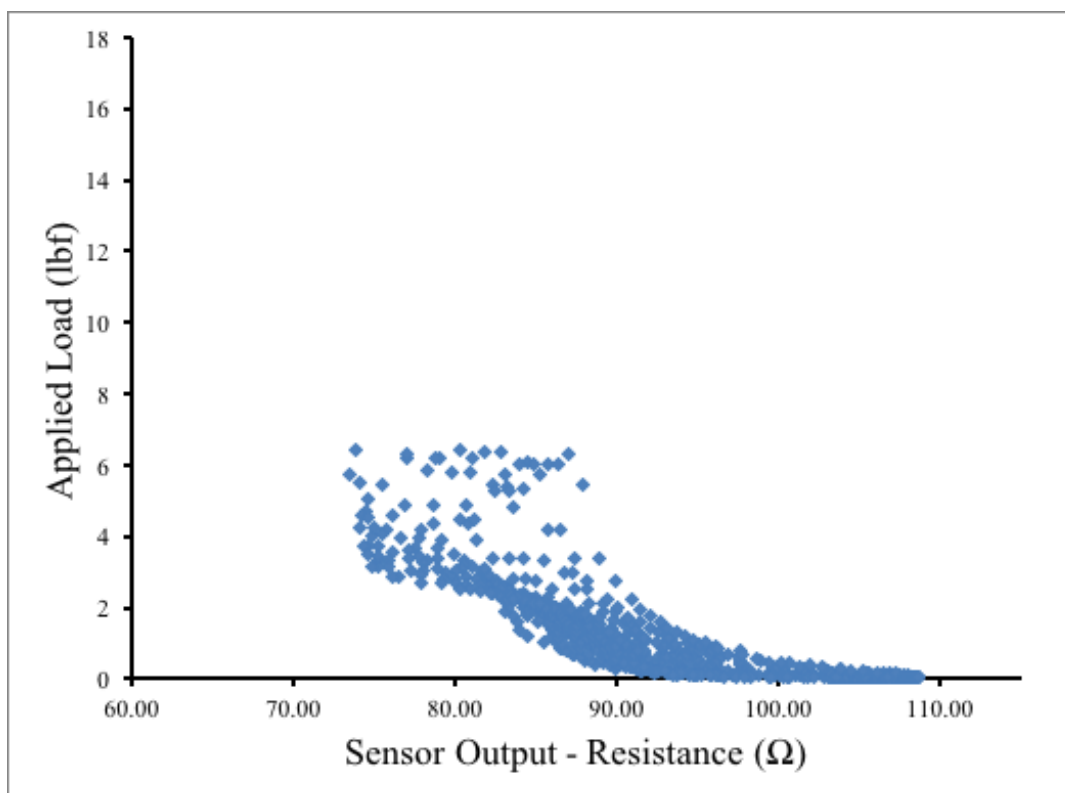


Figure 32. Coverstitch - 1/2" Green Polyester Squared

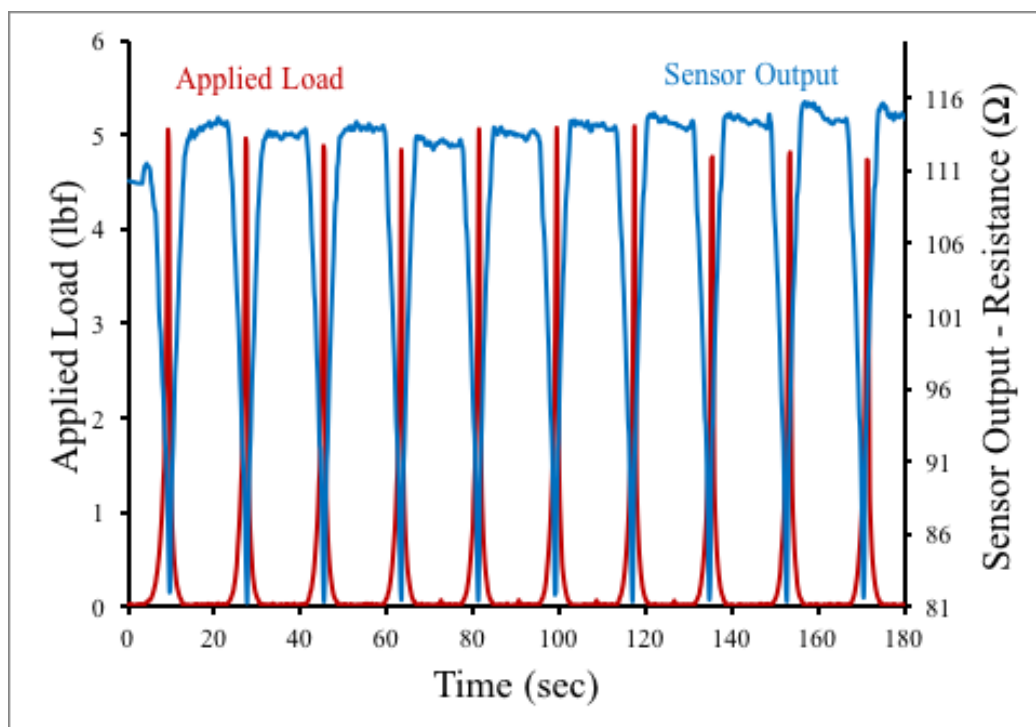


Figure 33. Coverstitch - 1/2" White Polyurethane Curved

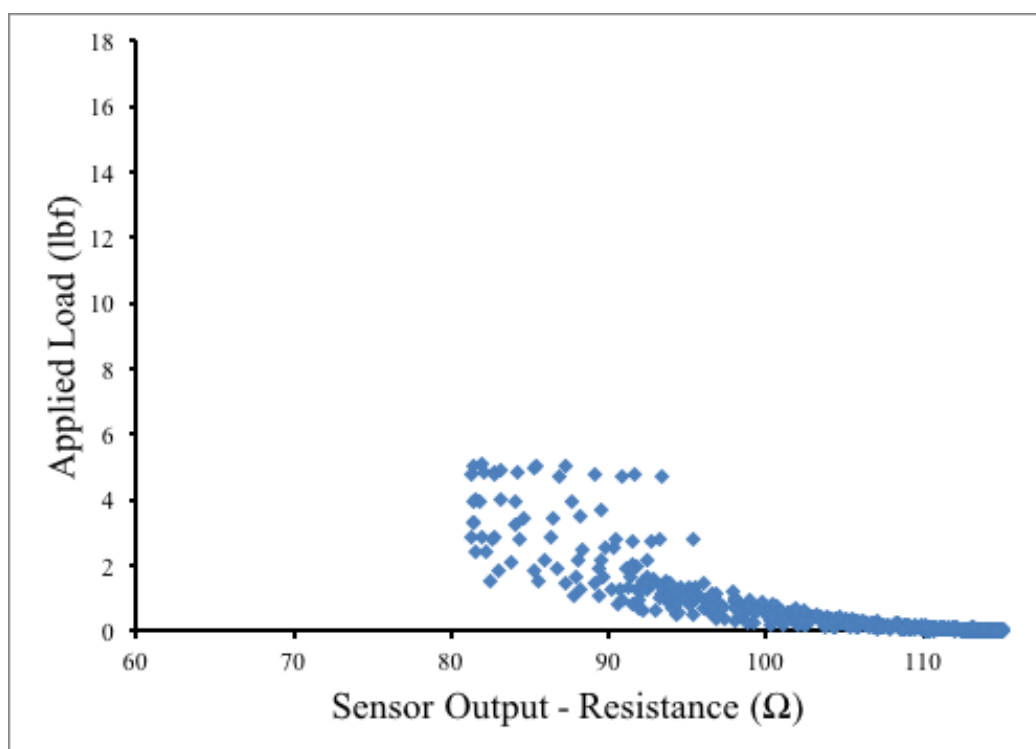


Figure 34. Coverstitch - 1/2" White Polyurethane Curved

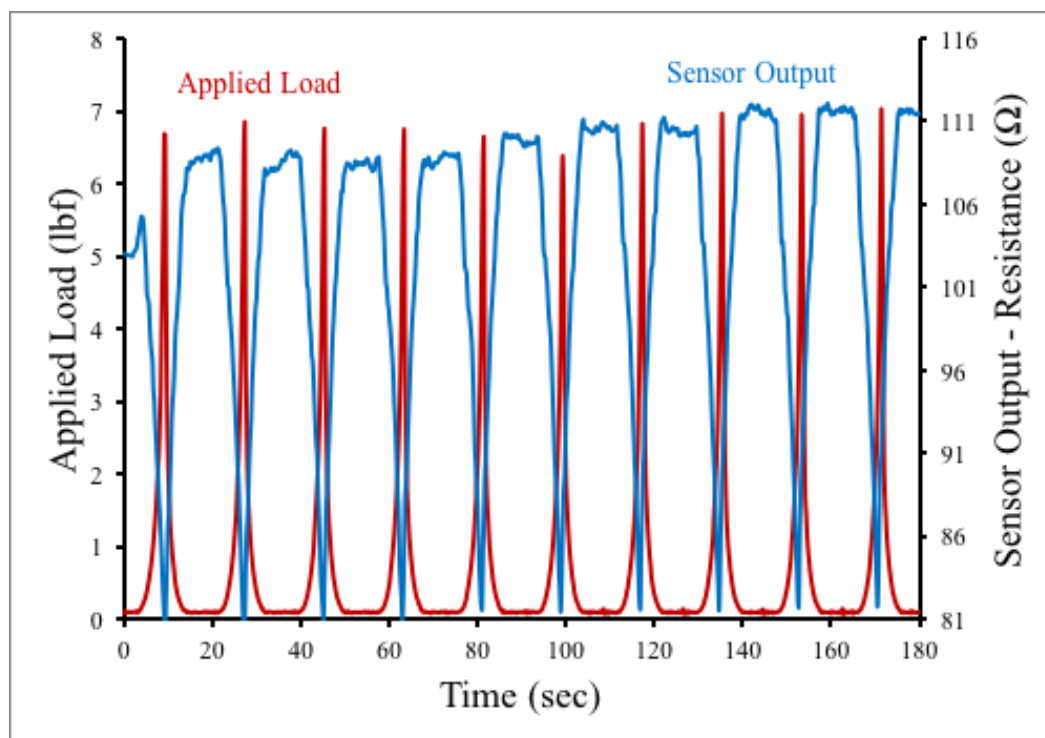


Figure 35. Coverstitch - 1/2" White Polyurethane Squared

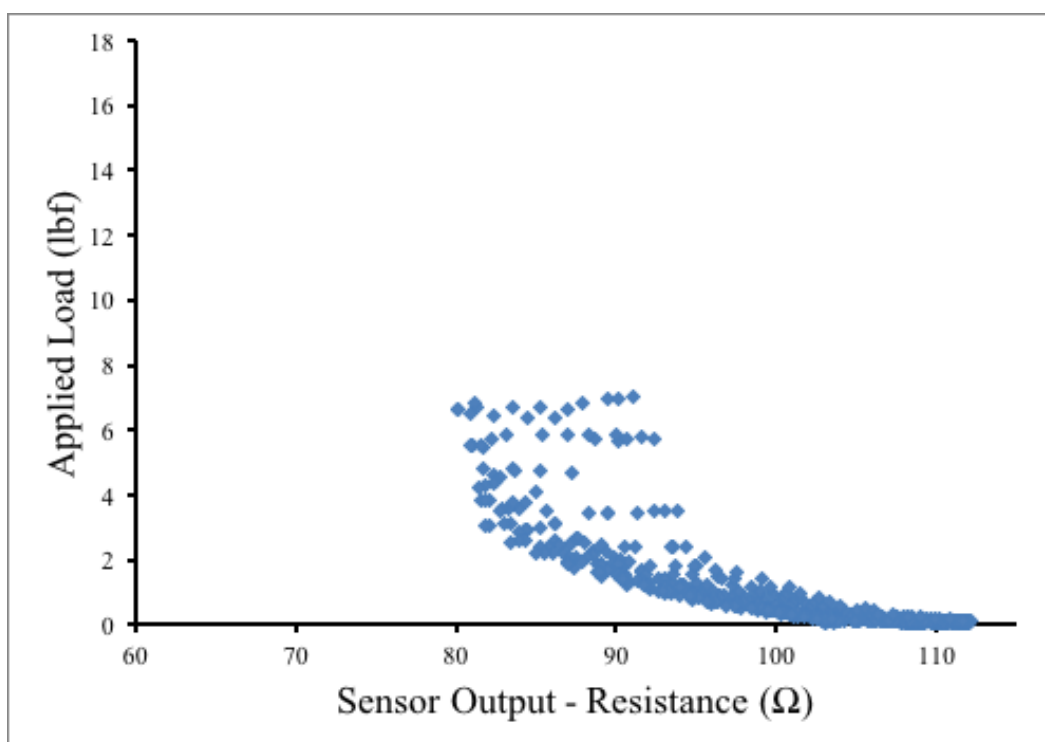


Figure 36. Coverstitch - 1/2" White Polyurethane Squared

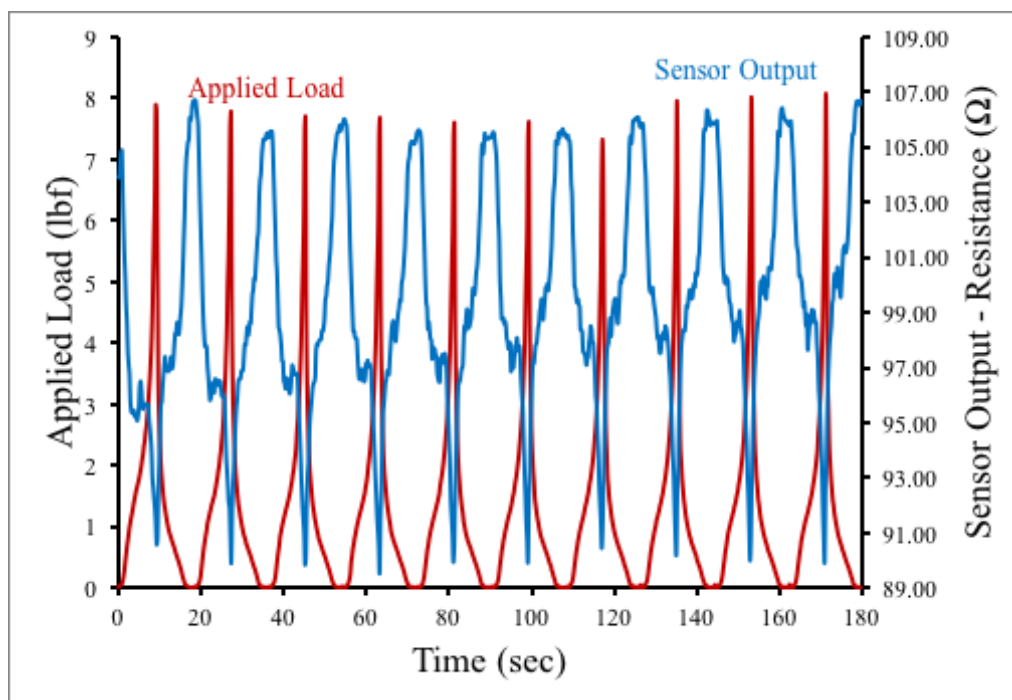


Figure 37 Coverstitch - 3/4" Green Polyester Curved

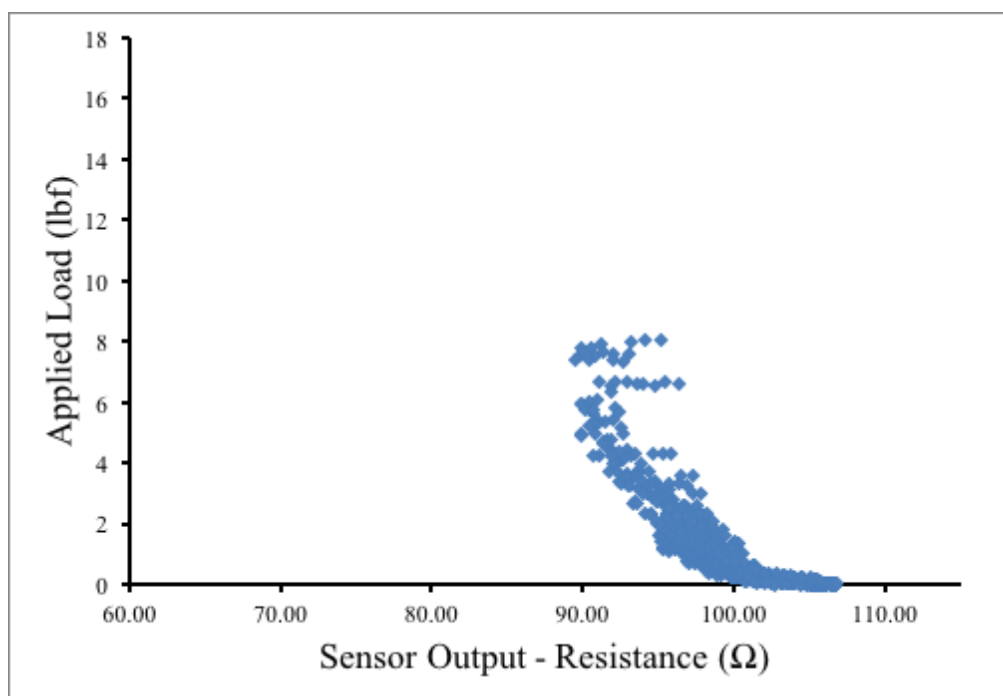


Figure 38. Coverstitch - 3/4" Green Polyester Curved

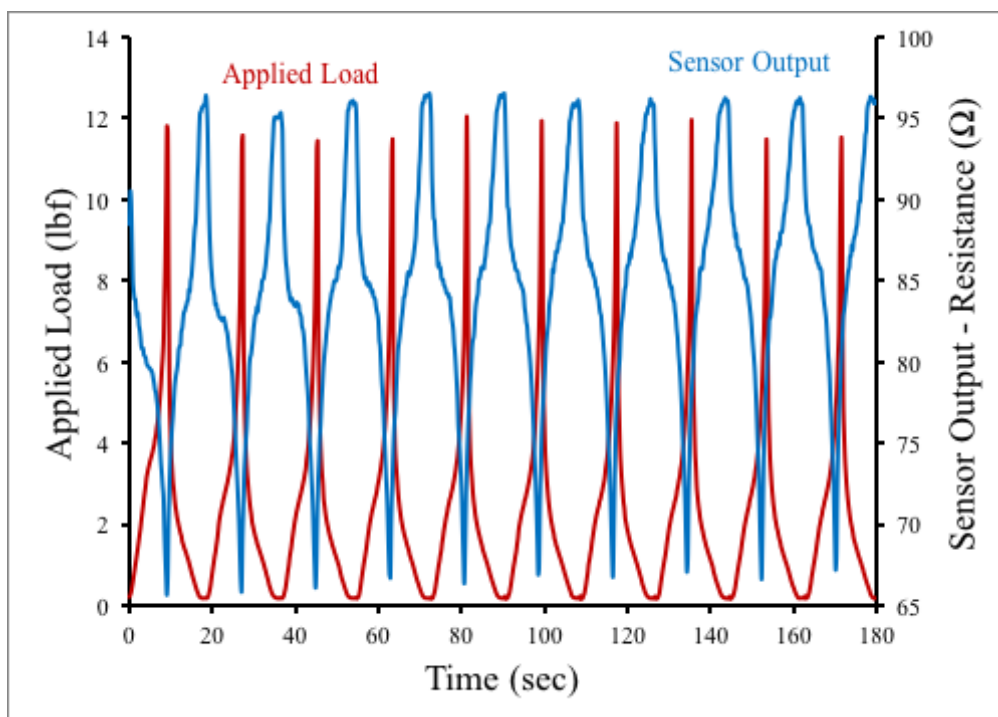


Figure 39. Coverstitch - 3/4" Green Polyester Squared

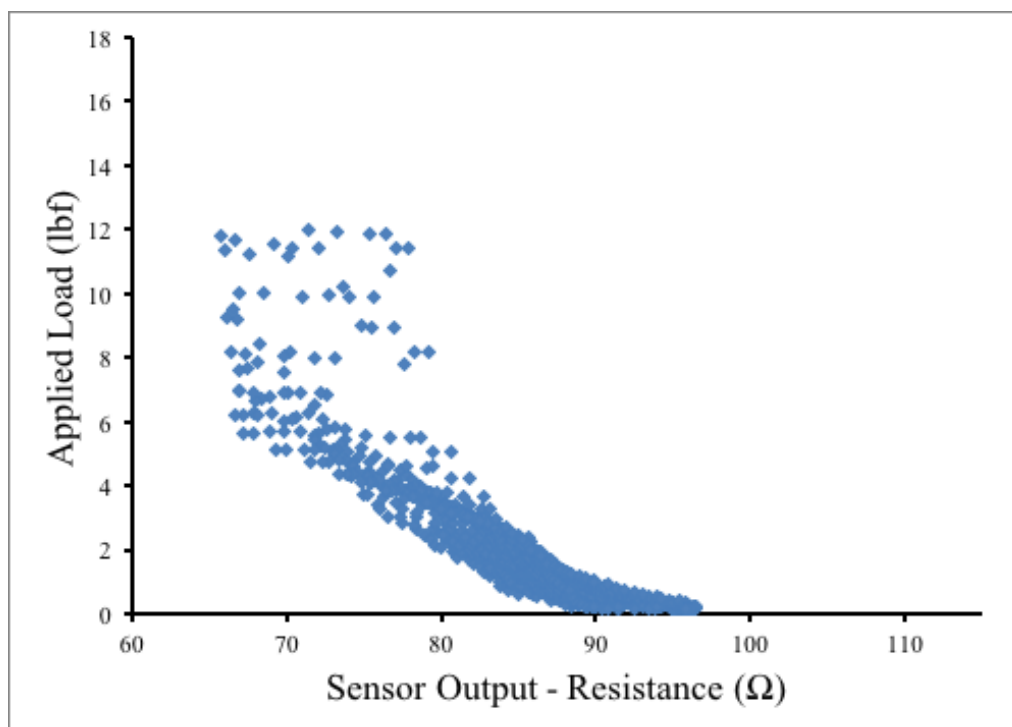


Figure 40. Coverstitch - 3/4" Green Polyester Squared

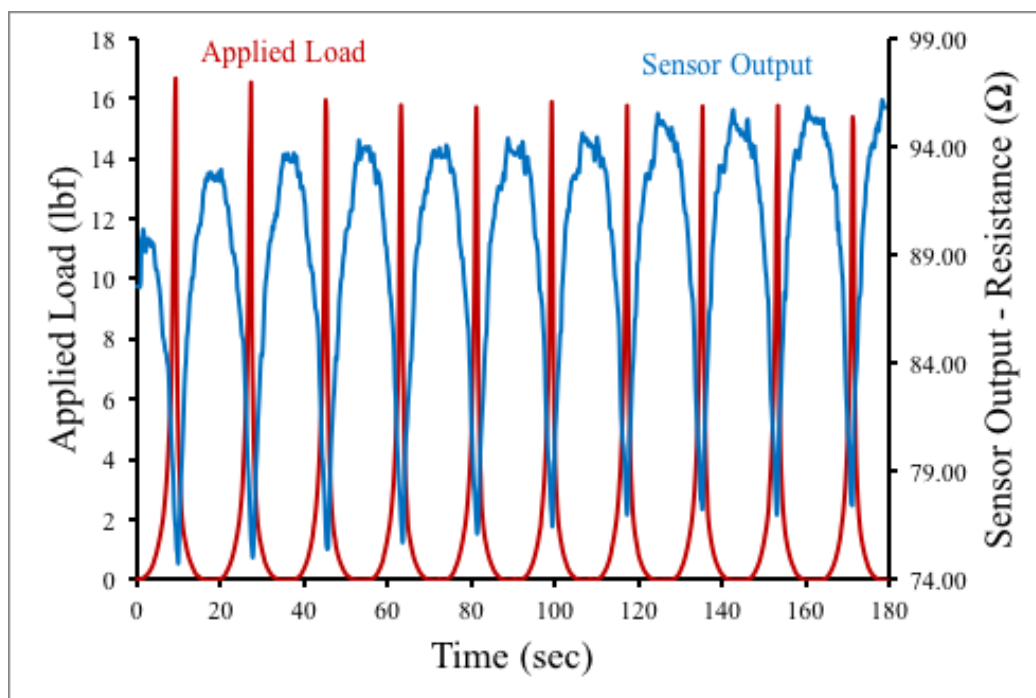


Figure 41. Coverstitch - 3/4" White Polyurethane Curved

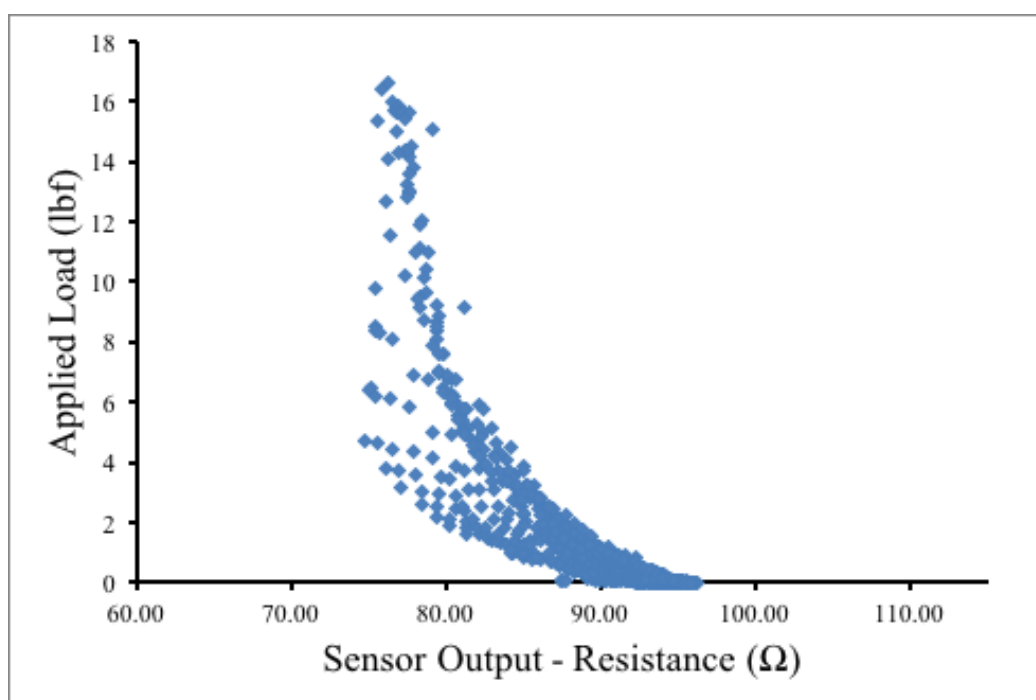


Figure 42. Coverstitch - 3/4" White Polyurethane Curved

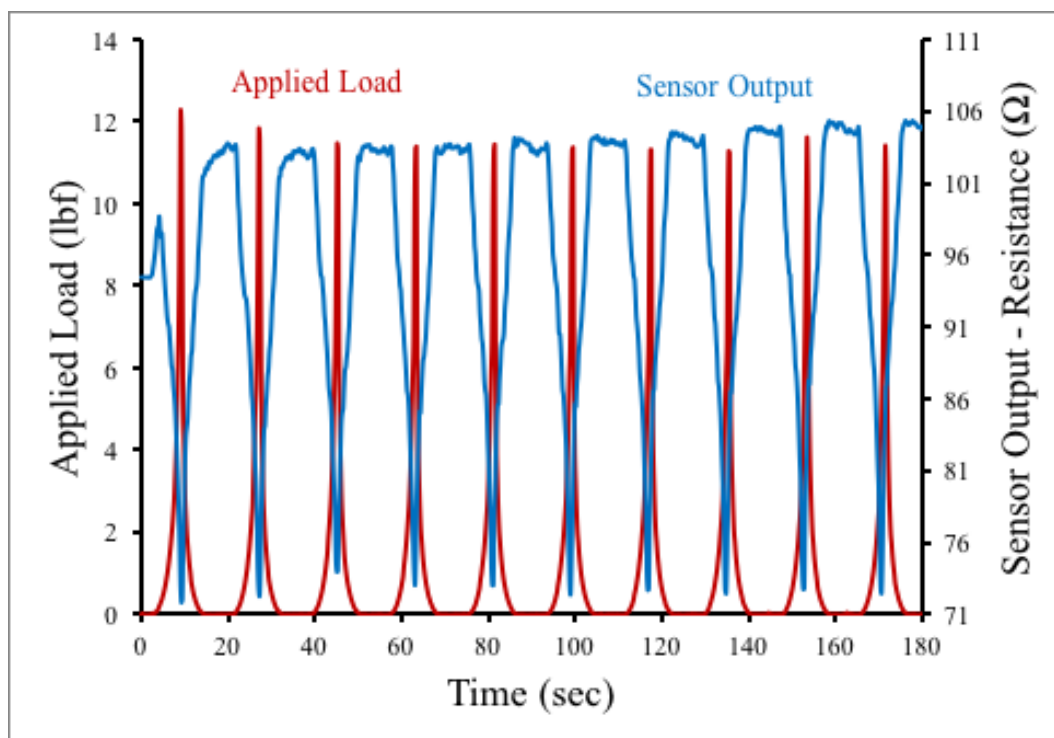


Figure 43. Coverstitch - 3/4" White Polyurethane Squared

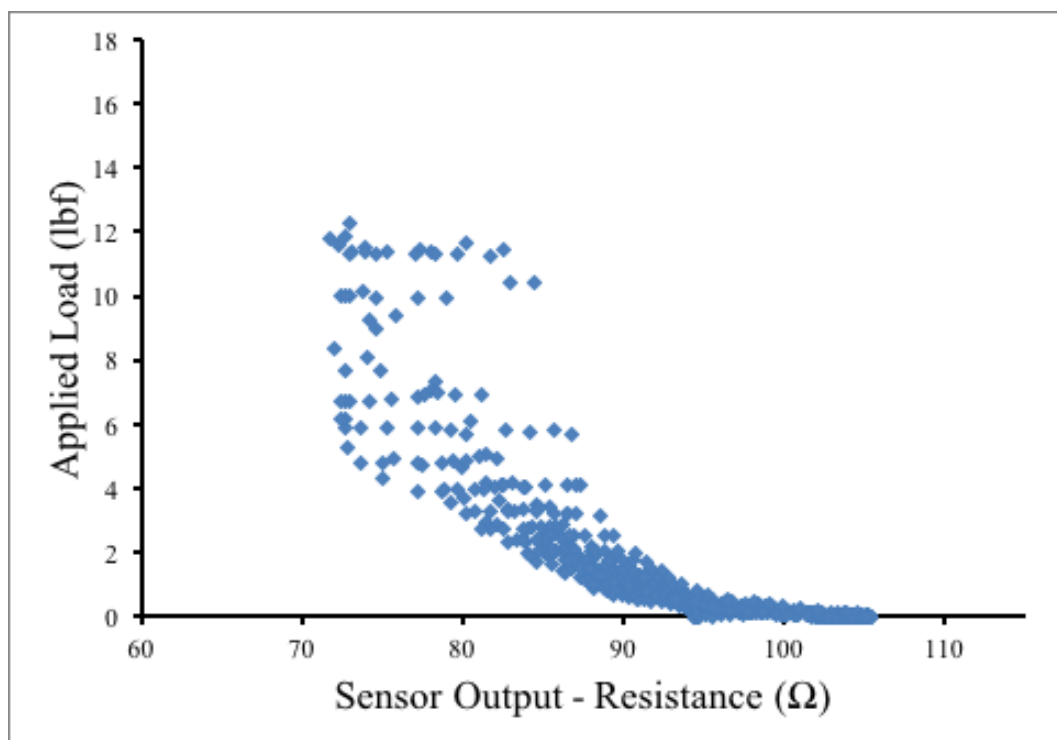


Figure 44. Coverstitch - 3/4" White Polyurethane Squared

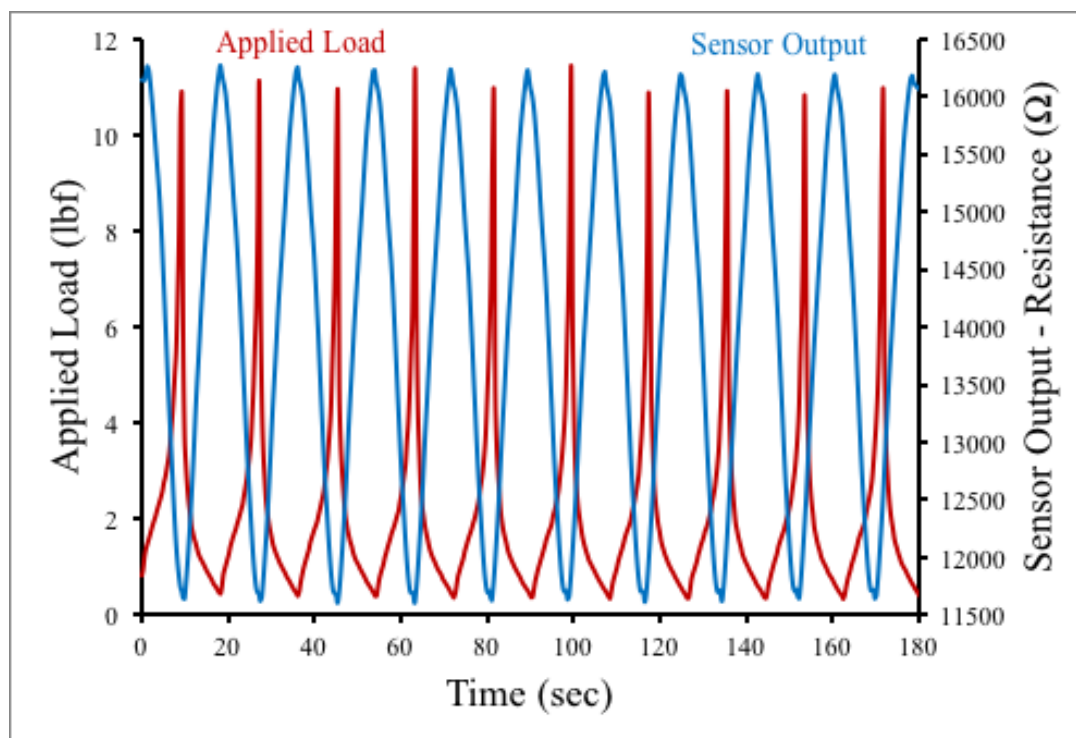


Figure 45. Flex Sensor - 1" Green Polyester Curved

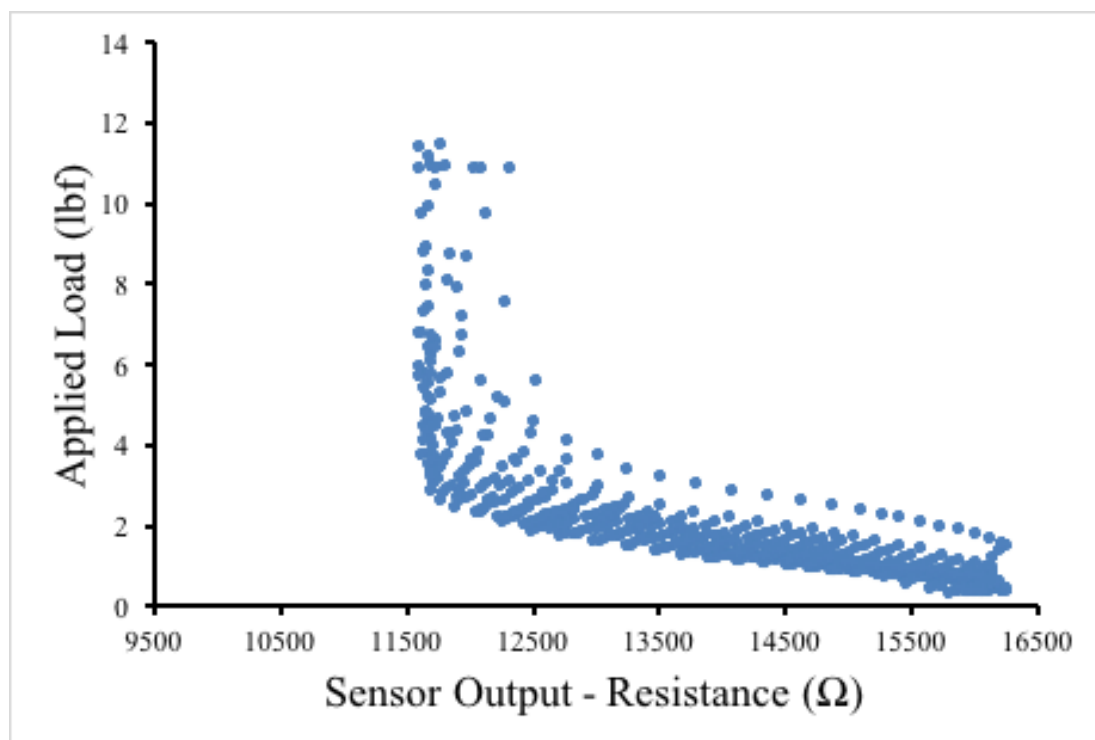


Figure 46. Flex Sensor - 1" Green Polyester Curved

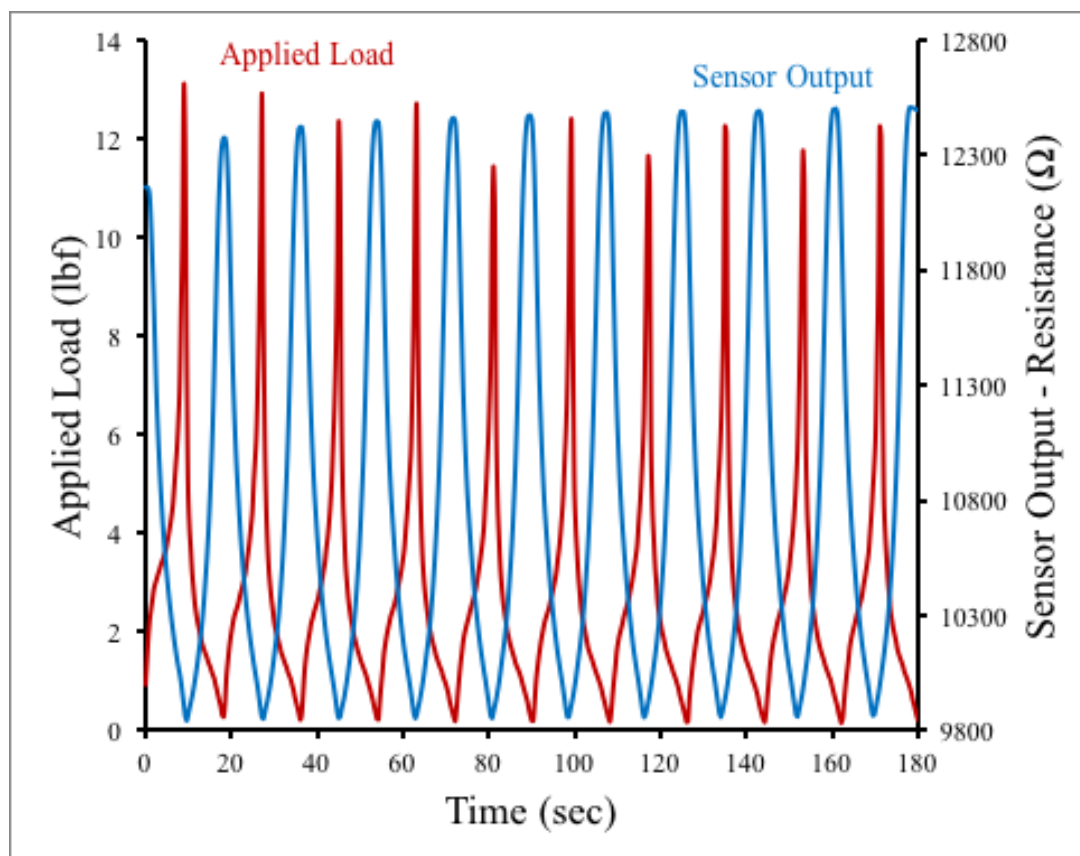


Figure 47. Flex Sensor - 1" Green Polyester Squared

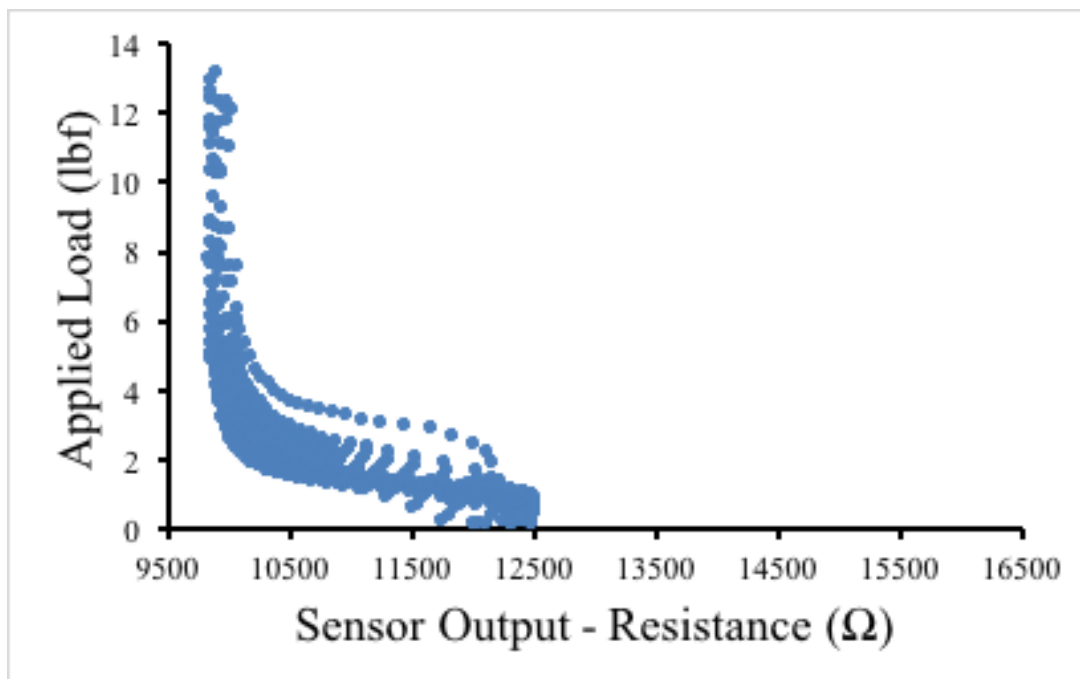


Figure 48. Flex Sensor - 1" Green Polyester Squared

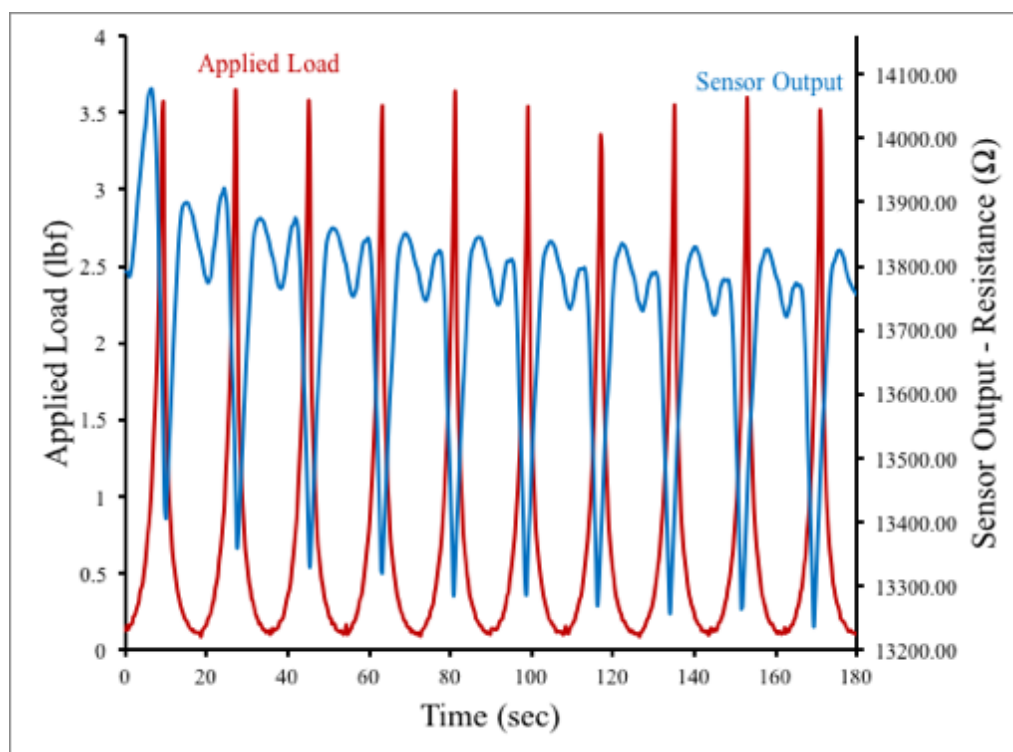


Figure 49. Flex Sensor - 1" White Polyurethane Curved

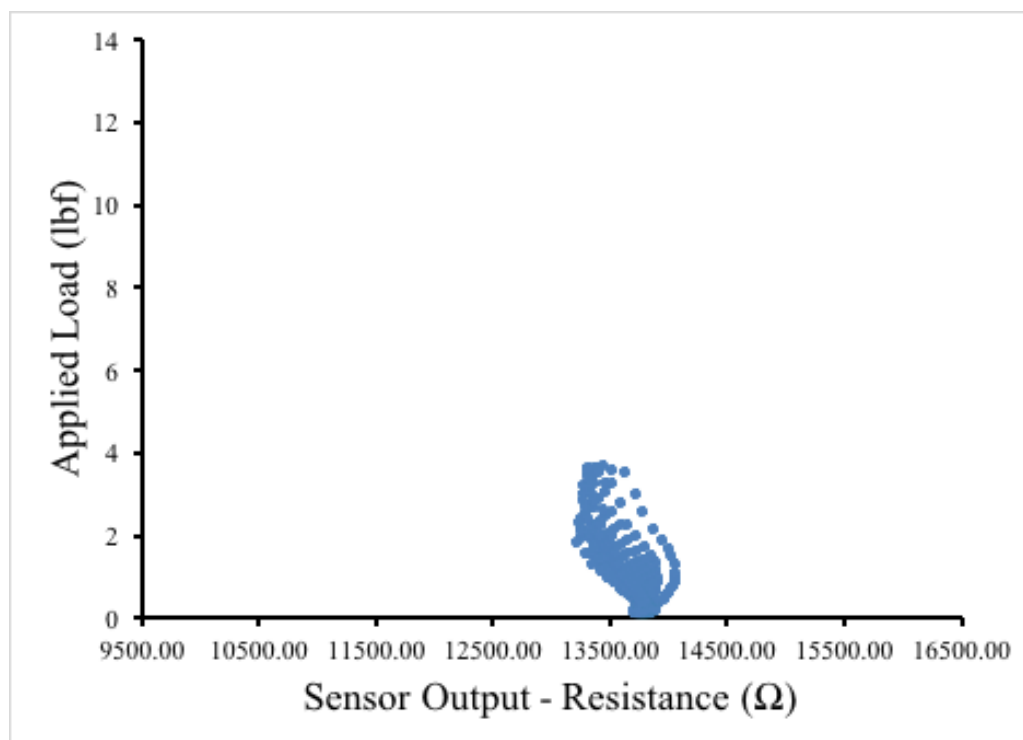


Figure 50. Flex Sensor - 1" White Polyurethane Curved

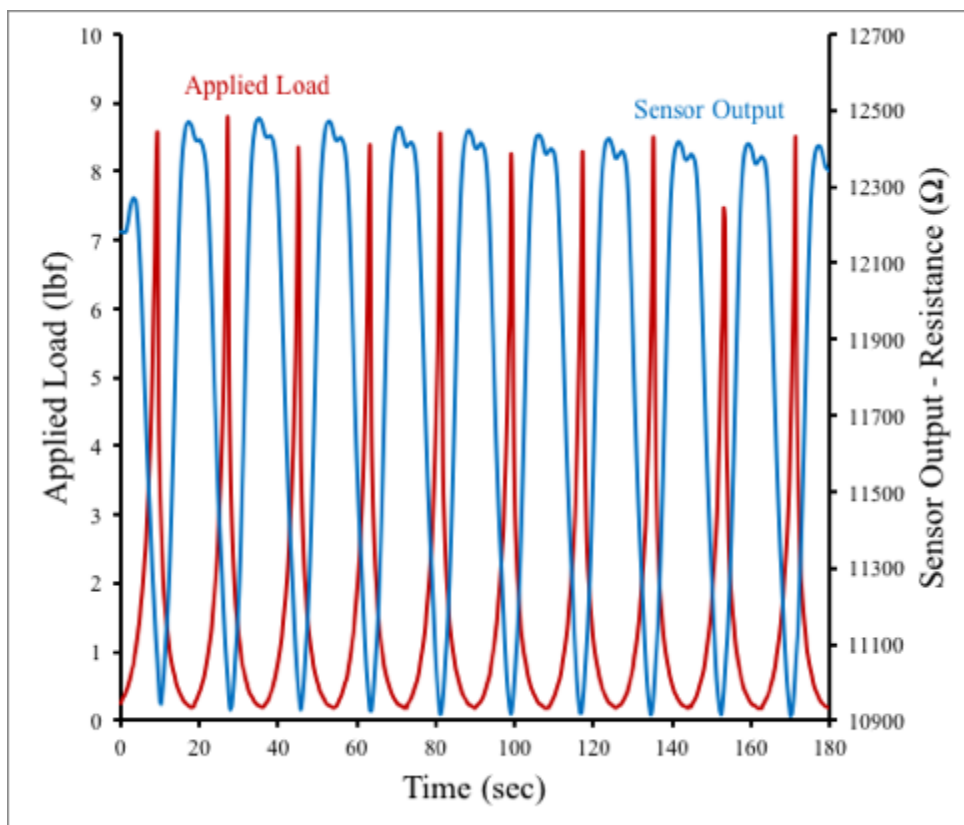


Figure 51. Flex Sensor - 1" White Polyurethane Squared

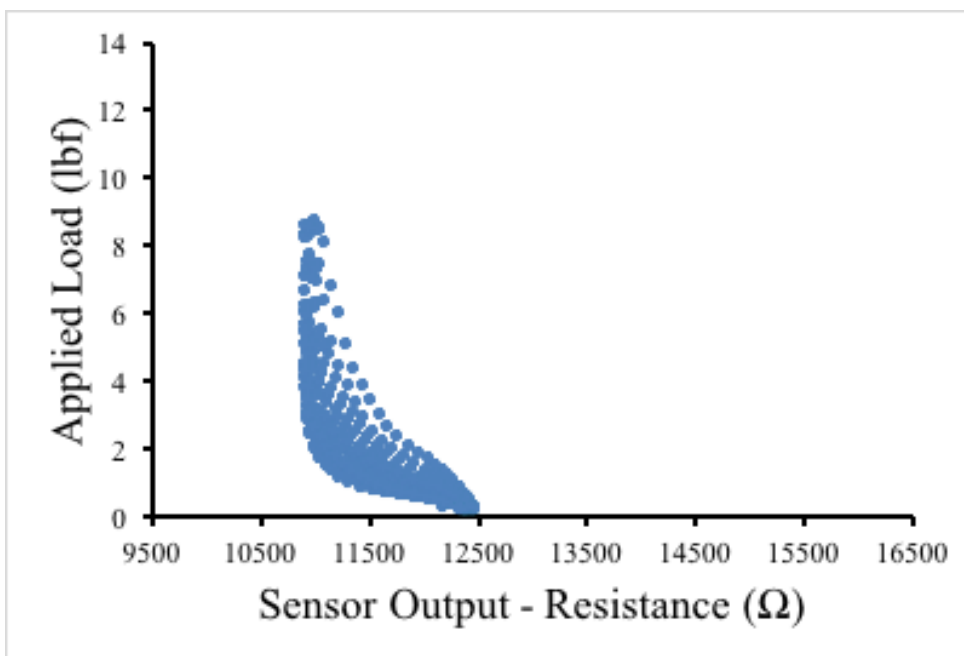


Figure 52. Flex Sensor - 1" White Polyurethane Squared

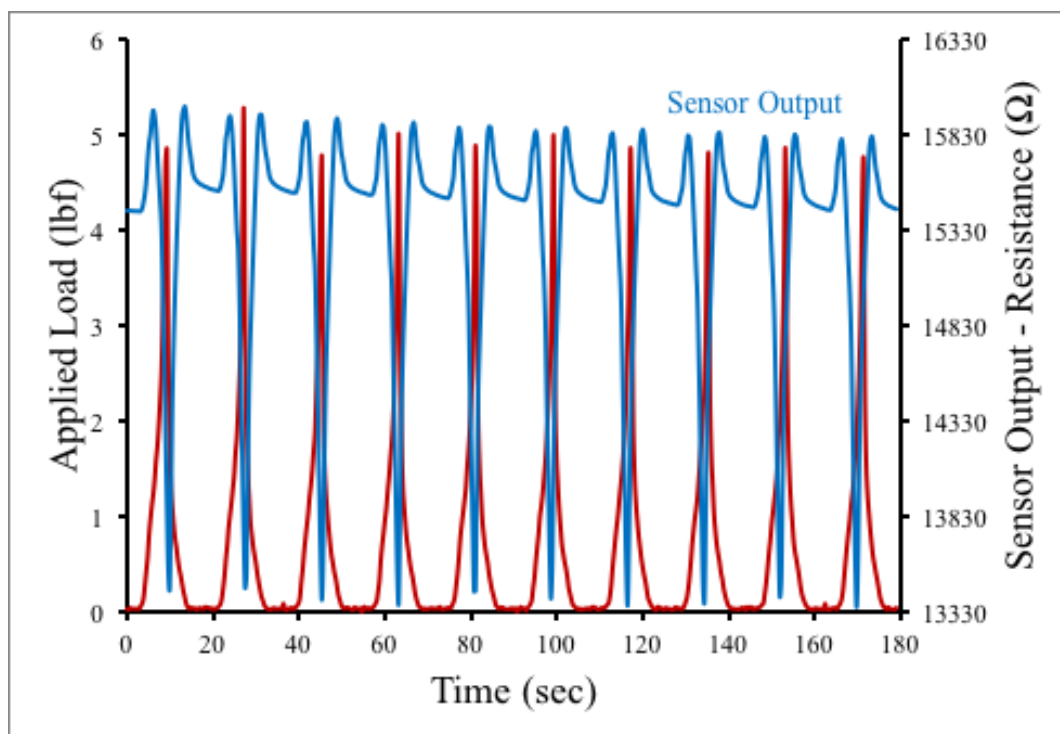


Figure 53. Flex Sensor – 1/2" Green Polyester Curved

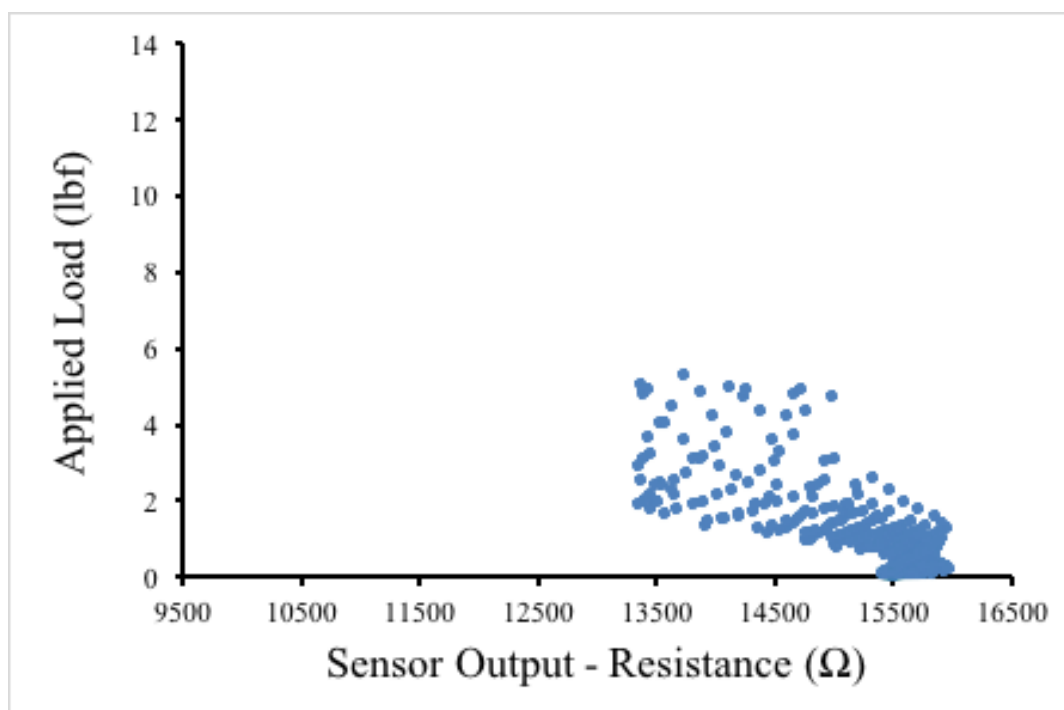


Figure 54. Flex Sensor – 1/2" Green Polyester Curved

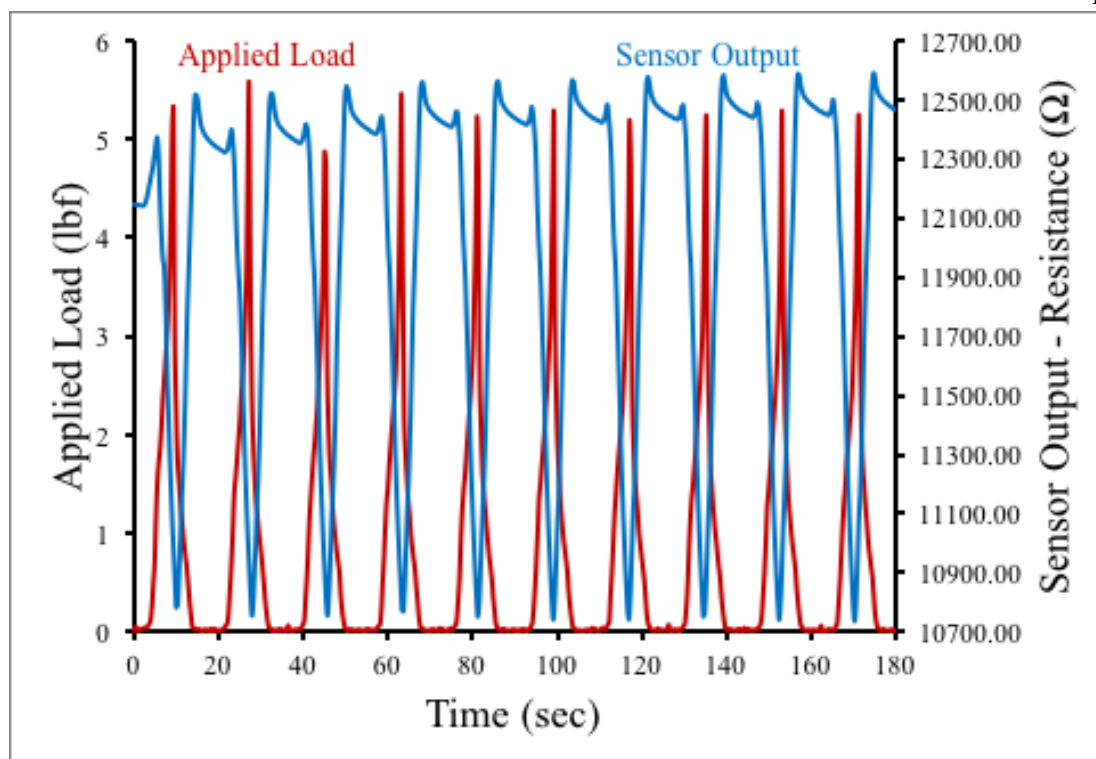


Figure 55. Flex Sensor – 1/2" Green Polyester Squared

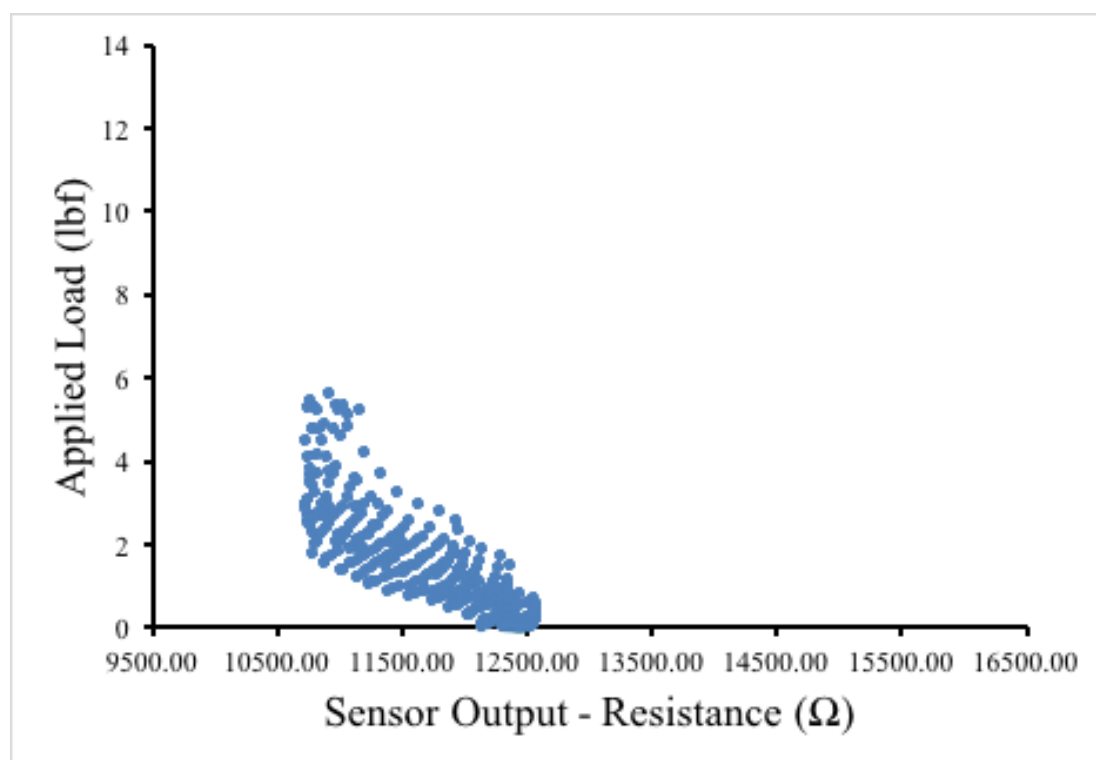


Figure 56. Flex Sensor – 1/2" Green Polyester Squared

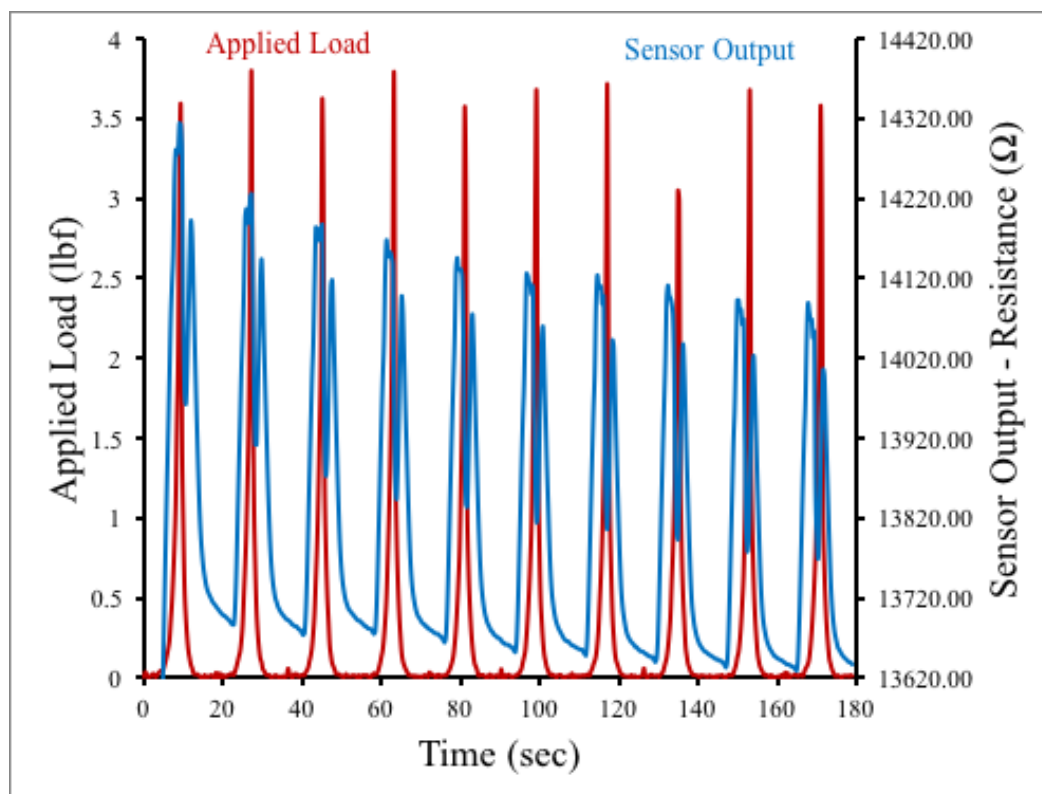


Figure 57. Flex Sensor – 1/2" White Polyurethane Curved

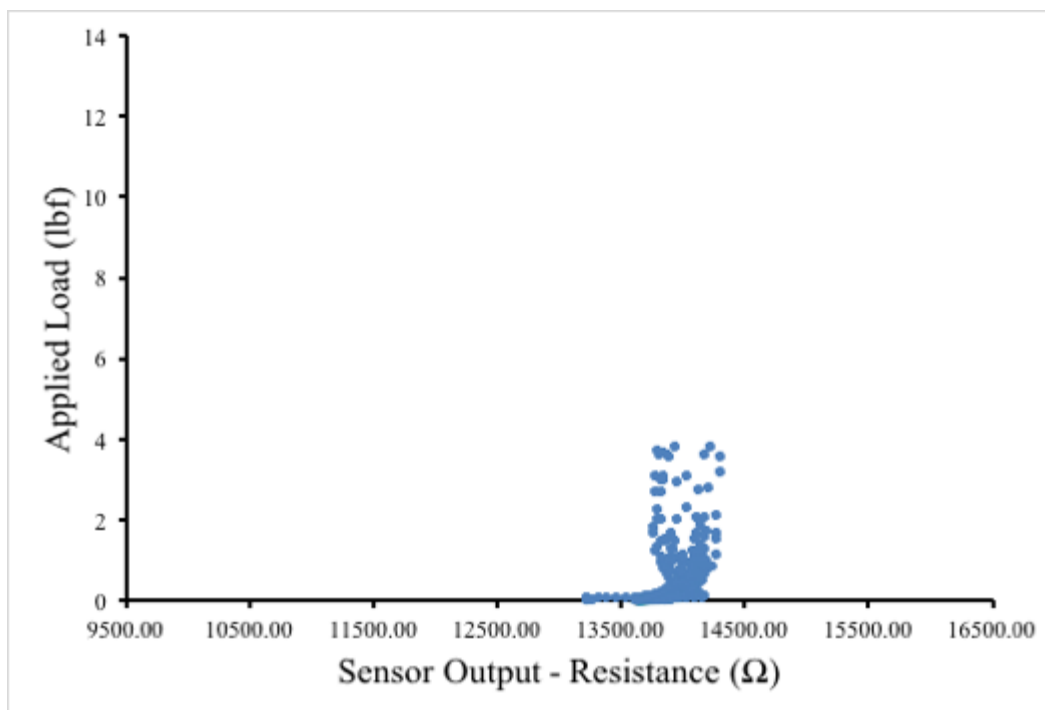


Figure 58. Flex Sensor – 1/2" White Polyurethane Curved

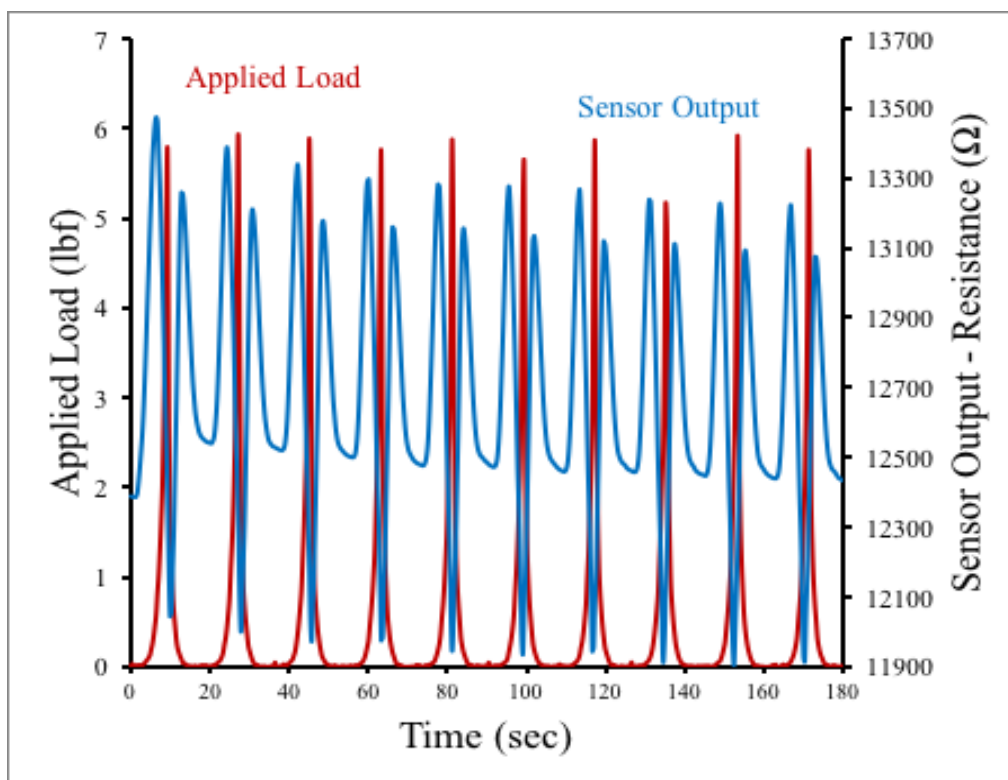


Figure 59. Flex Sensor – 1/2" White Polyurethane Squared

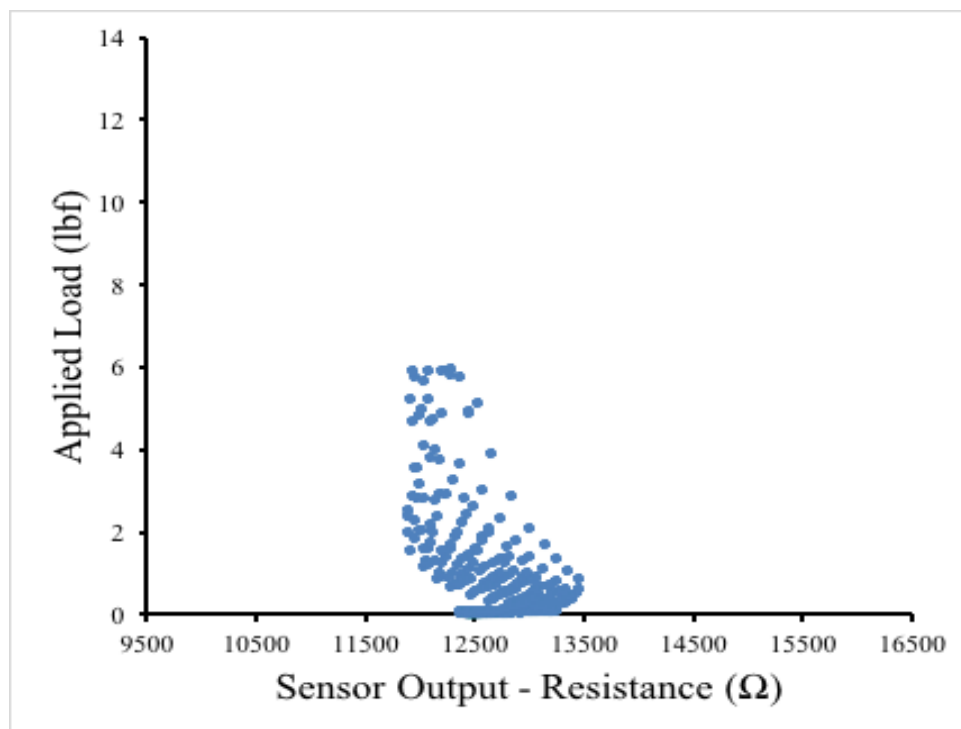


Figure 60. Flex Sensor – 1/2" White Polyurethane Squared

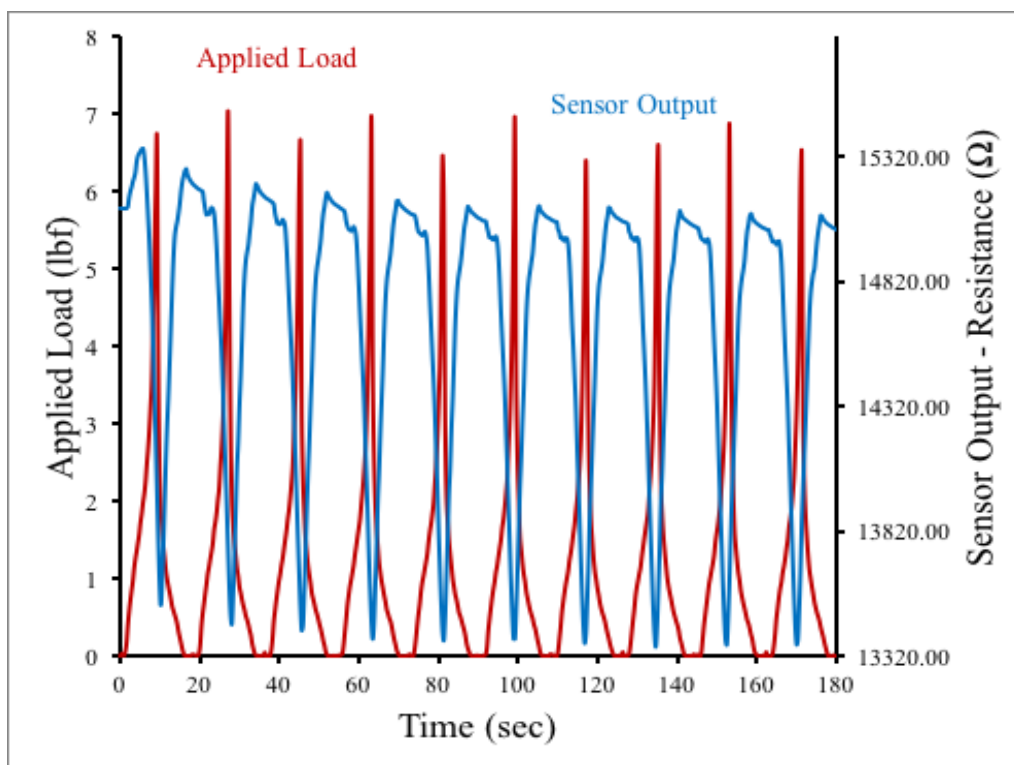


Figure 61. Flex Sensor - 3/4" Green Polyester Curved

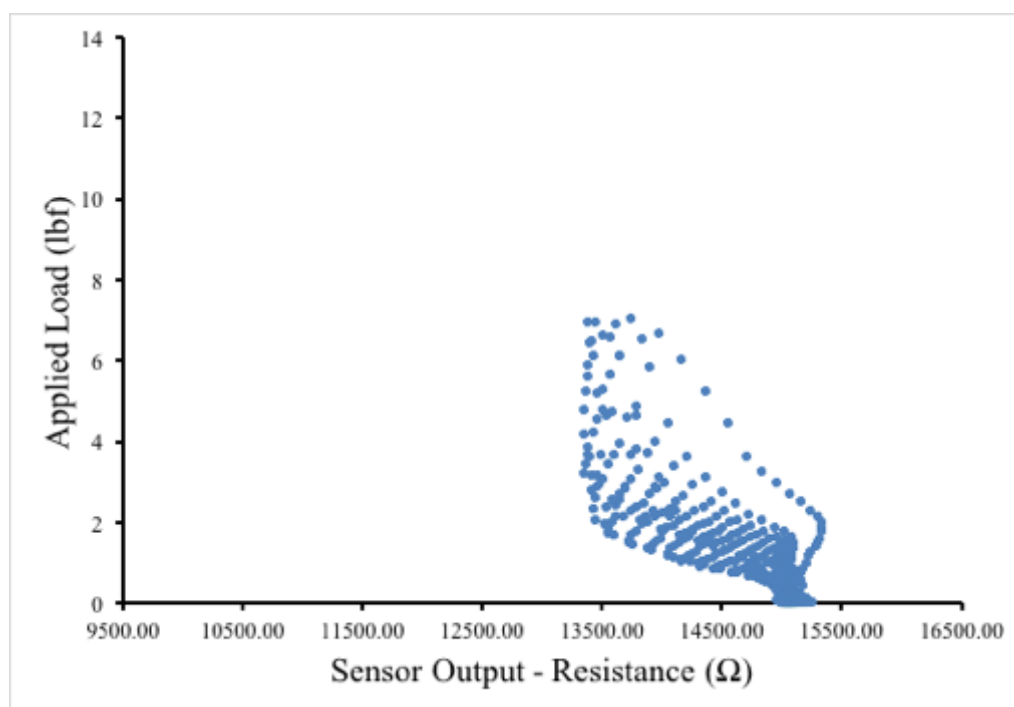


Figure 62. Flex Sensor - 3/4" Green Polyester Curved

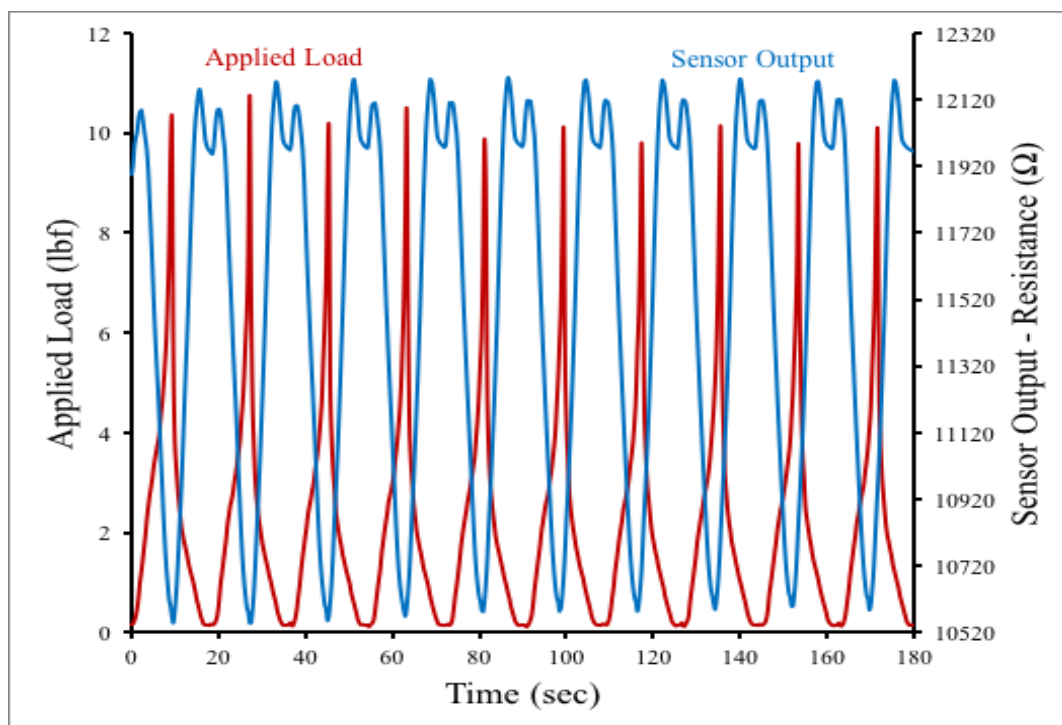


Figure 63. Flex Sensor - 3/4" Green Polyester Squared

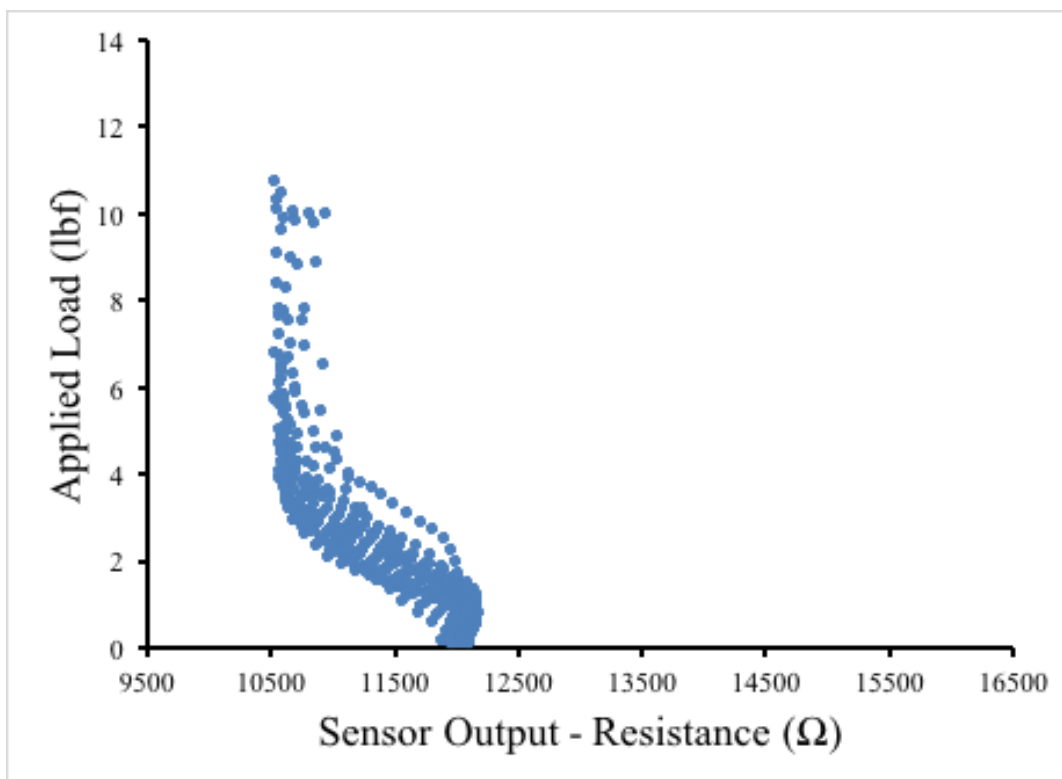


Figure 64. Flex Sensor - 3/4" Green Polyester Squared

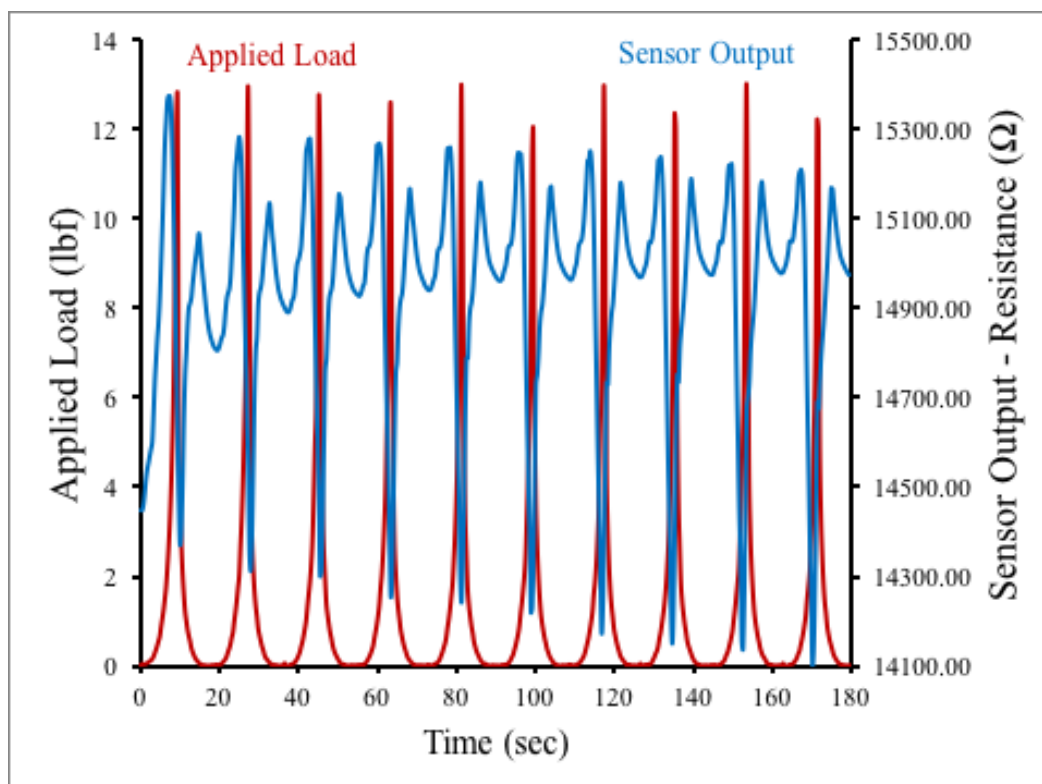


Figure 65. Flex Sensor - 3/4" White Polyurethane Curved

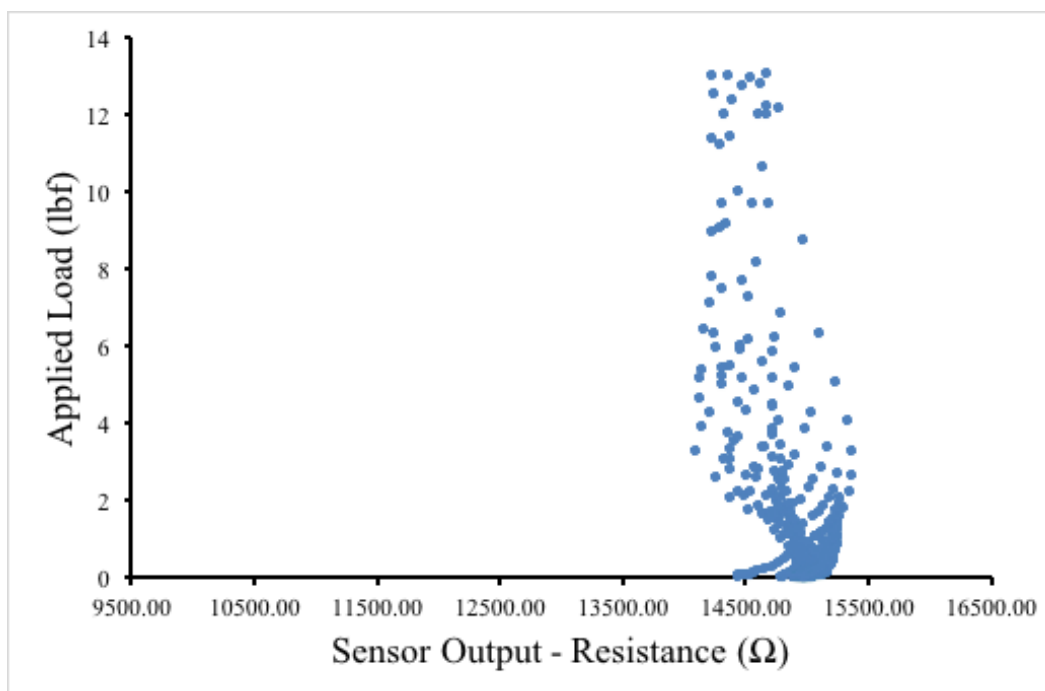


Figure 66. Flex Sensor - 3/4" White Polyurethane Curved

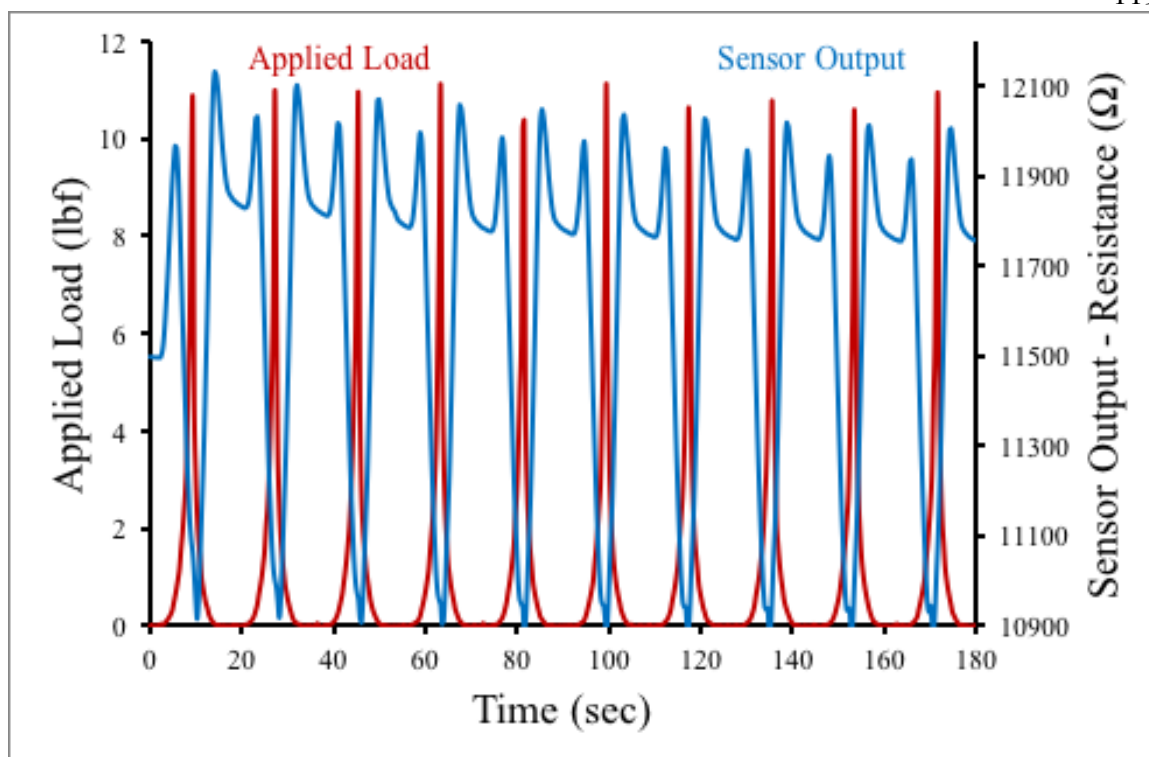


Figure 67. Flex Sensor - 3/4" White Polyurethane Squared

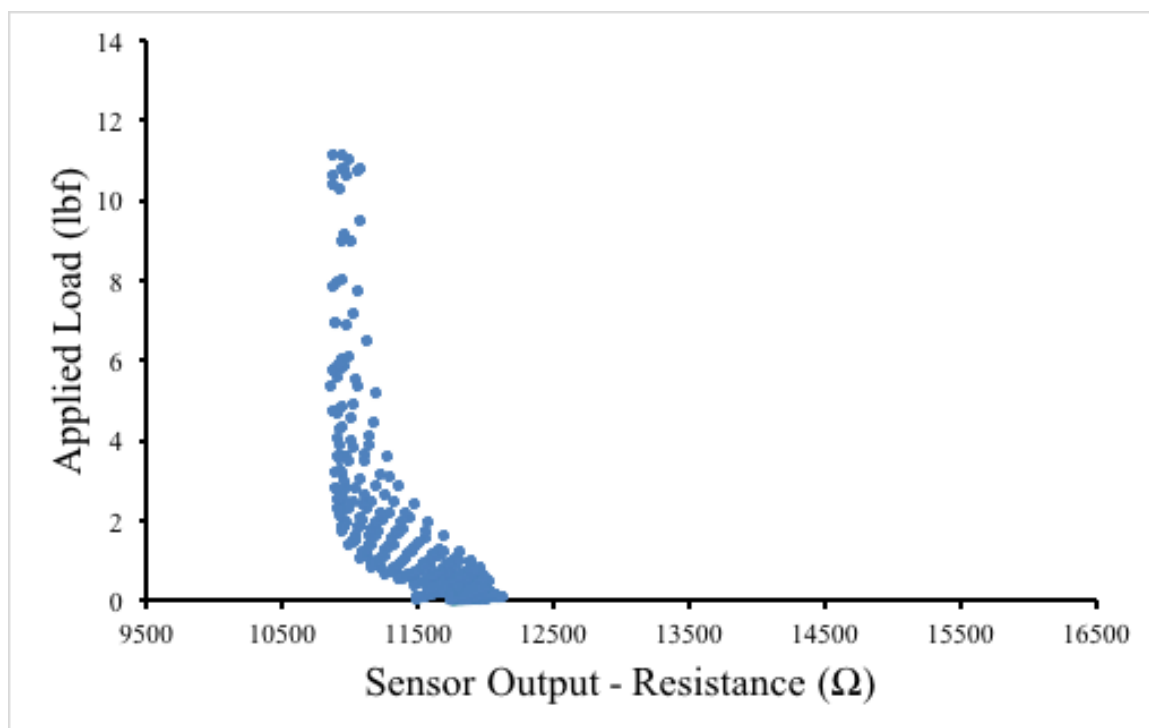
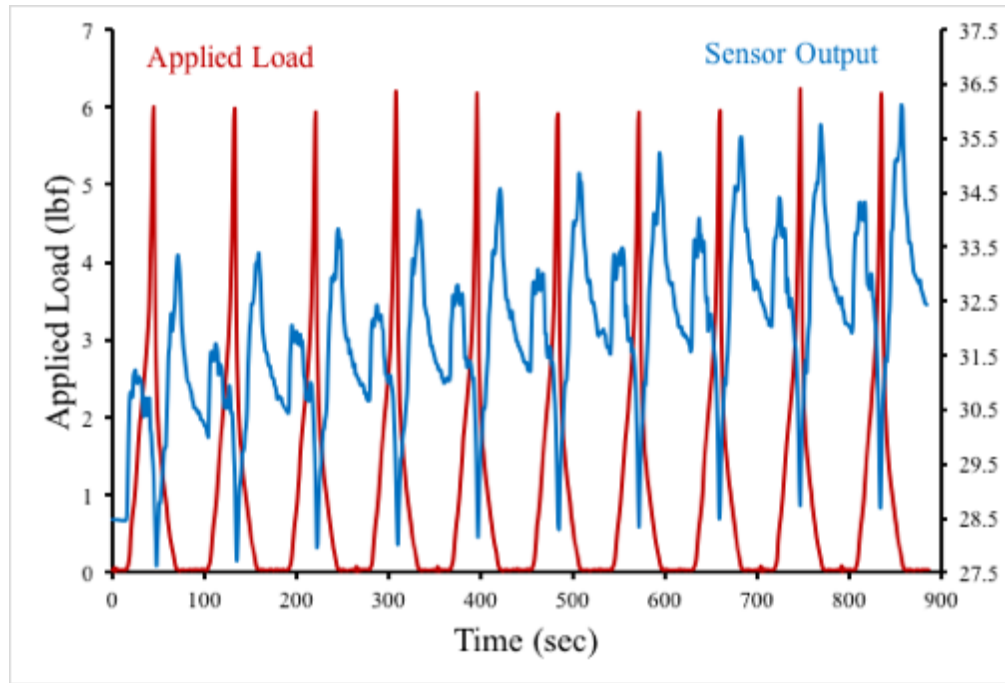
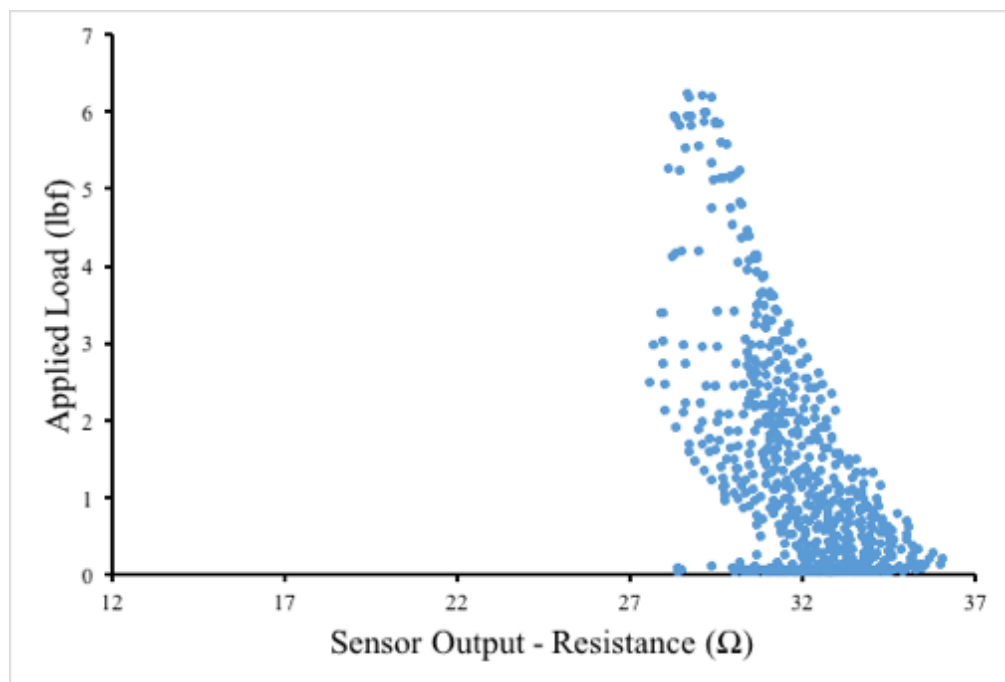


Figure 68. Flex Sensor - 3/4" White Polyurethane Squared

Appendix B: Additional Figures for Experiment 2**Figure 69. 4" Long 1/4" Thick****Figure 70. 4" Long 1/4" Thick**

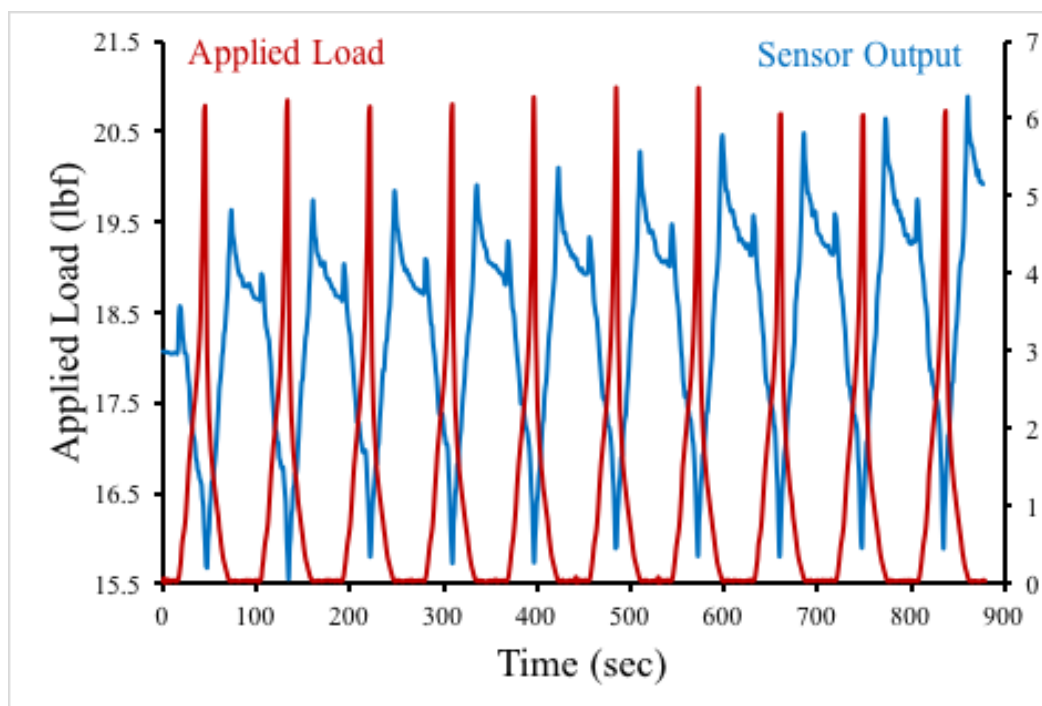


Figure 71. 4" Long 3/16" Thin

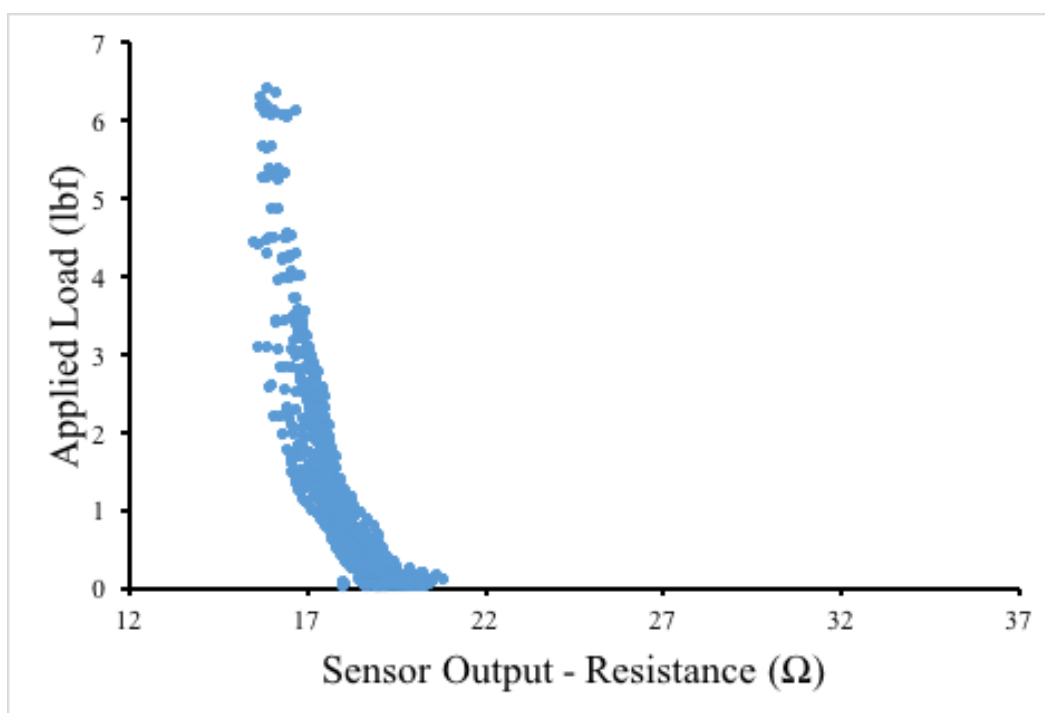


Figure 72. 4" Long 3/16" Thin

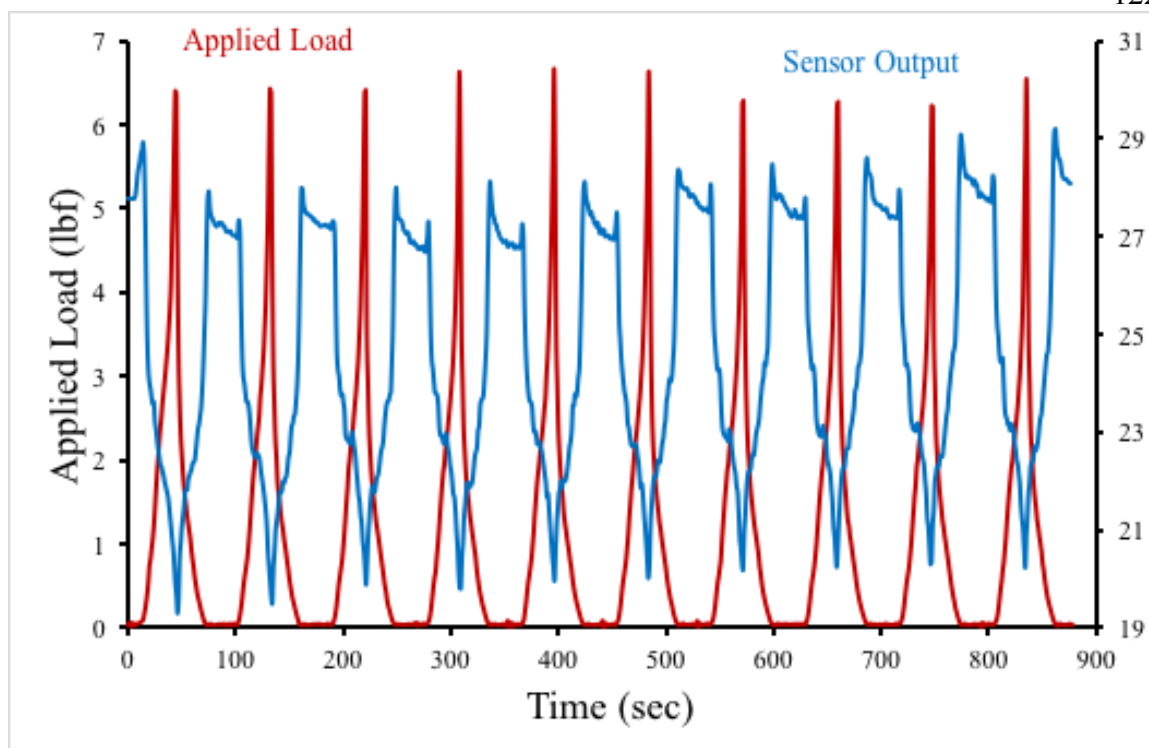


Figure 73. 3" Long 1/4" Thick

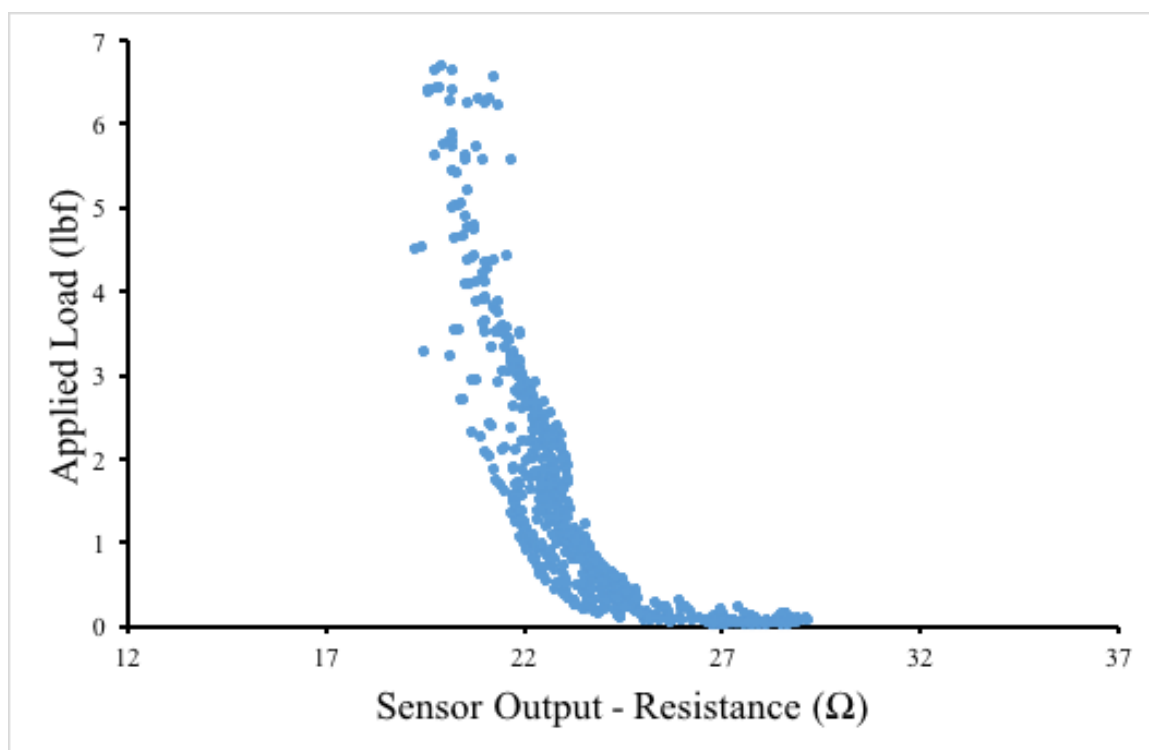


Figure 74. 3" Long 1/4" Thick

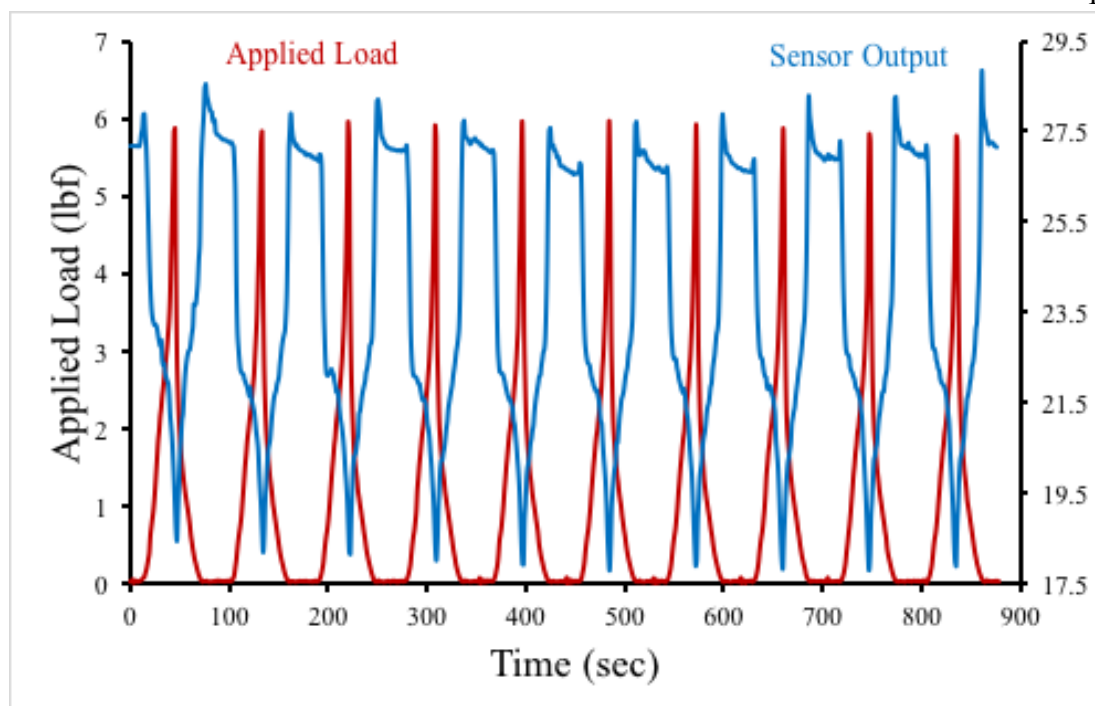


Figure 75. 3" Long 3/16" Thin

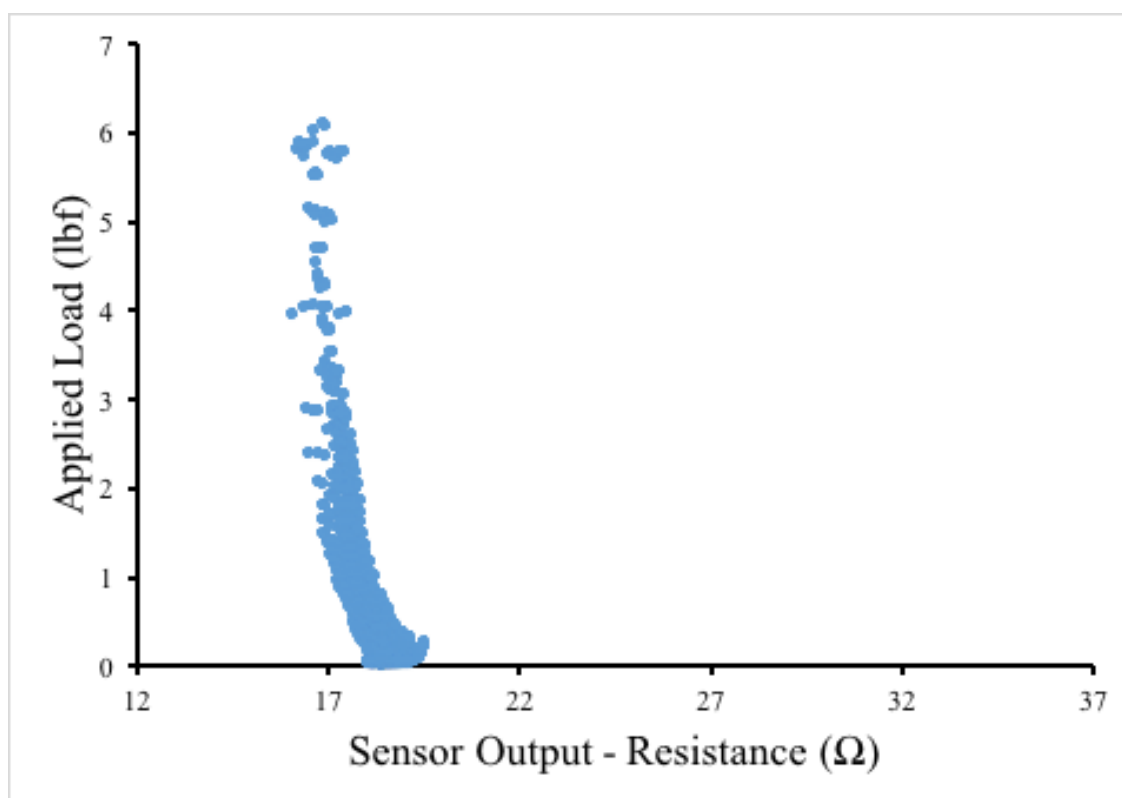


Figure 76. 3" Long 3/16" Thin

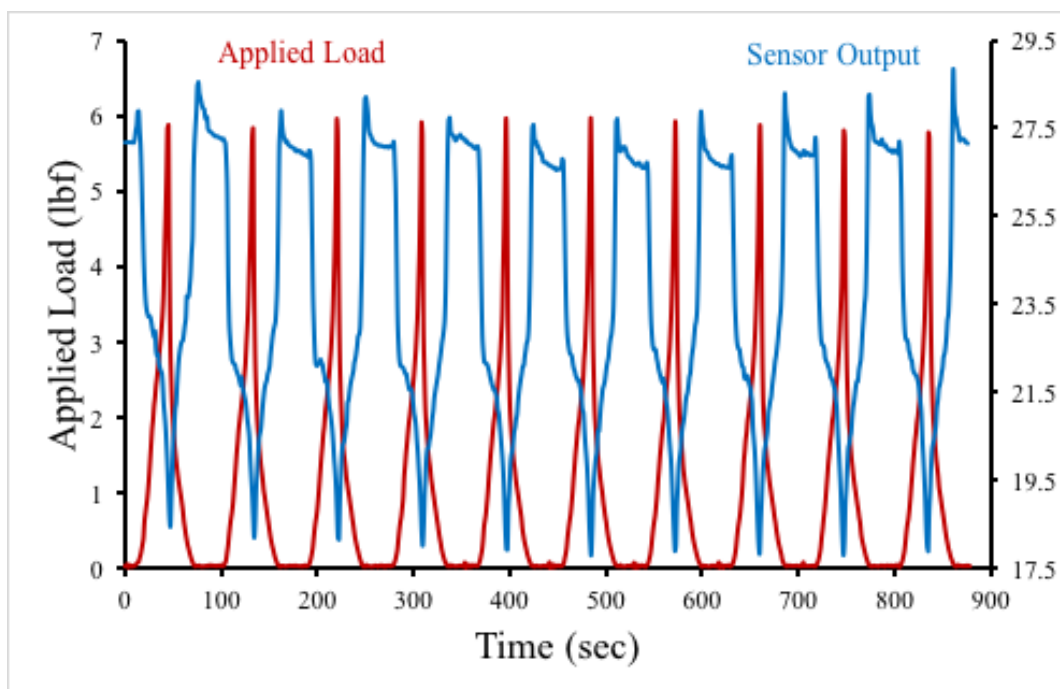


Figure 77. 2" Long 1/4" Thick

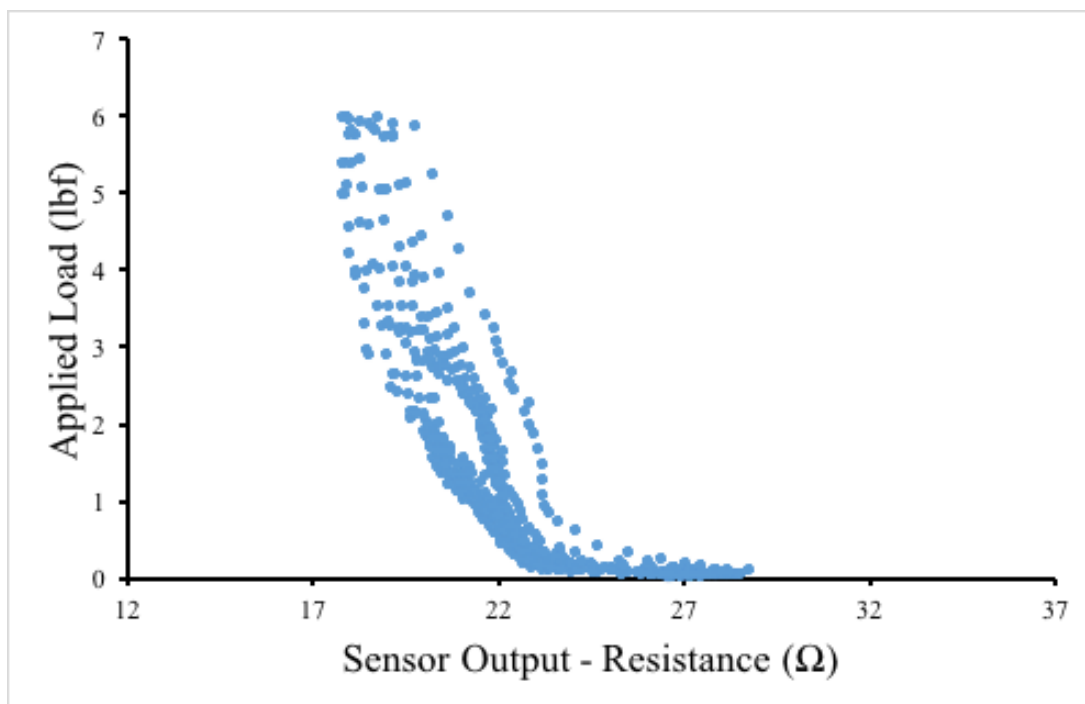


Figure 78. 2" Long 1/4" Thick

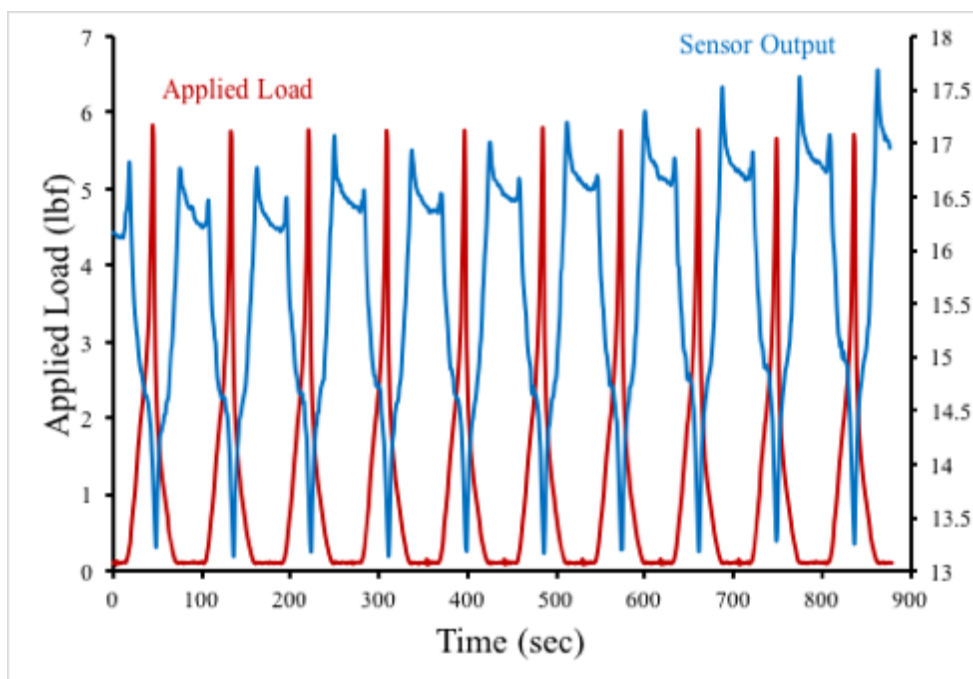


Figure 79. 2" Long 3/16" Thin

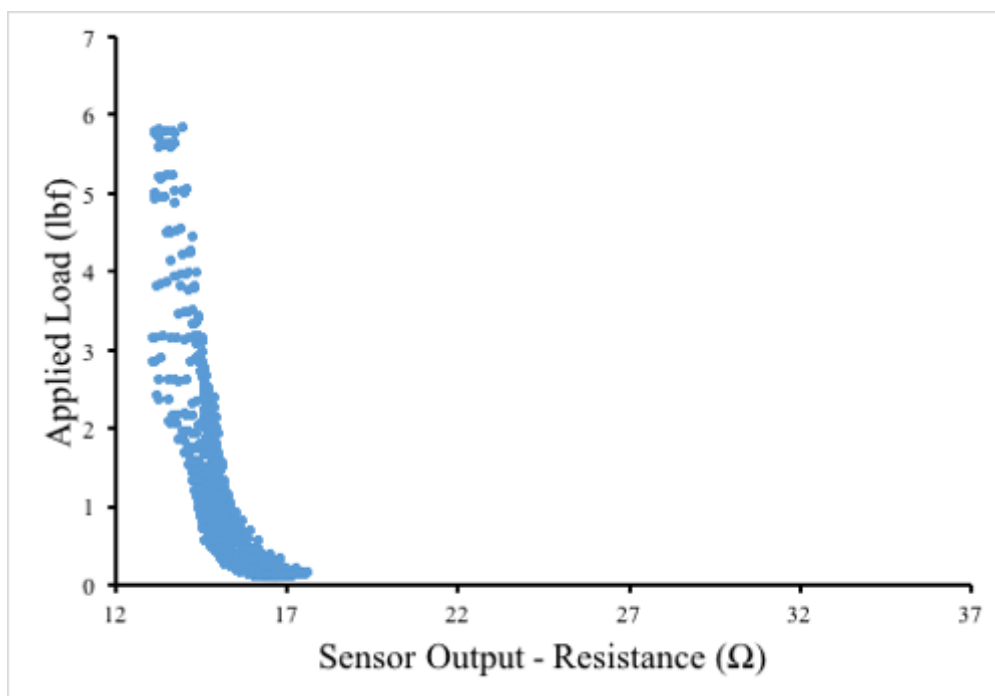


Figure 80. 2" Long 3/16" Thin

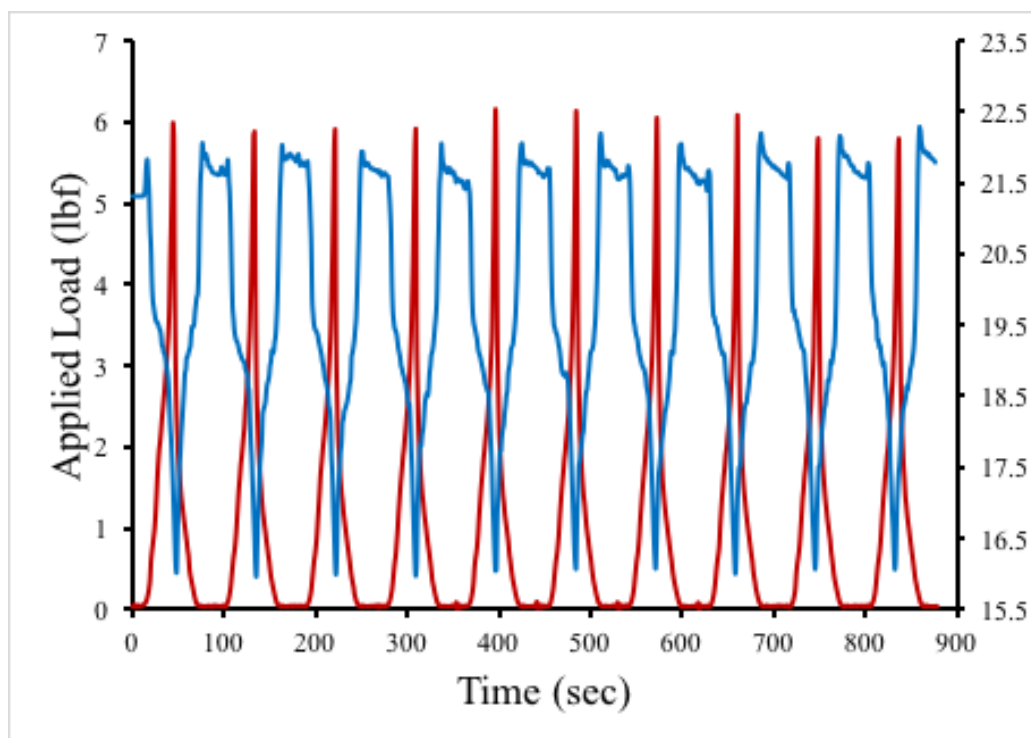


Figure 81. 1" Long 1/4" Thick

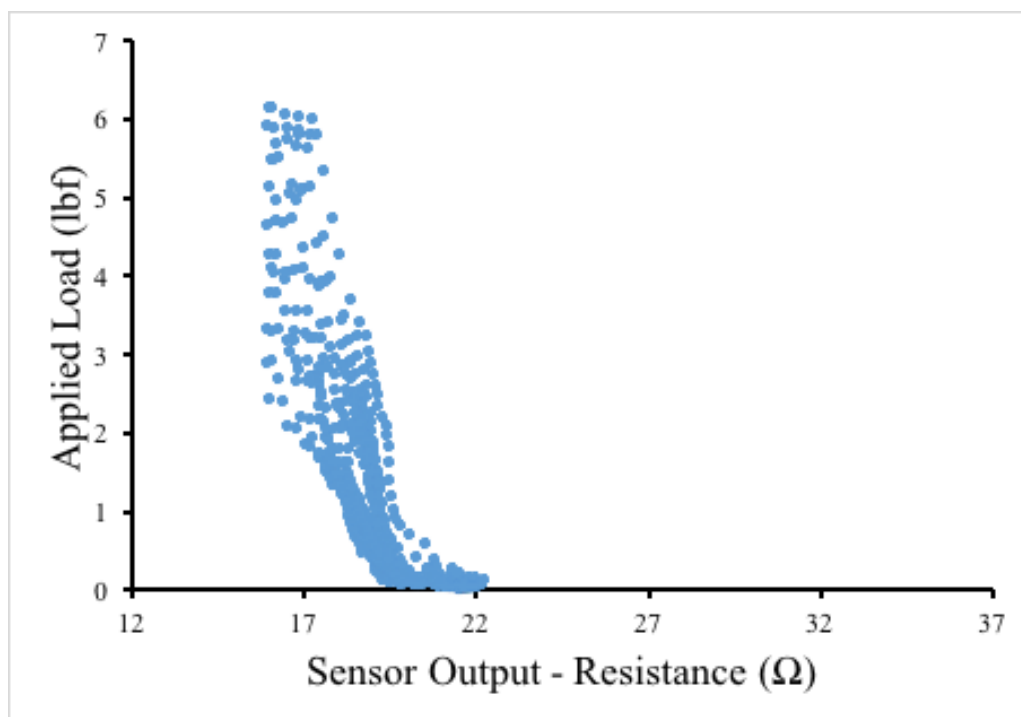


Figure 82. 1" Long 1/4" Thick

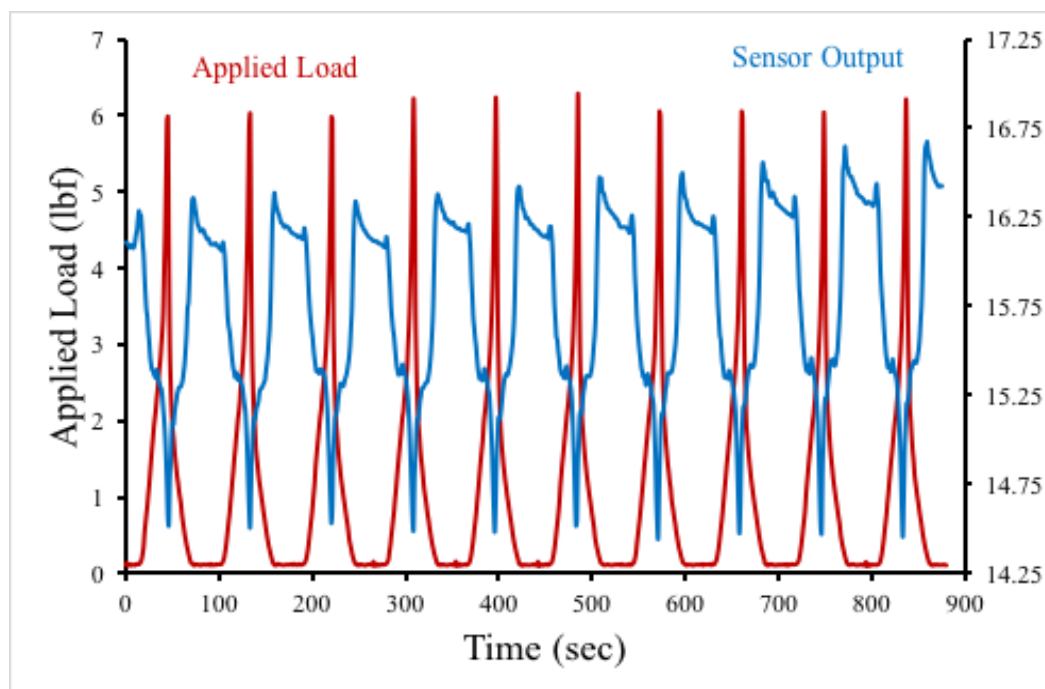


Figure 83. 1" Long 3/16" Thin

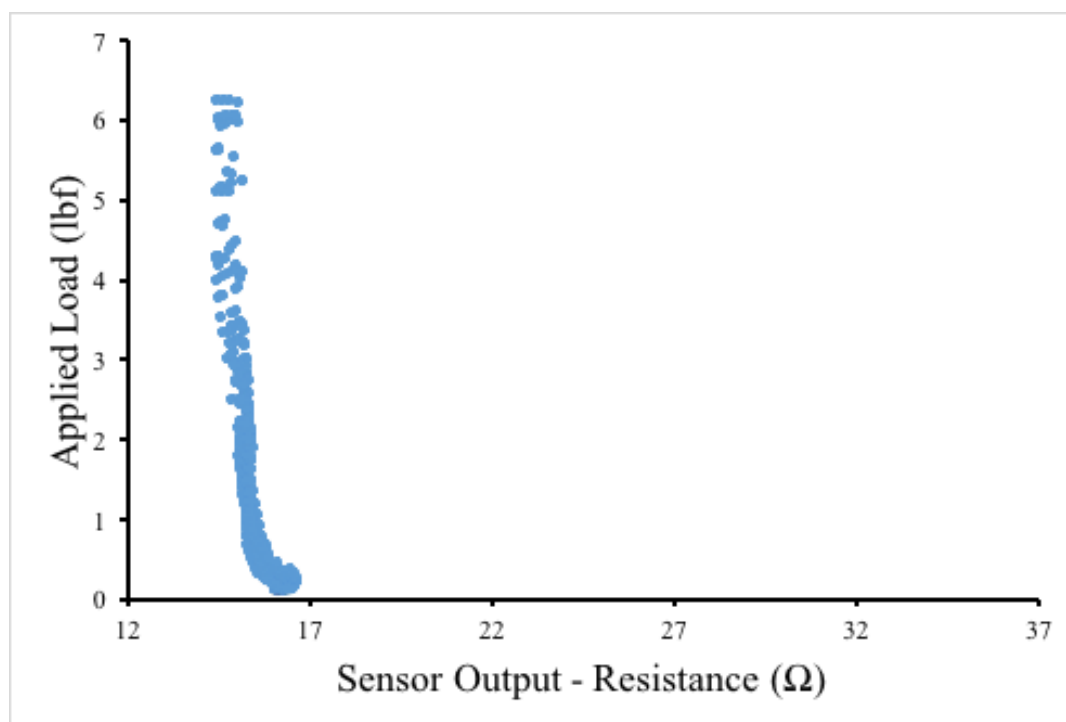


Figure 84. 1" Long 3/16" Thin

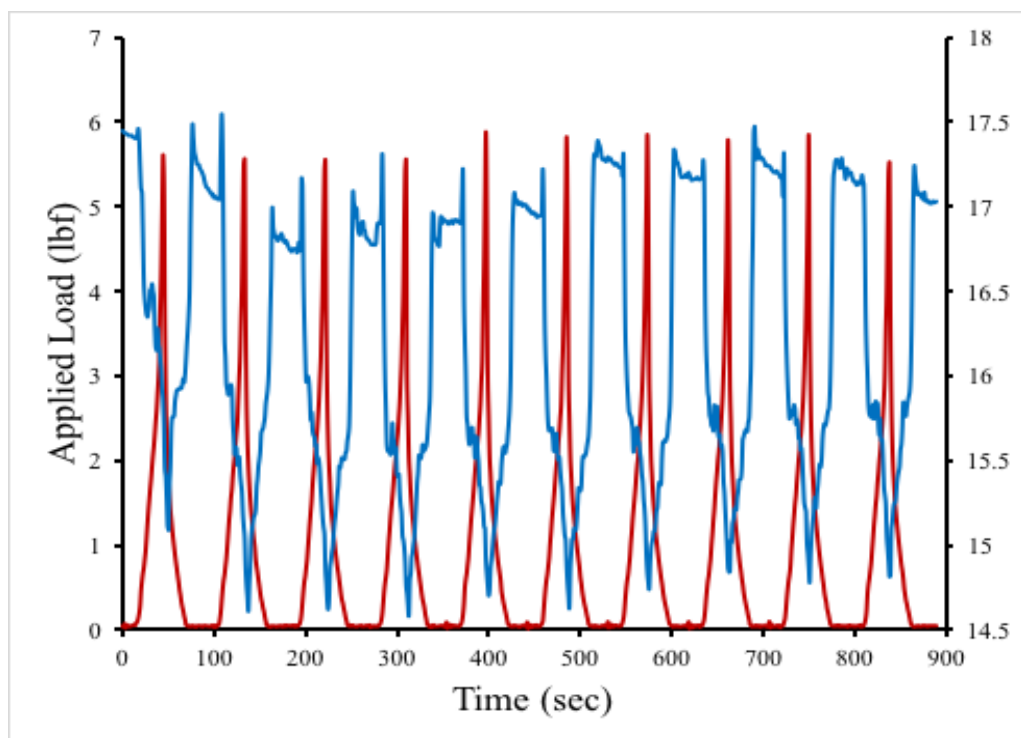


Figure 85. 1/2" Long 1/4" Thick

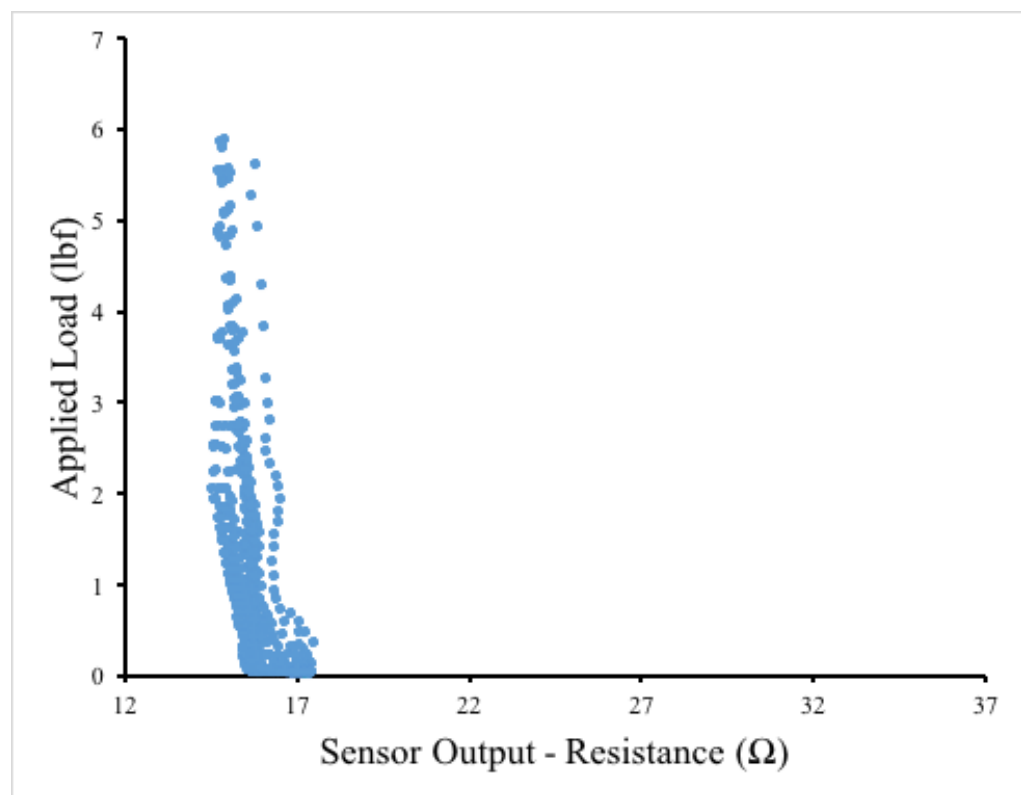


Figure 86. 1/2" Long 1/4" Thick

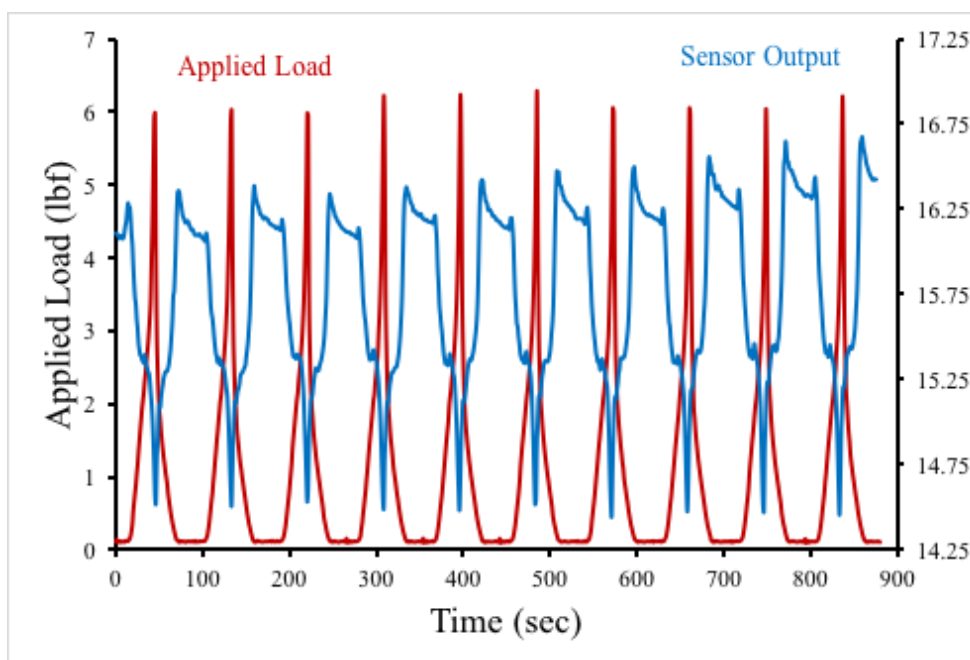


Figure 87. 1/2" Long 3/16" Thin

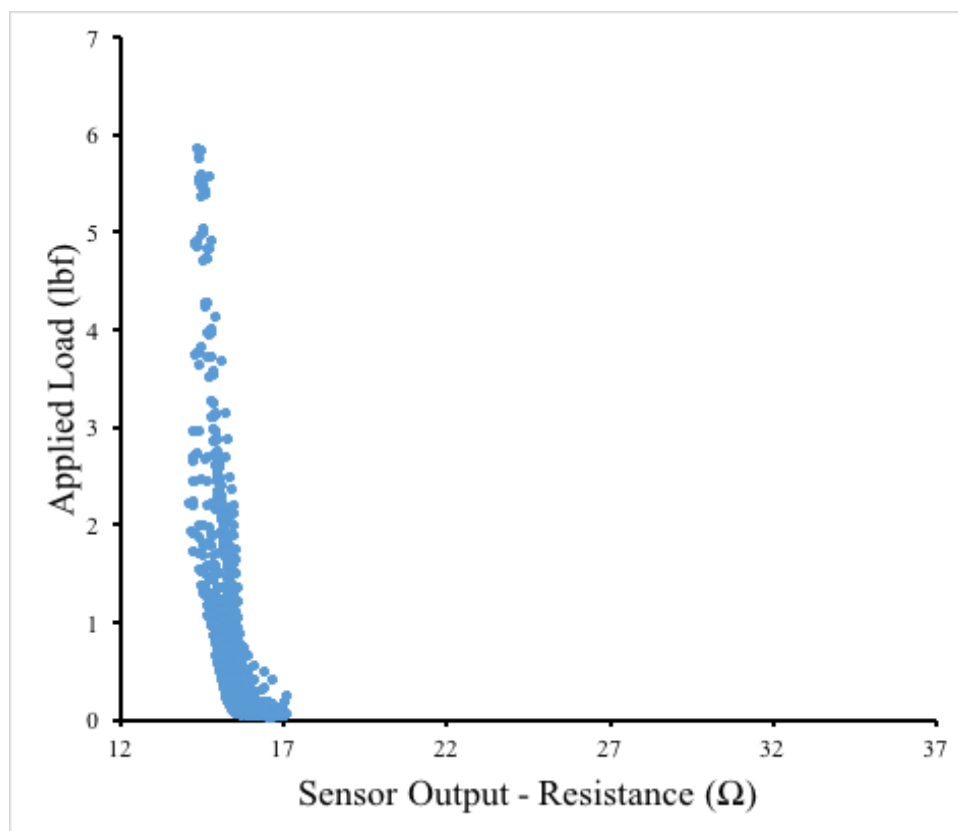


Figure 88. 1/2" Long 3/16" Thin

Appendix C: Additional Figures for Experiment 3

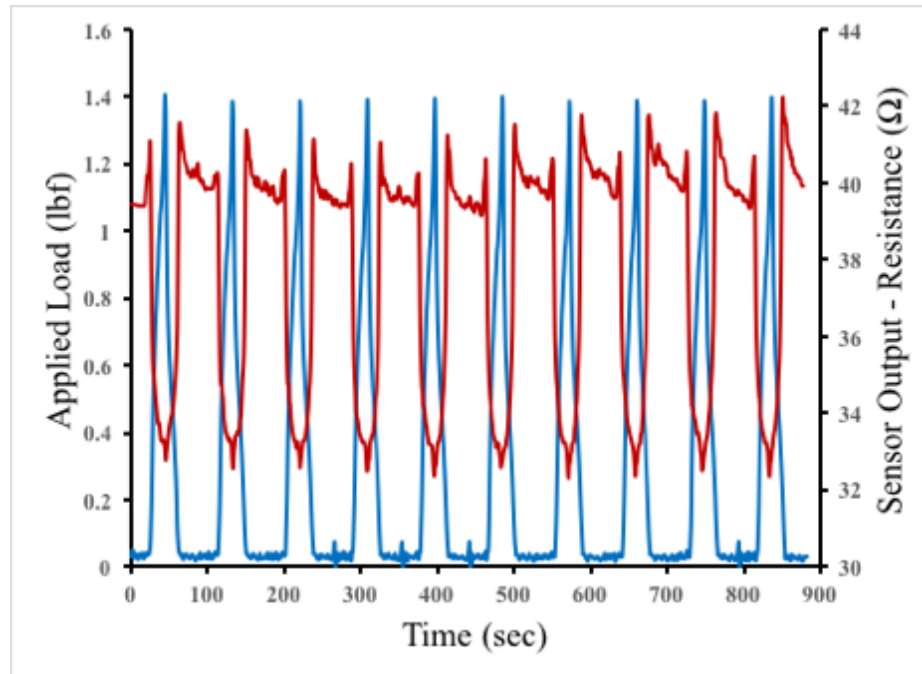


Figure 89. Flat Rubber

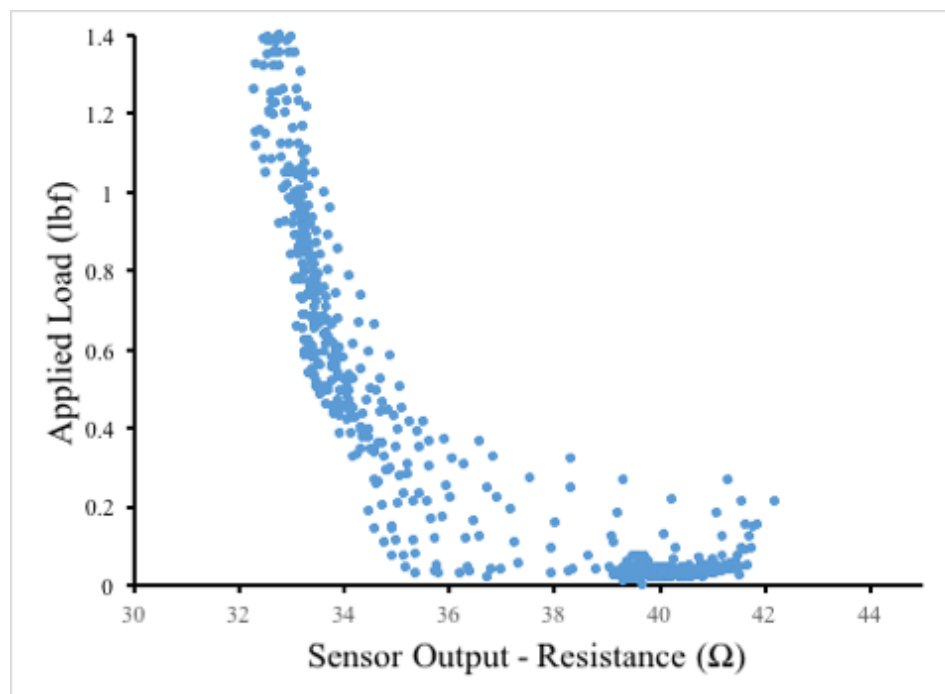


Figure 90. Flat Rubber

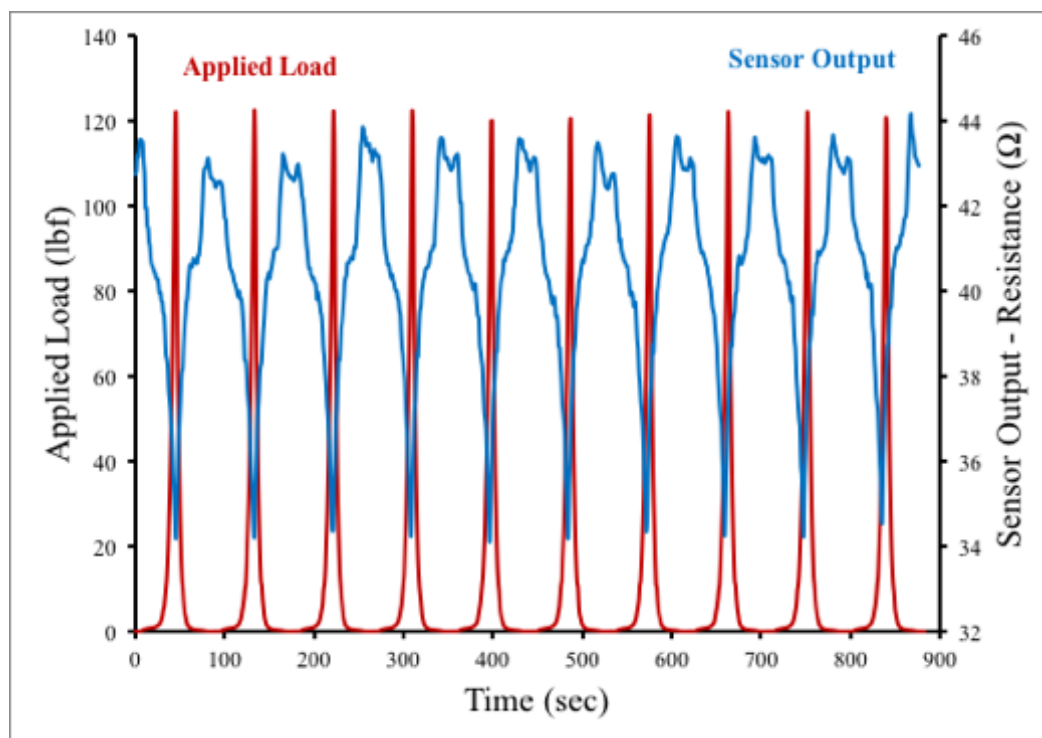


Figure 91. Rubber - 3/4" Diameter Sphere

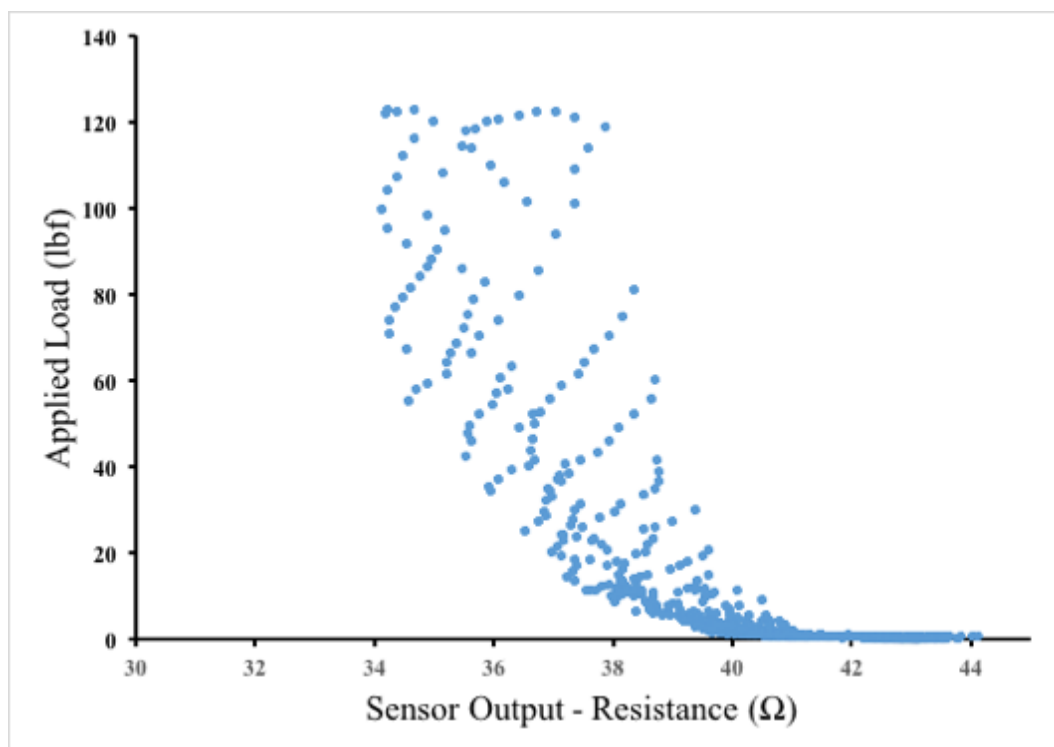


Figure 92. Rubber - 3/4" Diameter Sphere

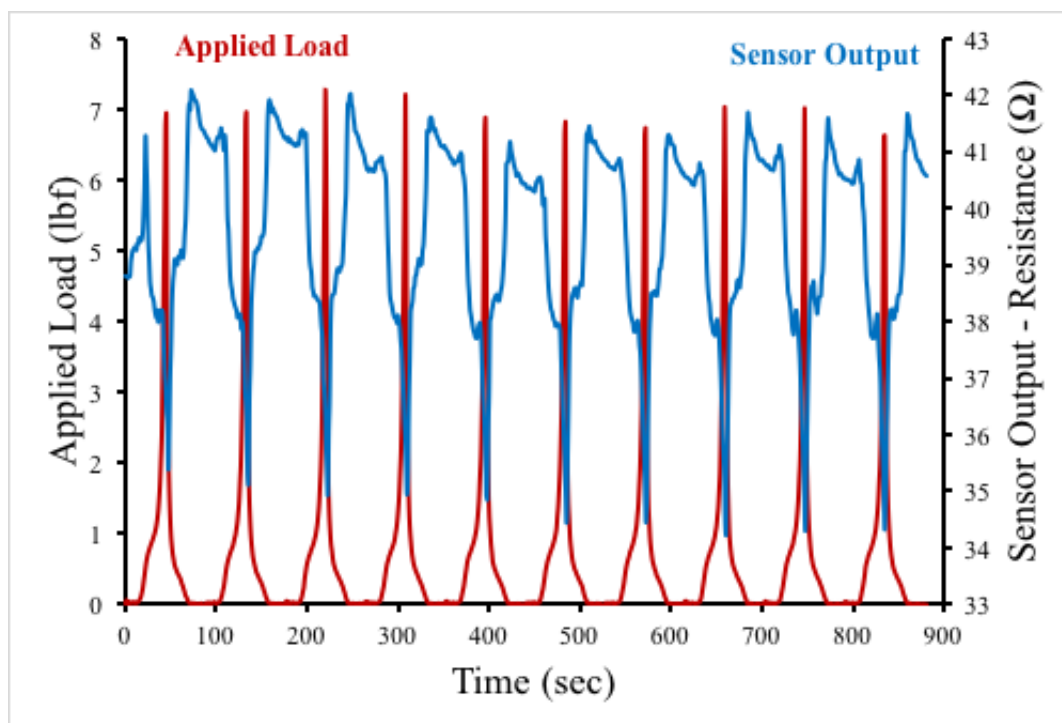


Figure 93. Rubber - 1/2" Diameter Sphere

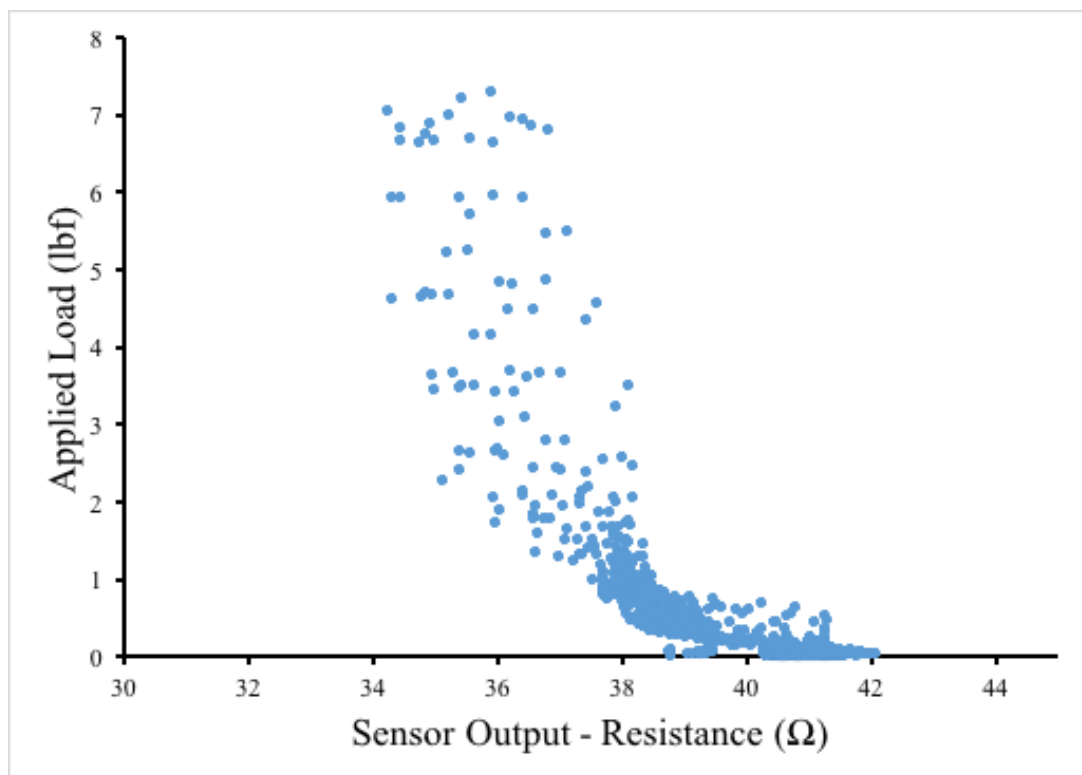


Figure 94. Rubber - 1/2" Diameter Sphere

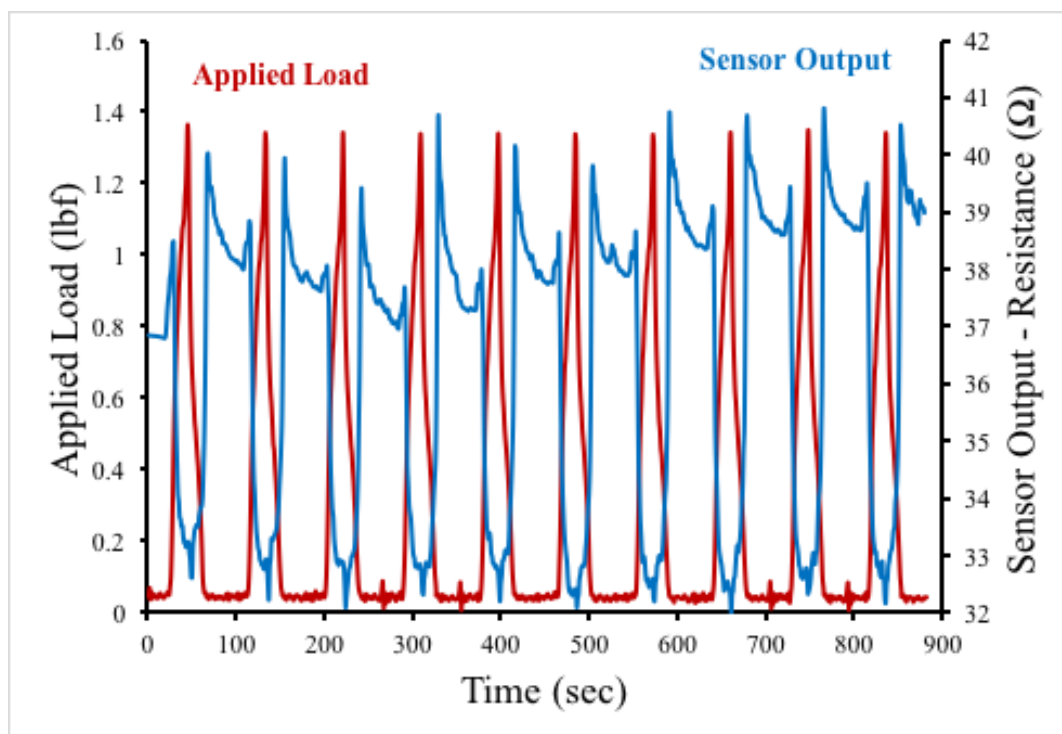


Figure 95. Rubber - 1/8" Diameter Sphere

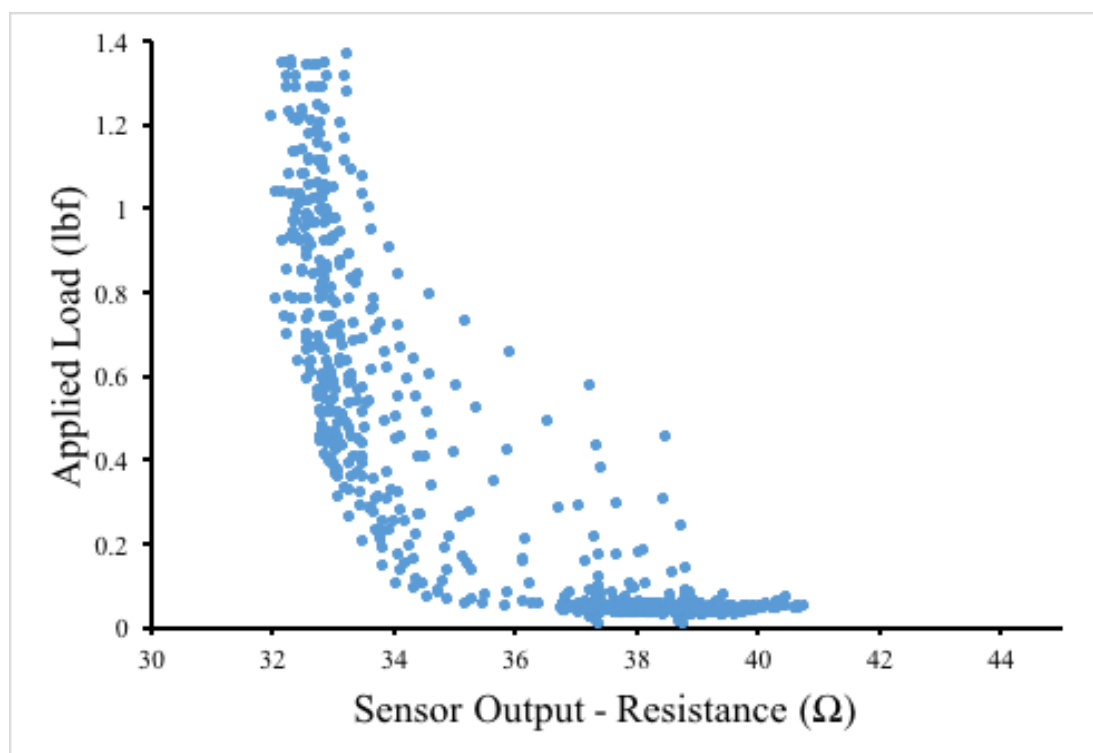


Figure 96. Rubber - 1/8" Diameter Sphere

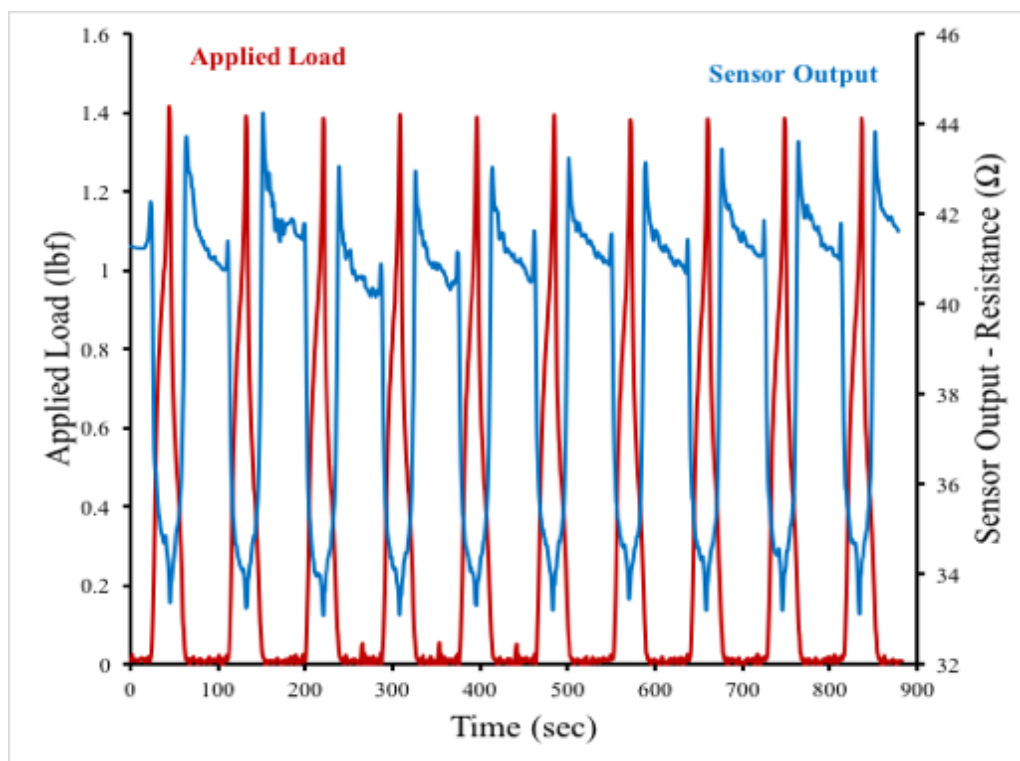


Figure 97. Flat Silicone

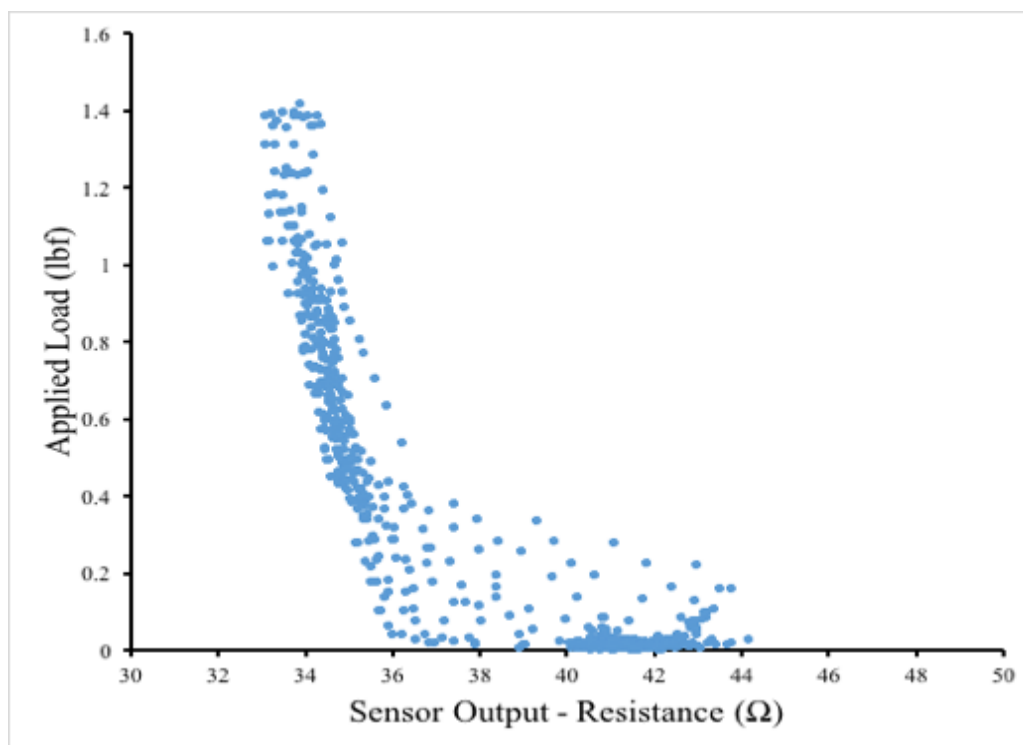


Figure 98. Flat Silicone

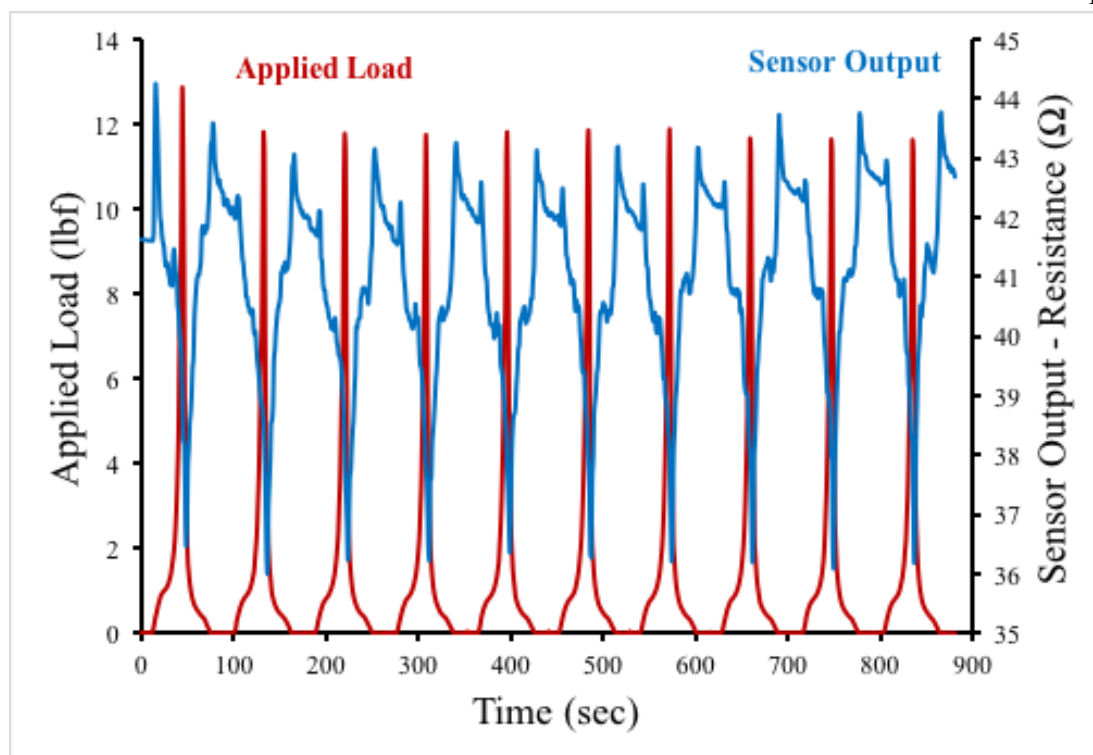


Figure 99. Silicone - 3/4" Diameter Sphere

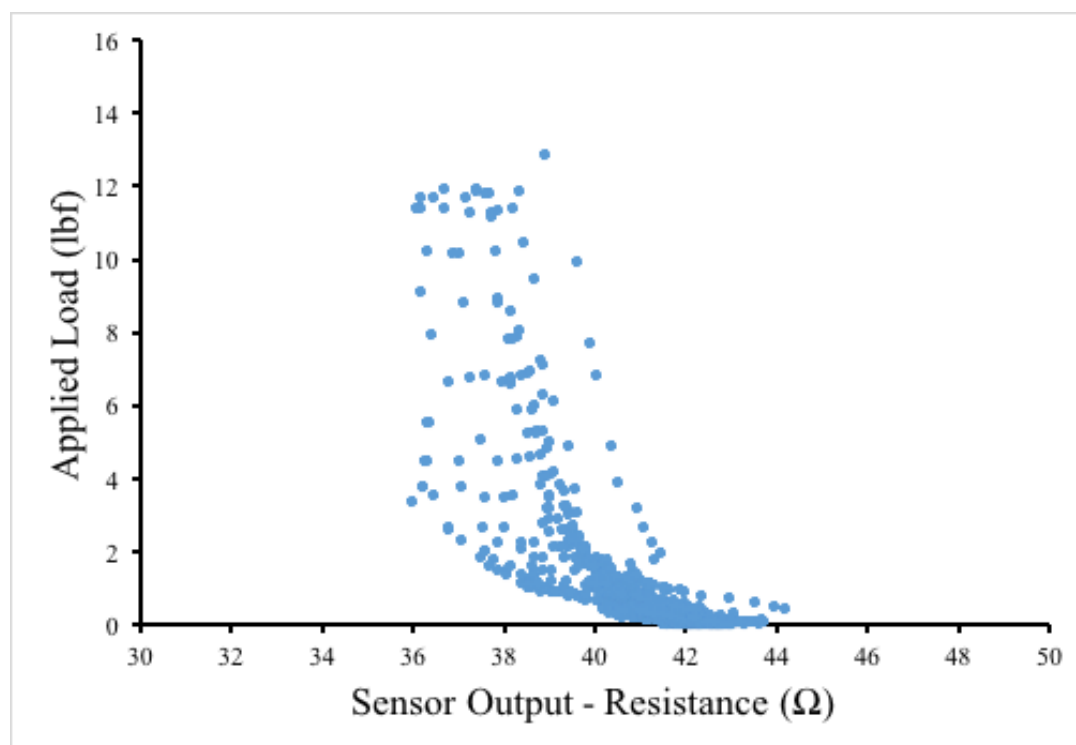


Figure 100. Silicone - 3/4" Diameter Sphere

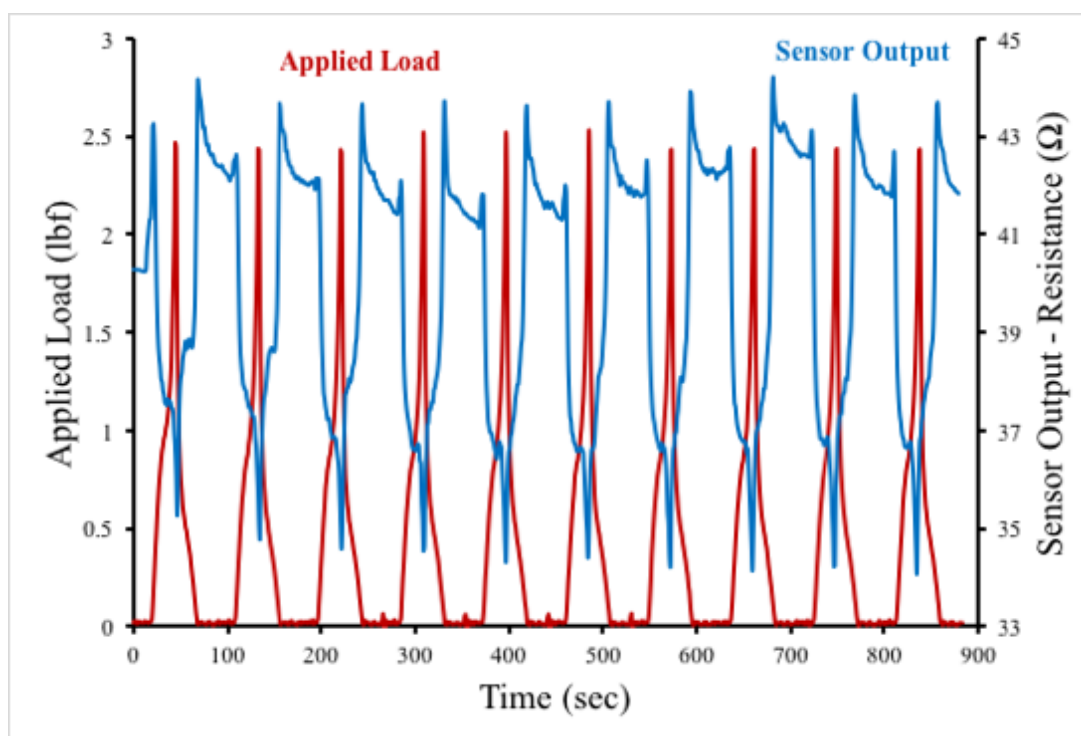


Figure 101. Silicone - 1/2" Diameter Sphere

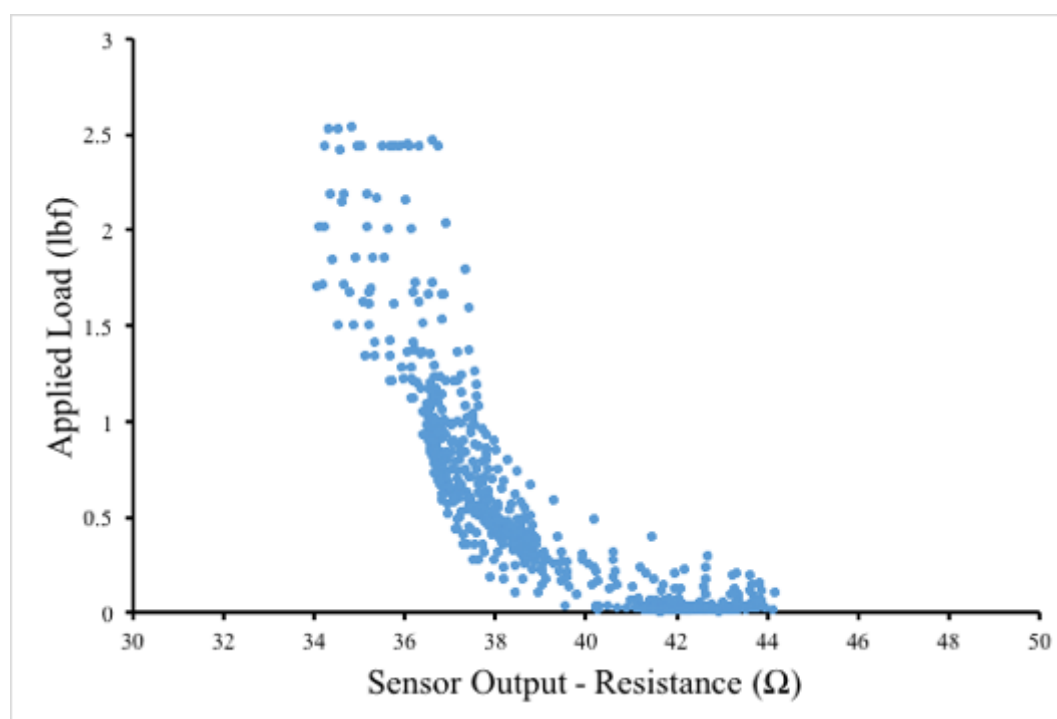


Figure 102. Silicone - 1/2" Diameter Sphere

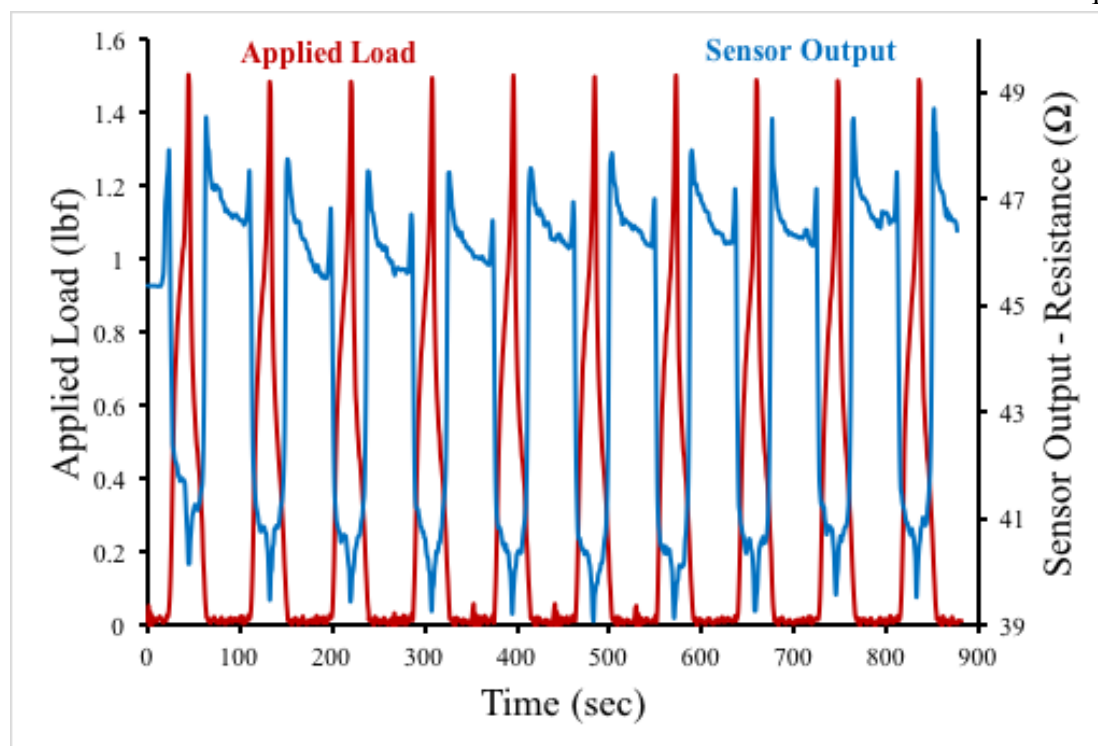


Figure 103. Silicone - 1/8" Diameter Sphere

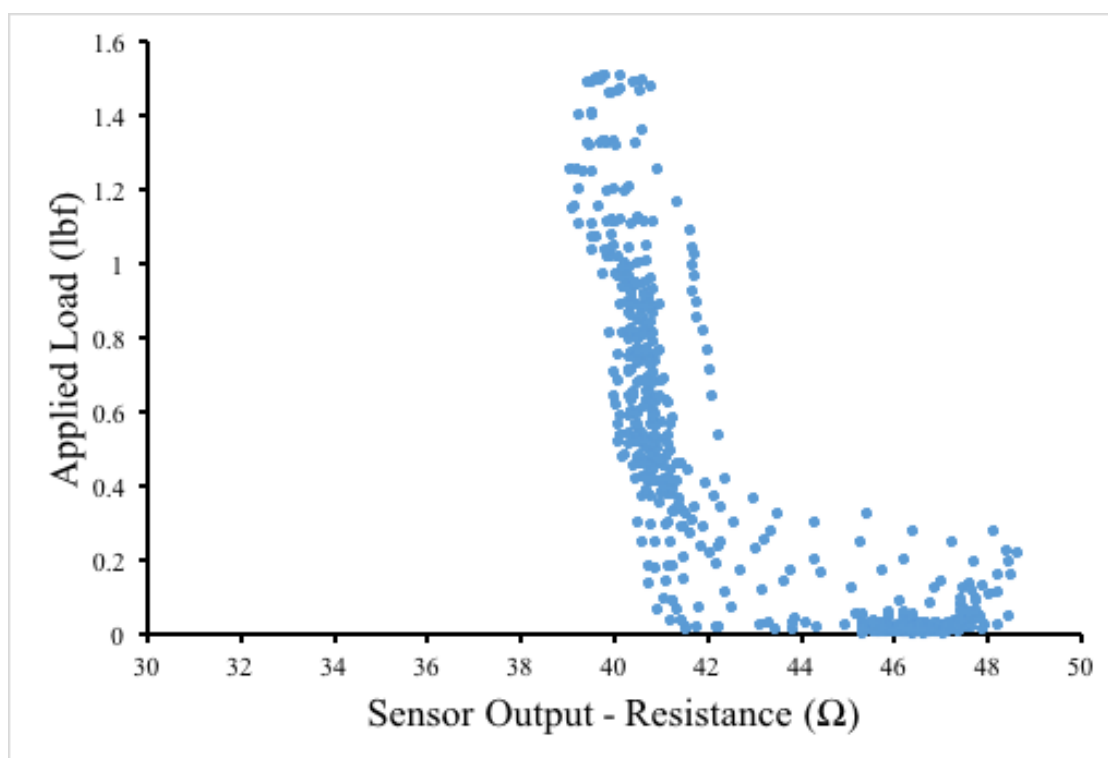


Figure 104. Silicone - 1/8" Diameter Sphere